CURING BEHAVIOR AND PROPERTIES OF 4,4’-BISMALEIMIDODIPHENYLMETHANE AND O,O’-DIALLYL BISPHENOL A: EFFECT OF PEROXIDES AND HYBRID SILSESQUIOXANE ADDITION

By

Jiang Zhu

A DISSERTATION

Submitted to
Michigan State University
in partial fulfillment of the requirements
for the degree of

Chemical Engineering and Materials Science-Doctor of Philosophy

2012

ABSTRACT

CURING BEHAVIOR AND PROPERTIES OF 4,4’-BISMALEIMIDODIPHENYLMETHANE AND O,O’-DIALLYL BISPHENOL A: FFECT OF PEROXIDES AND HYBRID SILSESQUIOXANE ADDITION

By

Jiang Zhu

The aim of this work is to provide a better understanding on the use of common organic free radical initiator and hybrid silsesquioxane on curing behavior, corresponding cured structures and thermal mechanical properties of organic bismaleimide (BMI) network consisted by 4,4’-bismaleimidodiphenylmethane (BMPM) and O, O’-diallyl bisphenol A (DABPA). Three kinds of peroxide, Dicumyl Peroxide (DCP), 2,5-Dimethyl-2,5-di(tert-butylperoxyl) hexane (Trigonox®101), 3,6,9-Triethyl-3,6,9,-trimethyl-1,4,7-triperoxonane (Trigonox®301) and two types of silsesquioxane, Octastyrenyl (OSTS) and N-Phenylaminopropyl cage mixture (APS) were investigated with BMI system. Specifically, onset of cure reaction and evolution of exothermic heat flow by the differential scanning calorimetry were used to study changes in the reaction mechanism when different initiators and/or silsesquioxane was added. Thermal mechanical properties of cured network, glass transition temperature and degradation kinetics were investigated as a function of additive types and concentration. The result of this work showed that Trigonox®101 was the most suitable initiator for BMPM/DABPA system due to its low onset curing temperature, around 130°C and mild initiation step which did not result in high homopolymerization rate of BMPM as compared to DCP. Glass transition temperature of

BMPM/DABPA with 0.3wt% Trigonox® 101 was significantly improved, 90°C higher than the systems without addition of peroxide additive.

To improve thermal stability of BMI thermoset network, hybrid silsesquioxanes were added into the system. OSTS is a cage $(SiO_{1.5})_8$ containing eight styrenyl functional groups surrounding the SiO core. The styrenyl functional groups of OSTS can react with BMPM through the free radicals formed by BMPM when heated to around 200°C. APS is a cage mixture of $(SiO_{1.5})_n$, where n is equal to 8, 10 or 12, with N-aminopropyl groups surrounding the SiO core. APS will react with BMPM at around 150°C through Michael addition reaction. This work showed that this secondary amine in silsesquioxane could effectively react with BMPM forming useful networks. The enhancement in thermal properties, such as glass transition temperature of BMI network by APS was more significant than the OSTS addition. BMI network with only 5wt% APS addition showed an enhancement of 30°C in glass transition temperature while system with 10wt% OSTS showed 20°C increase. Thermo-oxidative degradation rate was also greatly reduced with the addition of hybrid silsesquioxanes.

ACKNOWLEDGEMENTS

I would like to thank my advisor, Professor Andre Y. Lee, for his guidance and support during my pursuit of doctoral degree. He widened my eyesight by encouraging me to participate in undergraduate teachings that are out of the field of my own research activities. I also would like to express my gratefulness to the members of my committee, Professor Ramani Narayan, Professor James Lucas and Professor Rafael Auras for their input and guidance.

Special thanks go to the Air Force Research and Laboratory for the financial support. I also would like to thanks AkzoNobel Inc. for generous supplying materials used in this work. Last but not the least, I want to thank my family and friends who love me and supported me during the past years.

TABLE OF CONTENTS

LIST OF TABLES

LIST OF FIGURES

CHAPTER 1: INTRODUCTION

1.1 High performance thermosets

Thermosets resins are formed by low molecular weight oligomers with reactive groups that can further undergo crosslink reaction. One advantage of thermosets is that the ultimate properties of thermoset can be finely controlled by composition ratio and processing method [1]. High-performance thermosetting materials are designed to meet highly demanding environments. The criteria of high performance thermosets include its processability as well as final physical properties, such as high glass transition temperature around 300^{o}C and high temperature stability that can maintain material stable at 400^{o}C [2]. Most high performance thermoset is consisted by aromatic ring structure or heterocyclic segments. However, the high content of aromatic ring structure will drastically increase melt viscosity and reduce solubility of the resin [3]. When the resin becomes flowable at elevated temperature, it also starts rapid polymerization that made the fabrication process really difficult. As a result, poor processability of high performance thermosetting resin is a common concern during fabrication process.

High performance thermoset have found a broad range of application, such as structural materials in fiber reinforced composites, thin films in electronics packaging and so on. Composites based on thermoset are widely used in aerospace application, such as aircraft engines, missiles and rockets. Three most widely used thermoset system in industry includes polyimide, epoxy and bismaleimide.

Polyimides developed for aerospace application are consisted by highly aromatic chemical structure. It has gained considerable attention over the last two decades due to their excellent thermal and chemical stability. Polyimides can be produced from either condensation reaction or addition reaction. Condensation reactions are generally based on high molecular weight polyamic acid precursor [4]. During the condensation reaction, volatile will leave the system with voids. Condensation polyimides generally do not possess high heat resistance. On the other side, addition polyimides are usually made from low molecular weight resin with unsaturated moieties for crosslink reactions, which produce no volatile. The final matrix is theoretically void free. Addition polyimides are usually thermal resistant [1]. Thermoplastic polyimides as well as thermoset polyimides are available for commercial and aerospace applications [5]. Specifically polyimide systems will be discussed in detail later in this chapter.

Epoxy resin has been the most important class of thermoset system in industry. It is versatile in application, such as coating, structural adhesives and composites matrix. Besides, it is low in cost and easy for processing. Conventional epoxy resin based on diglycidyl ether of bisphenol A is still inadequate in thermal stability, $Tg<120^{o}C$. In order to meet the high performance requirement, tri as well as tetraglycidyl epoxy has been developed. N,N,N’,N’-tetraglycidyl-4,4’-diaminodiphenylmethane(TGDDM) has been probably the most useful high performance epoxy resin. Resin mixture consisted by TGDDM and diaminodiphenylsulfone (DDS) is commonly used as matrix for aerospace composites. The ultimate glass transition temperature is around $240^{o}C$ [1]. However, a very serious drawback of epoxy is that the high amount of water absorption around 4.0 to 6.5wt% brings deterioration in mechanical properties of the materials.

Thermoset bismaleimide resin (BMI) was developed to compromise this tradeoff between thermal stability and processability [5]. BMI can be processed like epoxy but still has high Tg up to 350^{o}C. Thus, among additional type polyimides, BMI is widely used in structural application due to its high performance to cost ratio [6]. The reactive group of bismaleimide is imide bond that is under electron withdrawing of adjacent carbonyl groups. Bismaleimide can undergo polymerization by simple heating without the addition of any initiator. Neat BMI is generally very brittle due to its high crosslink density. Diallyl bisphenol A (DABPA) has been commonly mixed with BMI to improve fracture toughness of the system. However, high temperature (>200^{o}C) was still needed for the crosslinking reaction [8-13]. As a result, their usage in the repair of conventional composites process was limited. Thus, reaction initiator would be needed to reduce the initial cure temperature. The initiators can either be peroxides that can form free radicals and initiate the cure reaction or some tertiary amines, imidazoles that can induce the bismaleimide to undergo the anionic reaction [14]. The goals of this work were to provide a better understanding on the use of common organic free radical initiator and hybrid silsesquioxane on the curing behavior, the corresponding cured structures and the thermal mechanical properties of organic bismaleimide (BMI) network. In the following sections, a brief review on thermosetting polyimides and common reactions for BMI are presented.

1.2 Polyimide

Marston started first produce in aromatic polyimides in 1908 [15]. Development in modern polyimide can be traced back to work conducted in DuPont during 1950s [16]. The most common method of fabricating polyimides is a two-step process. First step is condensation reaction of aromatic diamine and dianhydride to form poly(amic acid) as precursor and then followed by cyclodehydration step to form polyimide. The research of polyimide in DuPont developed Pyralin^{TM} for wire coating and Kaption-H^{TM} for film application [17]. However, the evolution of volatile by product, H_2O, is inevitable.

Investigation in addition curing polyimide started in early 1970s. The major goal was to improve the processibility without affecting the thermal stability and performance at high temperature. The most widely used higher performance polyimides include Polymerization of Monomer Reactant (PMR) type polyimides, phenylethynyl terminated imides and bismaleimides. The most popular polyimide in PMR family is PMR-15 developed at NASA Lewis Research Center [18]. The fabrication of PMR-15 based composites was to impregnate reinforcement fibers with a solution of dialkyl ester of 3, 3', 4, 4'-benzophenone tetracarboxylic acid with methylene dianiline and monoalkyl ester of 5-norbornene-2,3-dicarboxylic acid in a low-boiling alkyl achohol, typically methanol or ethanol. The chemical structures of materials in PMR-15 were shown in Figure 1.1. Around 200^{o}C, these monomers undergo imidization to form norbornyl end-capped polyimide oligomers with theoretical molecular weight around 1500. These end-cap norbornyl groups will undergo crosslink reaction at temperatures above 300^{o}C

[19]. The crosslink reaction occurs directly on the fiber surfaces resulting composites with stable thermal mechanical property for high temperature aerospace application [20]. Melt viscosity of PMR resin can be controlled through varying the monomer stoichiometry. Lower viscosity helps to remove volatile byproducts produced during the imidization reaction and leads to low void content in the final product. PMR-15 has a relatively high Tg around 365^{o}C and a good retention in its mechanical properties after expose in air for over 10,000h up at temperature around 200^{o}C. However, composites materials produced by the condensation reaction still have to face the challenge in low void content. Besides, two primary concerns of PMR-15 existed which were the health issue caused by methylene dianiline and the high cost of fabrication due to processing limitations [21].

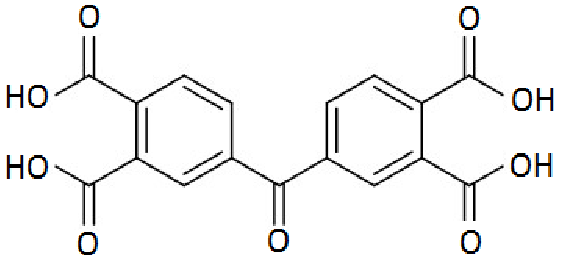

3,3’,4,4’-benzophenone tetracarboxylic acid

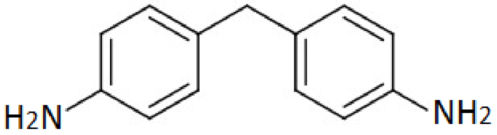

Methylene dianiline

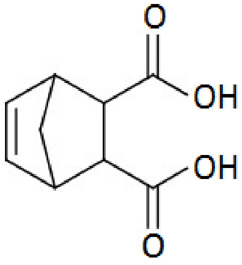

5-norbornene-2,3-dicarboxylic acid

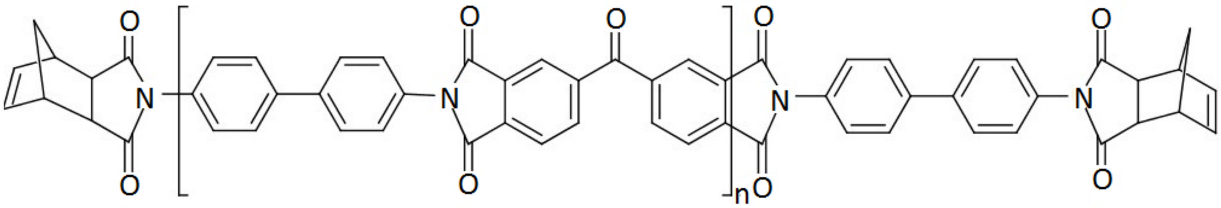

Oligomer of PMR-15

Figure1.1: Schematic chemical structures of PMR-15 origin materials

Beside PMR type polyimides, acetylene end capped polyimides have also been under extensive study [22-24]. Although acetylene terminated imides have even higher Tg and better thermal oxidative stability than PMR 15, but the crosslink reaction of acetylene groups was at about the same temperature as the imidization temperature [25]. As a result of this, it was not beneficial to remove condensation by product during processing. Due to this concern, increasing polymerization temperature of acetylene end capped polyimides was taken into consideration. This objective had been obtained by introducing phenyl rings on the acetylene groups. Most notable research was on the application of end capping agent 4-phenylethynylphthalic anhydride (PEPA) to various polyimides. NASA’s PETI-5, as shown in Figure 1.2, was one of the most successful applications of PEPA during the development of High Speed Civil Transport Program. The crosslink reaction temperature is around 350°C and the final thermoset has great hot/wet stability, high toughness as well as decent Tg around 270°C. The major disadvantage of PEPA is its high cost to performance ratio [5].

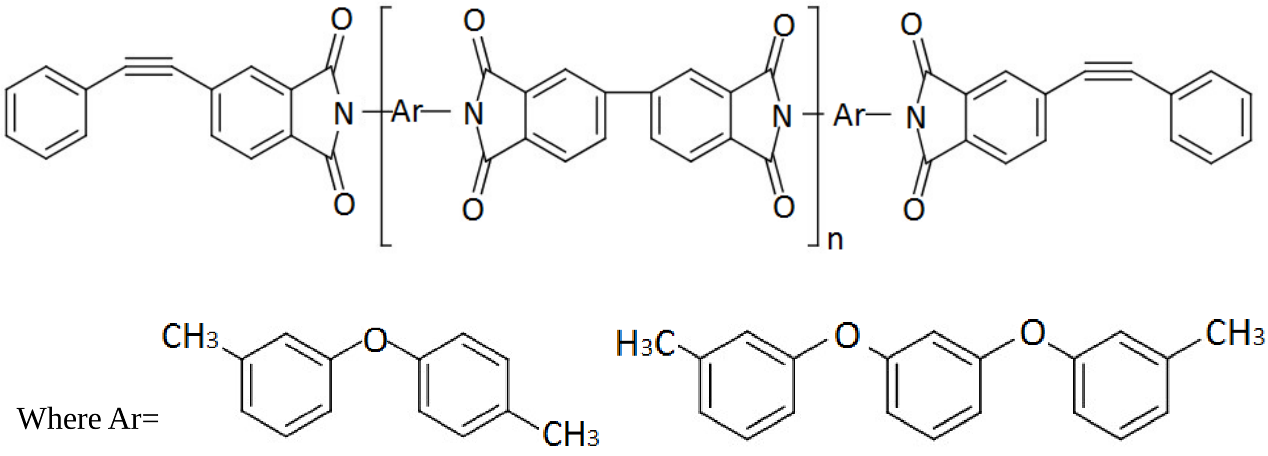

Figure1.2: Schematic structural of NASA PETI-5

1.3 Bismaleimide

Thermoset bismaleimide resin (BMI) was developed to compromise the tradeoff between thermal stability and processability [5, 6]. BMI can be processed like epoxy but still has high Tg up to 350°C. Thus, among additional type polyimides, BMI is widely used in structural application due to its high performance to cost ratio [26]. The good thermal stability and low moisture uptake property of bismaleimide allow its applications in the aerospace and electronics industry [26]. The general molecule of bismaleimide is shown in Figure 1.3.

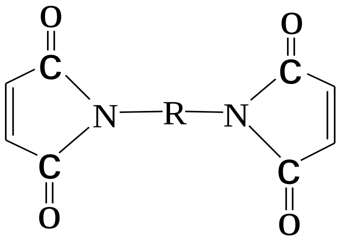

Figure1.3: General Bismaleimide molecule

Reactive groups of bismaleimide are the double bonds that are under electron withdrawing of adjacent carbonyl groups. Bismaleimide can undergo polymerization by a simple heating without the addition of any initiator or hardening agents [26]. Neat BMI is generally very brittle due to its high crosslink density. Addition of reactive elastomers, copolymerization with monomer containing allyl groups, mixture of bismaleimide monomers and modification with thermoplastics had all been used to modify bismaleimide thermosets [27].

Diallyl bisphenol A (DABPA) has been commonly mixed with BMI to improve the fracture toughness of BMI network. The allyl groups in DABPA can react with bismaleimide via “Ene” type addition. The linear chain of bismaleimide is thus extended and crosslink density is controlled. The most widely used bismaleimide system are based on 4,4’-bismaleimidodiphenylmethane (BMPM) and O, O’-diallyl bisphenol A (DABPA), as shown in Figure 1.4.

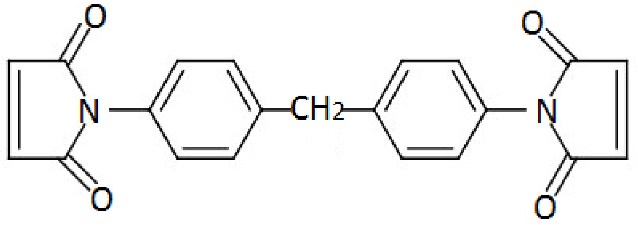

4,4’-bismaleimidodiphenylmethane (BMPM)

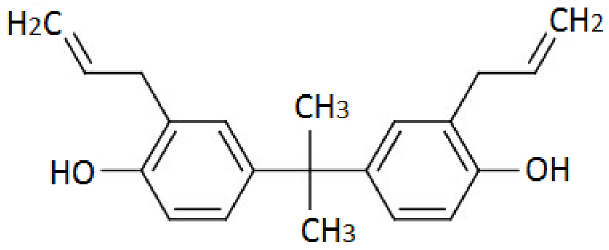

O, O’-diallyl bisphenol A (DABPA)

Figure1.4: Schematic chemical structure of BMPM and DABPA

The reaction of BMPM and DABPA has been well studied by previous researches [7-10]. Although the reactions between BMPM and DABPA were complex, the following reaction types have been proposed and accepted by most researchers: “Ene”, Diels-Alder, homopolymerization of BMPM and alternating copolymerization of BMPM and DABPA [11]. The reaction routes were shown in Figure 1.5. Around 150°C, the BMPM and DABPA monomers react forming “Ene” molecule which contains three active C=C double bonds. In Figure 1.5, three possible reactive sites were shown as the ally site labeled as “A”, the propenyl site labeled as “B” and the maleimide site labeled as “C”. At above 200°C, these three sites will undergo the rapid free radical polymerization [12].

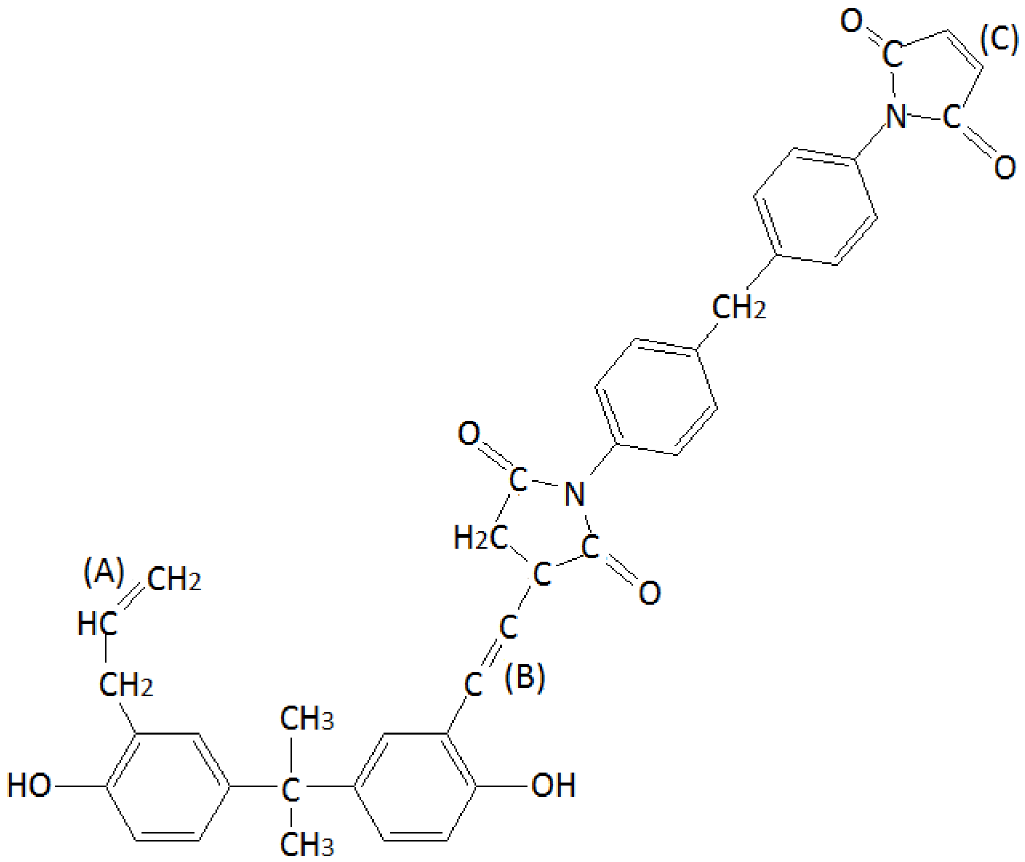

Figure1.5: Free radical polymerization sites in BMPM/DAPBA “Ene” adduct prepolymer

1.3.1 Thermal polymerization

The major crosslink reaction of bismaleimide resin is their homopolymerization at elevated temperatures. In general, bismaleimide resin showed an onset reaction temperature as low as 150^{o}C and peak reaction temperature no more than 300^{o}C by differential scanning calorimetric study [1]. Few researchers have studied pure bismaleimide thermal polymerization. The following reaction pathway has been suggested to occur during the crosslink reaction between BMPM. One pathway is the homopolymerization of BMPM by the reaction of maleimide C=C double bonds. The resulting network has formation of a four-member ring structure [28]. The other possible pathway is also the homopolymerization of BMPM, but the reaction is between three BMPM molecules through C=C double bonds [29]. In general, the maleimide ring addition is the only observable reaction in bismaleimides polymerization.

The reaction mechanism of bismaleimide crosslink reaction is free radical polymerization. When free radicals are formed during the heating of BMPM, these free radicals can quickly transferred to other double bonds in BMPM to form growing polymer chain. The pendant double bonds at the ends of these chains can further react with another growing chain for network formation. When the molecular weight of the growing polymer reaches a certain level, a gel-like structure is formed. At the gel point, substantial fraction of pendent maleimide bonds still can remain in the system. The concentration of these pendent double bonds in the thermoset can be calculated from the consumption of monomers [30].

The disadvantage of pure bismaleimide resin is its high crosslink density. The final network is very brittle, thus limit its application for structural materials. Besides, system reaches the gel point too quickly leaving many unreacted maleimide bonds. As a result, at the end of the cure, the reaction generally cannot reach completion. Any kind of further crosslink reaction during application may cause the system become even more brittle.

1.3.2 Michael addition with amine

Due to the brittleness of pure bismaleimide network, modification by adding co-reactants was needed. Addition of amine as a co-reactant had been actively investigated due to the Michael addition reaction between them [31-41]. The amine addition reaction result in a chain extension of the network resulted in lower crosslink density of the final cured BMI network as the increase in the distance between crosslinks.

The Michael addition between bismaleimide and amine occurs readily at a lower temperature than the homopolymerization of the maleimide double bonds [31]. The amine addition reaction and homopolymerization of bismaleimide and amine were shown in Figure 1.6. The final network properties were a combination of these two reaction effects. Tungare and Martin [32] did a systematic research on 1,1’-(methylenedi-4,1-phenylene) bismaleimide and 4,4’-methylenedianiline (MDA) with different stoichiometric ratio in order to investigate the curing behavior of bismaleimide resin. They found that the amine addition to the maleimide double bond occurred by a second-order reaction mechanism and gave the network an extended chain structure. The homopolymerization of bismaleimide can also be modeled by a thermal initiation step, radical mechanism and finally leads to crosslinked network. The amine addition occurred more rapidly than the chain propagation by BMPM homopolymerization at lower temperatures. Varma and Sangita investigated how different amines can affect the final bismaleimide network [33]. It was found that the Michael addition reaction rate depends on the reactivity of amines. Amines that are more basic in character can react with bismaleimide at lower temperature. They also found that the thermal stability of cured resin was better when amine contains phosphorous groups. Marie and Louis studied on the influence of steric hindrance on the reactivity for the bismaleimide-diamine system [34]. They investigated those diamines containing different alkyl substituents at the ortho position to the amine function. The electron donating effect of alkyl groups were considered as a reinforcement factor on the basicity of the amine functions. With a higher electron density, the amine reactivity will be higher. However, the steric hindrance of larger alkyl groups can also reduce the reactivity of amine [35]. From their study, with the steric effect of diamine increased, less addition reaction would take place. The system will favor the homopolymerization of bismaleimide. Although with amine modified bismaleimide thermoset showed improvement in fracture toughness, thermal properties such as decomposition temperature, glass transition temperature and thermal stability of the resin were negatively impacted [40, 41].

1.3.3 Eutectic mixture of Bismaleimide monomers

Bismaleimide itself have relatively high melting point which oriented the researchers to study mixture of maleimide systems with lower melting point for better processing ability. Binary system of bismaleimide has been investigated before, showing reduced melting temperatures [36, 37]. In general, these binary mixtures were consisted by two bismaleimide monomers containing aromatic structure with defined stoichiometric ratio. Studies have been focused on mixing BMPM with other low melting temperature bismaleimide. Nagai's research showed that the melting point of the mixture was decreasing with more content of low melting temperature bismaleimide in the system [37]. The maximal decreased temperature was observed corresponded to a eutectic mixture that shows a minimal temperature.

Bismaleimide eutectic mixtures have been under research by industry. However, the reaction mechanisms of these bismaleimide mixtures were not well discussed or published [36]. Afsoon studied a mixture of two or more different kinds of bismaleimide monomers. Their study showed that the melting of BMI mixture was lowered with more content of low melting temperature BMI monomer in the system. There is a certain composition of the mixture when a significant lower melting temperature (eutectic temperature) that was lower than the melting temperature of each BMI monomer [68]. Varma proposed mechanism via copolymerization of bismaleimide molecules. On the other side, Nagai found that no change in the peak reaction temperature of eutectic mixture as compared to each bismaleimide monomers, indicating no copolymerization occurred [37]. Grenier and Cunha further investigated on the reaction using solid-state spectroscopy and confirmed that the copolymerization between bismaleimide monomers was definitely took place. Moreover, the more reactive monomer was consumed faster at the onset of reaction. However, in the later stage, the consumption of both monomers was about the same [34].

1.3.4 Copolymerization with monomer containing allyl groups

BMI resin with alkenylphenol oligomers was developed due to the improvement in toughness and humidity resistance by incorporating allyl groups into the network [38]. Maleimide groups react with allyl via an “Ene” reaction as mention before. The cure mechanism of the network was then mainly consisted by chain polymerization and polycondensation reaction [39]. For chain polymerization is from the maleimide and the propenyl groups generated by the “Ene” reaction. The condensation reaction is the dehydration reaction of phenol groups. A ladder structure developed from Diels-Alder reaction between maleimide bonds and “Ene” product was postulated as part of the network formation and most researchers accepted this mechanism. On the other side, Roger and coworkers investigated on mono-functional groups of maleimide and allyl functional groups to further understand the reaction mechanism, they found that the Diels-Alder reaction only take place in mono-functional system. The steric hindrance in the “Ene” molecule of BMPM and DABPA did not allow the reaction occurs.

The most popular resin based on bismaleimide and alkenylphenol is Matrimid 5292B by Ciba-Geigy. Prepolymer was formed by ene reaction between maleimide and allylphenyl coreactant upon heating around 150°C. The toughness of final thermoset is significantly enhanced. Fracture toughness of pure Matrimid 5292A (BMPM) is around 0.14in-lb/in^2 while the combined 5292B with 5292A is around 1.2in-lb/in^2. Great hot/wet strength and low moisture absorption were also observed.

Other allyl compounds were also developed to incorporate into BMI network. For example, Guozheng and Aijuan synthesized N,N'-diallylaminodiphenyl methane (ADM) and mixed with BMPM at various mole ratios [42]. They found that the reaction peak temperature of BMPM/ADM system was relatively lower than BMPM/DABPA system. When BMPM/ADM at weight ratio of 1 to 0.68, the peak reaction temperature was 38°C lower than BMPM/DABPA at weight ratio of 1 to 0.87. They showed that BMPM/ADM at weight ratio of 1 to 0.4 has better thermal stability than BMPM/DAPBA network. However, it might be due to the higher amount of BMPM in the system that would give the network higher crosslink density.

1.3.5 Initiator initiated polymerization

When bismaleimide was thermally cured, high temperature was needed to initiate the crosslink reaction. All the above-discussed bismaleimide and co-reactant system can only solve the high crosslink density issue of pure bismaleimide. However, further crosslink reaction still needed high temperature so that bismaleimide can form free radicals by itself. This high curing temperature limits the application of bismaleimide in conventional composites processing. Thus, researchers turn their way to initiators to reduce the cure temperature. The initiators can be peroxides initiating free radical polymerization [43-46]. It can also be imidazole that resulting anionic polymerization [47]. Seris and coworkers did systematic research on anionically initiated by imidazole. The addition of imidazole can lower the onset reaction temperature up to 20^{o}C with 0.2wt% imidazole added. Their study suggested that the anionic curing of bismaleimide was more homogeneous than the thermally initiated system. This might be due to a faster initiation step as compared to the propagation step. However, the heat of reaction decreased with increasing amount of imidazole. The system reached gel stage very fast, leaving a lot of imide bonds unreacted [48].

Takashi and Toshiro did research on both imidazole and peroxide type initiators on mono-functional maleimide resin. They investigated N-phenylmaleimide (PMI) and a mixture of PMI/N, N'-diphenylaspartimide (API). API was synthesized from PMI with aniline at 1 to 1 molar ratio. Both PMI and PMI/API system was studied with imidazole and dicumyl peroxide (DCP). Imidazole accelerated the reaction of PMI at 170^{o}C. The presence of API did not significantly affect the reaction of PMI with the addition of imidazole. With DCP initiated system, API hindered the catalytic effect of DCP. They found that with increasing amount of API in PMI system, the polymerization rate of PMI decreased [49].

1.3.6 Bismaleimide nanocomposites

During recent years, nanocomposites made from the combination of polymer matrix and nano-sized inorganic fillers have been proven to exhibit excellent property and performance.

These nano-sized inorganic fillers often exhibit dramatic physical and chemical properties that are superior to their micro-phase counterpart. One of the nanoscopic inorganic fillers, Polyhedral Oligomeric Silsesquioxanes (POSS), has received a lot of attention in recent years. POSS are nanomolecules that contain [$RSiO_{1.5}$] repeat units. There are four general structures of POSS: random, ladder, partial cage and cage. The framework of POSS is consisted by oxygen and silicon with organic groups cover the outer space. The organic groups can be reactive or non-reactive functional groups. Thus, POSS are hybrid compounds containing both organic and inorganic elements, which can be simply considered as functionalized silica. POSS molecules have characteristic size in the nano region (1-3nm). POSS molecules with organic functional groups are compatible with polymer, thus it provides vast possibilities for designing new hybrid materials with well-defined dimensions and nanophase behavior [50].

POSS containing one or more reactive functional groups have been synthesized and studied. It can be prepared via grafting, surface bonding, transformation or polymerization [51]. Large-scale process for POSS monomer synthesis has already developed in the early 2000 [52]. Now, POSS monomers containing various reactive or nonreactive groups are commercially available as solids or oils. POSS nanostructured monomers can be homopolymerized or copolymerized with other monomers, grafting, or blending with polymer [53]. The incorporation of POSS into polymer can always lead to significant improvement in mechanical and physical properties, such as extended temperature range, reductions in flammability during processing [54]. These improvements have already been widely shown in the application of POSS in various thermoplastics as well as some thermosets [55-62].

In general, there are two methods to incorporate POSS into polymer. One method is mostly concerned with POSS containing reactive functional groups. POSS with monofunctional group can copolymerize with an organic monomer to produce a linear hybrid copolymer [60]. Another method is simple blending POSS into polymer. The organic groups on the POSS cage can provide compatibility between POSS and polymer matrix.

BMI/Octaaminophenyl POSS was studied by Fuwei Huang and Zhongping Li et al [63]. Their study showed that Octaaminophenyl POSS can react with the bismaleimide system. The Tg of neat BMI was 320°C while the Tg of BMI/5wt% POSS was 350°C. This was due to the hinder effect of bulky POSS cage on the mobility of the polymer chain. But with more POSS addition, Tg decreased, which was possibly due to the increased free volume with POSS addition [64]. The decomposition temperatures of the cured resin stayed the same under N_2 atmosphere and decreased in ambient air atmosphere with more POSS added into the system. The char yield was increased with more POSS loading, which was due to the rising of silica content. Hongwei Cao did research on BMI/ Octamaleimidophenyl POSS (OMPS) system [65]. With 1wt% OMPS addition, storage modulus as well as onset decomposition temperature were enhanced slightly. However, these properties were further impaired with higher OMPS content. The char yield increased with higher OMPS content, which was due to the stable Si-O core of POSS. BMI/Octaphenyl POSS nanocomposite was studied by Fuwei Huang [66]. It was assumed that Octaphenyl POSS was dispersed homogenously into BMI. Glass transition temperature of the nanocomposites with 12.7wt% POSS addition was 33°C higher than the parent resin. It was again due to the chain mobility hindrance caused by the POSS cage. Onset degradation temperature was higher for the nanocomposites, owing to the thermal stability of POSS as well.

1.4 Program goals

1.4.1 Curing and thermal properties of 4,4’-bismaleimidodiphenylmethane and O, O’-diallyl bisphenol A based Bismaleimide network assisted by free radical initiators

Although free radical initiators in bismaleimide resin have been under research for many years, most of the researches were related with industry and not published. The effect of initiators on the thermal mechanical properties of bismaleimide resin was not systematically studied. Since the thermal structure is related with network formation, the study of thermal properties, such as glass transition temperature and thermal degradation behavior can give some insight into the network structure due to low temperature initiated crosslink reaction.

The decomposition rate and temperature of peroxides is the primary factor in choosing particular peroxide for certain application. Dicumyl peroxide (DCP) has shown to be a popular choice in assisting cure reaction of thermosets due to its favorable decomposition rate at elevated temperature. It has been widely applied into thermoplastics to control molecular weight. It is also an important crosslink agent for rubber industry. Typically, two-step decomposition process will occur in bi-functional peroxides with the formation of strong abreacting alkoxy radical. The amount of initiators in system would significantly affect the reaction of bismaleimide system.

Choosing the right amount of initiator was necessary for optimal network formation since free radical polymerization made bismaleimide reach gel state very fast. Investigation in this dissertation will cover the efficient amount of DCP peroxide to add into bismaleimide as well as try to understand the reaction mechanism of bismaleimide and peroxide system.

Besides DCP, 2,5-Dimethyl-2,5-di(tert-butylperoxyl) hexane (Trigonox®101) and 3,6,9-Triethyl-3,6,9,-trimethyl-1,4,7-triperoxonane (Trigonox®301) have been shown their ability in abstract H bonds on polymer backbone and inducing branching in polymer chain and possible crosslinking reaction [67]. The lifetime of these strong abstracting radicals will affect the peroxides overall efficiency significantly. As a result, cure reaction rate will be quite different from each other. In this work, the influence of different kind of peroxide initiators on the reaction as well as thermal and mechanical properties of bismaleimide thermoset will be evaluated. This kind of study was an important step for process optimization as well as for the better understanding of structure-property relations in the final thermoset network.

1.4.2 Curing and thermal properties of 4,4'-bismaleimidodiphenylmethane and O, O'-diallyl bisphenol A based Bismaleimide network with Polyhedral Oligomeric Silsesquioxane

The low temperature curing of bismaleimide resin with peroxide can enhance the crosslink density of the network, but thermal stability such as degradation behavior cannot be significantly improved due to the organic nature of polymer. The study of BMI/POSS was to investigate the effect of POSS on final thermal properties of BMI/POSS nanocomposites. As mentioned in the BMI/POSS composites review above, the inorganic core nature of POSS will protect the system from fast degradation. Besides, the reaction between POSS and bismaleimide may further enhance the glass transition temperature of the network. In this study, understanding the structure-property relationships of POSS modified thermoset network and optimizing the best performance for BMI/POSS nanocomposites is very important for bismaleimide application in aerospace and other industries.

For the researches have been done on BMI/POSS composites, results either showed little improvement in thermal stability with limited POSS addition or no significant enhancement with large amount of POSS content. Most researchers use POSS with similar functional groups to the polymer matrix. However, the reactivity of POSS to the co-monomer was not well understood. It was assumed that the reaction of POSS to the monomer increased the crosslink density of the network with small amount of POSS addition. When large amount of POSS added, the POSS cage might increase the free volume in the polymer matrix, thus lower down the thermal stability of the system. The reaction between reactive POSS monomer to the polymer matrix may affect the reaction between the polymer original compounds, such as the crosslink reaction between BMPM and DABPA. As a result, the overall crosslink density may be decreased with more reactive POSS addition. With lower crosslink density, the thermal properties would be inevitably impaired.

1.4.3 Curing and thermal properties of 4,4’-bismaleimidodiphenylmethane and O, O’-diallyl bisphenol A based Bismaleimide network with Polyhedral Oligomeric Silsesquioxane assisted by free radical initiator

Both peroxide and POSS have been shown its ability to enhance glass transition temperature of thermoset as well as thermoplastics. The combined effect of peroxides and POSS will be further investigated with bismaleimide network to understand if there is any synergic effect of these two different factors on the thermal mechanical properties of bismaleimide. The enhancement of peroxides on the glass transition temperature of the network is very significant while POSS can enhance the thermal stability of the network. It is possible that by combining peroxide with POSS may help to obtain a final network with balanced and excellent thermal properties. In this work, the efficient amount of POSS to combine with peroxide will be under study. Any reaction between POSS and peroxide will be considered. Pervious researchers have not done this kind of research, understanding this provides a basis for future combination of peroxide and POSS into bismaleimide system as composites matrix.

REFERENCES

REFERENCES

1. Lin, S.C. Pearce, E.M. High performance thermosets, New York: Hanser publishers, 1993.

2. Meador M.A., Cavano P.J., Malarik D.C., Structural composites: design and processing technologies, Sixth annual ASM/ESD advanced composite conference, pp529–539, 1990.

3. Staniland P.A., Macromolecular design of polymeric materials, New York: Dekker publisher, 1997.

4. Ghosh, M.K. and Mittal, K.L., Polyimides: Fundamentals and applications, New York: Marcel Dekker, Inc., 1996.

5. Jason, E.L. Michigan State University, Ph.D. thesis, 2001.

6. Wilson, D., Stenzenberger, H.D. and Hergenrother P.M., Polyimides, New York: Chapman and Hall Inc, 1990.

7. Boris, A.R., Emma, A.D., Roger, J.M. and Eugene, E.S., The polyaddition, chain and polycondensation mechanisms of formation of networks based on bismaleimides, Macromolecular Symposia, vol.171, pp87-96, 2001.

8. Boris, A.R, Emma, A.D., Roger, J.M. and Eugene, E.S., High-performance bismaleimide matrices: cure kinetics and mechanism, Polymers for advanced technologies, vol.13, pp837-844, 2002.

9. Thomas, M.D. and David, R., Relationships in a bismaleimide resin system. Part I: cure mechanisms, Polymer engineering and science, vol.32, pp409-414, 1992.

10. David, B.C., Brett, A.C. and James, M.C., Cure reaction pathways of bismaleimide polymers: a solid state NMR investigation, Macromolecules, vol.31, pp6776-6782, 1998.

11. Mijovic, J. and Andjelic, S., Study of the mechanism and rate of bismaleimide cure by remote in-situ real time fiber optic near-infrared spectroscopy, Macromolecules, vol.29, pp239-246, 1996.

12. Roger, J.M., Eugene, E.S. and Jason, E.L., Handbook of thermal analysis and calorimetry, Vol.3, Elsevier Science, 2002.

13. Morgan, R.J., Kong, F.M., Structure-property relations of polyethertriamine-cured Bisphenol A-diglycidyl ether epoxy, Polymer, vol.25, pp375-386, 1984.

14. Seris, A., Feve, M., Mechin, F. and Pascault, J.P., Thermally and anionically initiated cure of bismaleimide monomers, Journal of applied polymer science, vol.48, pp257-269, 1993.

15. Ohya,H., Kudryavtsev, V.V., Semenova, S.I., Polyimide membrane applications, fabrications and properties, Tokyo: Kodansha Ltd., 1996.

16. Sroog, C.E. Polyimides, Progress in polymer science, vol.16, pp561–694, 1991.

17. Michael, A.M., Recent advances in the development of processable high temperature polymers, Annual review of materials science, vol.28, pp599-630, 1998.

18. Serafini, T.T., Delvigs, P., Lightsey, G.R., Thermally stable polyimides from solutions of monomeric reactants, Journal of applied polymer science, vol.16, 905-915, 1972.

19. Wong, A.C., Ritchey, W.M., Nuclear magnetic resonance study of norbornene end capped polyimides. 1. Polymerization of N-phenylnadimide, Macromolecules vol.14, pp825–31, 1981.

20. Pater, R.H., Thermosetting polyimides- a review, Sample Journal, vol.30, pp29-38, 1994.

21. Current Intelligence Bull. 47, Methylenedianiline, U.S. Department of Health and Human Service, July 28, 1986.

22. Bilow, N., Landis, A.L., Miller, R.J., Copolymers of ethynyl terminated polyimides and diethynylbenzene, U.S. Patent No. 3,845,018, 1974.

23. Landis, A.L., Bilow, N., Boschan, R.H and Lawrence, R.E., Thermosetting polyimide adhesives, Polymer Preprint, vol.15, pp537–41, 1974.

24. Bilow, N, Keller, L.B., Landis, A.L., Boschan, R.H. and Castillo. A., New development in acetylene substituted polyimides, Proceedings of the 23rd national SAMPE symposium, vol.23, pp791–805, 1978.

25. Hergenrother, P.M. and Johnston, N., Status of high temperature laminating resins and adhesives, ACS Organic coatings and plastics chemistry, vol.40, pp460-468, 1979.

26. Li, Y., L., Gu, A.J., Liang, G.Z., Microcapsule modified bismaleimide (BMI) resins,

Composites science and technology, vol.68, pp2107-2113, 2008.

27. Boey F., Xiong, Y. and Rath, S.K., Glass transition temperature in the curing process of bismaleimide modified with diallylbisphenol A, Journal of applied polymer science, vol.91, pp3244-3247, 2004.

28. Lee, B., Chaudhari, M. A. and Galvin, T., Rubber toughener for bismaleimide thermoset, 17th National SAMPE technical conference, vol.17, pp172-175, 1985.

29. Fry, C. G., and Lind, A. C., Curing of bismaleimide polymers: a solid-state C13 NMR study, new polymer materials, vol.2, pp235-254, 1990.

30. Dusek, K., Matejka, L., Spacek, P.and Winter, H., Network formation in the free-radical copolymerization of a bismaleimide and styrene, Polymer, vol.37, pp2233–2242, 1996.

31. Stenzenberger, H.D., Herzog, M and Norman, J.R. Development of thermosetting polyimide resins, British polymer journal, vol.15, pp2-12, 1983.

32. Tungare, A.V. and Martin, G.C., Analysis of the curing behavior of bismaleimide resins, Journal of Applied Polymer Science, vol.46, 1125-1135, 1992.

33. VARMA, I. K., and VARMA, D. S., Addition polyimides. III. Thermal behavior of bismaleimides, Journal of Polymer Science: Polymer chemistry edition, Vol. 22, pp1419-1433, 1984.

34. Marie, F.G.L and Louis, D.C., Influence of steric hindrance on the reactivity and kinetics of molten-state radical polymerization of binary bismaleimide-diamine systems, Polymer, vol.39, 1799-1814, 1998.

35. Gunnar, O.N. and Jon, S. Solvent properties of dichloromethane. II. The reactivity of dichloromethane toward amines, Acta chemical scandinavica B, vol.38, pp469-477, 1984.

36. Varma, I. K. and Tiwari, R., J., Thermal characterization of bismaleimide blends, Thermal Analysis, vol. 32, pp1023-1037, 1987.

37. Nagai, A., Takahashi, A., Suzuki, M., Katagiri, J. and Mukoh, A., Thermal behavior and cured products of mixture of two different bismaleimide, Journal of applied polymer science, vol.41, pp2241-2250, 1990.

38. Zahir, A.C. and Renner, A., Process for the manufacture of crosslinked polymers which contain imide groups, U.S. Patent, 4100140, 1978.

39. Rozenberg, B.A., Dzhavadyan, E.A., Morgan, R., and Shin, E., High-performance bismaleimide matrices: Cure kinetics and mechanism. Polymer for advanced technologies, vol.13, pp837–844, 2002.

40. Crivello, J.V., Polyaspartamides: condensation of aromatic diamines and bismaleimide compounds, Journal of polymer science, polymer chemistry edition, vol.11, 1185-1120, 1973.

41. White, J.E. Synthesis and properties of high molecular weight step growth polymers from bismaleimides, Industrial & engineering chemistry product research and development, vol.26, pp395–400, 1986.

42. Liang, G.Z. and Gu, A.J., Toughening bismaleimide resins by N-allyl aromatic amine, Polymer journal, vol.29, pp553-556, 1997.

43. Stenzenberger, H., Structural adhesives, Elsevier, London, 1986.

44. Varma, I.K., Gupta, S.P. and Varma, D.S., Effect of triallyl cyanurate on the properties of bismaleimide resins, Journal of applied polymer science, vol.33, pp151-164, 1987.

45. Kwiatkowski, G.T., Robeson, L.M. and Bedwin, A.W., Thermosetting diphenyl sulfone-based maleimide, Journal of polymer science: polymer chemistry edition, vol.13, pp961-972, 1975.

46. Acevedo, M., Abajo, J.D. and Campa, J.G.D.L., Kinetic study of the crosslinking reaction of flexible bismaleimides, vol.31, 1955-1959, 1990.

47. Stenzenberger, H.D., Herzog, M. and Canning, M., Compimides: a family of high performance bismaleimide resins, 30th National SAMPE Symposium, vol.30, pp1568-1584, 1985.

48. Seris, A., Feve, M. and Pascault, J.P., Thermally and anionically initiated cure of bismaleimide monomers, Journal of applied polymer science, vol.48, pp257-269,1993.

49. Enoki, T., Takeda, T. and Ishii, K., Effects of initiators on the model reactions of several maleimide resin systems- (I) Amine modified maleimide, High performance polymer, vol.6, pp385-393, 1994.

50. Pielichowski, K. and Njuguna, J. Polyhedral Oligomeric Silsesquioxane (POSS)-containing nanohybrid polymers, Advances in polymer science, vol.201, pp225-296, 2006.

51. Lichtenhan, J.D. and Schwab, J.J., Nanostructured chemicals: a new era in chemical technology, Journal of Chemical innovation, vol.31, pp3-5, 2001.

52. Ellsworth, M.W. and Gin, D.L., Recent advances in design and synthesis of polymer inorganic nanocomposites, Polymer news, vol.24, pp331-341, 1999.

53. Haddad, T.S. and Stapleton, R., Nanostructured hybrid organic/inorganic materials. Silsesquioxane modified plastics, Polymer preprints, vol.40, pp496-497, 1999.

54. Li, G.Z. and Wang, L.C., Viscoelastic and mechanical properties of vinyl ester (VE)/multifunctional polyhedral oligomeric silsesquioxane (POSS) nanocomposites and multifunctional POSS-styrene copolymers, Polymer, vol.43, pp4167-4176, 2002.

55. Schwab, J.J. and Lichtenhan, J.D. Polyhedral oligomeric silsesquioxane (POSS)-based polymers, Applied organometallic chemistry, vol.12, pp707-713, 1998.

56. Shochey, E.G. and Bolf, A.G., Functionalized polyhedral oligomeric silsesquioxane (POSS) macromers: new graftable POSS hydride, POSS α-olefin, POSS epoxy, and POSS cholorosilane macromers and POSS-siloxane triblocks, Applied organometallic chemistry, vol.13, pp311-327, 1999.

57. Abad, M.J. and Barral, L., Epoxy networks containing large mass fractions of a monofunctional polyhedral oligomeric silsesquioxane (POSS), Macromolecules, vol.36, pp3128-3135, 2003.

58. Chandramohan, A., Dinkaran, K. and Kumar, A.A., Synthesis and characterization of epoxy modified cyanate ester POSS nanocomposites, High performance polymers, vol.24, pp405-417, 2012.

59. Mather, P.T. and Jeon, H.G., Mechanical relaxation and microstructure of poly(norbornyl-POSS) copolymers, Macromolecules, vo.32, pp1194-1203, 1999.

60. Haddad, T.S.and Lichtenhan, J.D., Hybrid organic-inorganic thermoplastics: styryl based polyhedral oligomeric silsesquioxane polymers, Macromolecules, vol.29, pp7302-7304, 1996.

61. Lee, A. and Lichtenhan, J.D., Viscoelastic responses of polyhedral oligosilsesquioxane

reinforced epoxy systems, Macromolecules, vol.31, pp4970-4974, 1998.

62. Fu, B.X., Namani, M.and Lee, A. Influence of phenyl-trisilanol polyhedral silsesquioxane on properties of epoxy network glasses, Polymer, vol.44, pp7739-7747, 2003.

63. Huang, F.W., Rong, Z.X. and Shen, X.N., Organic/inorganic hybrid bismaleimide resin wih octa(aminophenyl)silsesquioxane, Polymer engineering and science, vol.48, pp1022-1028, 2008.

64. Ni, Y., Zheng, S.X. and Nie, K.M., Morphology and thermal properties of inorganic-organic hybrids involving epoxy resin and polyhedral oligomeric silsesquioxane, Polymer, vol.45, pp5557-5560, 2004.

65. Cao, H.W., Xu, R.W. and Yu, D.S., Thermal and dielectric properties of bismaleimide-triazine resins containing octa(maleimidophenyl) silsesquioxane, Journal of applied polymer science, vol.109, pp3114-3121, 2008.

66. Huang, F.W., Huang, F.R. and Zhou, Y., Nanocomposites of a bismaleimide resin with octaphenylsilsesquioxane or Nano-SiO_2, Polymer composites, vol.32, pp125-130, 2011.

67. Valeria, D.R., Helson, M.C., Marisa, C.G.R. and Ailtion S.G., Study of different peroxide types on the modification of LLDPE. Part 1. Factorial experimental design and thermal properties, Polymer testing, vol.25, pp306-312, 2006.

68. Afsoon, F., Laleh, R. and Faramarz, A.F., DSC analysis of thermosetting polyimides based on three bismaleimide resin eutectic mixtures, Iranian polymer journal, vol.20, pp161-171, 2011.

CHAPTER 2: CURING AND THERMAL PROPERTIES OF 4, 4’-BIS-MALEIMIDODIPHENYLMETHANE AND O, O’-DIALLYL BISPHENOL A BASED BISAMLEIMIDE NETWORK ASSISTED BY DICUMYL PEROXIDES

2.1 Introduction

Thermosetting polyimides can be produced from either condensation reaction or addition reaction. Addition polyimides are usually made from low molecular weight resin with unsaturated groups, such as maleimide [1]. Bismaleimide are generally cured by thermally induced addition reaction of maleimide groups. Bismaleimide can be processed like epoxy and end with higher glass transition temperature. Thus, among additional type polyimides, bismaleimide is widely used in airplane structural application due to its high performance to cost ratio [2]. High thermal stability and low moisture uptake properties of bismaleimide allow its applications in electronic application [3]. In particular, they were utilized as the matrix material in carbon fiber composites for aerospace applications and some high-end motherboards in electronic applications [4].

When bismaleimide were thermally cured, high temperature (>200^{o}C) was needed to initiate cure reaction. As a result, their usage in repairing conventional composites was limited. Reaction initiator can effectively reduce initial cure reaction temperature. The initiators can either be peroxides that can form free radicals and initiate the cure reaction or some tertiary amines, imidazoles that can induce bismaleimide to undergo anionic reaction [4].

The decomposition rate of peroxides was the primary factor in choosing particular peroxide for certain application. Dicumyl peroxide (DCP) has shown to be a popular choice in assisting cure reaction of thermosets due to its favorable decomposition rate at elevated temperature. Typically, two-step decomposition process will occur in bifunctional peroxides with the formation of strong abreacting alkoxy radical. Although there were some references of bismaleimide with initiator system, the reaction mechanism in the system was not systematic investigated [15-18]. The primary objective of this chapter was to understand the effect of DCP initiator on curing kinetic of BMI thermoset. Thus, understanding how this different curing process affects the final thermoset network when compared to original BMI system is important. Besides, the optimal percentage of peroxide concentration that can give the thermoset most balanced thermal and mechanical properties will be investigated also.

2.2 Experimental Techniques

2.2.1 Materials

The Bismaleimide resin (BMI) utilized was the Matrimid® 5292 system (Huntsman Co.) consisted by 4, 4'- Bismaleimidodiphenyl Methane (BMPM) and O, O'- Diallyl Bisphenol A (DABPA) monomers with stoichiometric molar ratio of 1 to 1. Different amount of Dicumyl Peroxide (DCP) (Aldrich Co.) ranging from 0.5 to 4wt% was added into the BMI resin. Besides, off stoichiometric molar ratio of BMPM to DABPA was also investigated with a fixed amount of DCP. The amount of DCP was controlled at 0.5wt%, while the molar ratio of BMPM to DABPA was 1.5 to 1 and 1 to 1.5 respectively, which represented BMPM rich and DABPA rich system. All chemical compounds were used as received with no further purification. A schematic chemical structure of these components was shown in Figure 2.1.

During mixing, the amber viscous liquid of DABPA monomers was poured into a glass beaker with magnetic stir bar. It was heated on a hot plate at 150^{o}C until viscosity decreased. Corresponding amount of yellow crystalline BMPM powder was then added into DABPA slowly and the BMPM/DABPA mixture was stirred for about 30min until a homogenous solution was obtained. The mixture was then cooled down to 100^{o}C and DCP was added in and quickly stirred in until dissolved. Finally, BMI resin panels were prepared by pouring the mixture into aluminum round disks. All panels were cured in a convention air oven at 150^{o}C for 2h and 250^{o}C for 6h.

2.2.2 Sample preparation

A diamond saw was utilized to cut cured BMI resin panels into desired size. Surface oxidation and porosity on the resin were removed by polishing with grit paper. The final specimen thickness was around 1.5mm. All samples were then cleaned with de-ionized water, followed by drying in a convention air oven at 80^{o}C until no weight change observed.

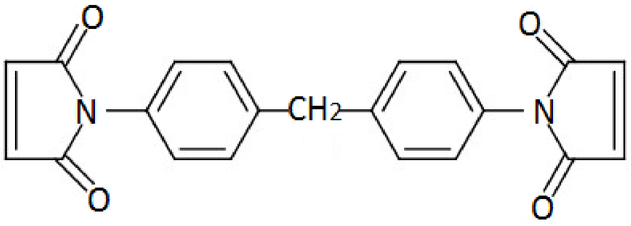

4,4’-bismaleimidodiphenylmethane (BMPM)

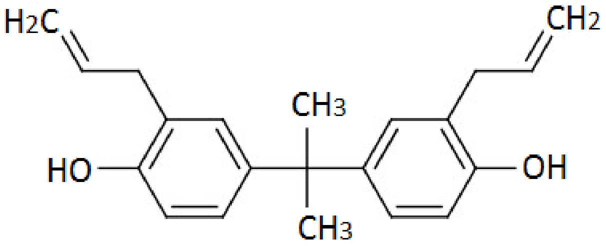

O, O’-diallyl bisphenol A (DABPA)

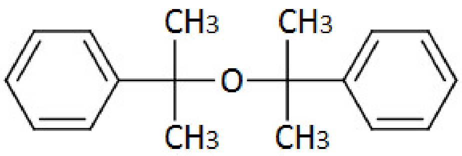

Dicumyl Peroxide (DCP)

Figure 2.1: Schematic structure of BMPM, DABPA and DCP

2.2.3 Characterization Techniques

DSC analysis of BMPM/DABPA/DCP resin was studied using around 10mg mixture in Mettler Toledo DSC-1. Dynamic heating rates of 10^{o}C/min were used to determine the heat of reaction during curing process. The heating range was from 50-350^{o}C with nitrogen gas at a flow of 50ml/min. The assumption of DSC analysis was that the area underneath the curves is proportional to the extent of reaction. The extent of cure α at any time was defined as

$$\alpha = \frac{\Delta H}{\Delta Hr}$$

where ΔH is the partial heat of reaction at any determined time while ΔH_r is the overall heat of reaction.

DMA was carried out on a Rheometric Solid Analyzer III with a 350g transducer. BMPM/DABPA/DCP samples were cut into rectangular bars with a width of 5mm and thickness of 1.5mm. Torsion mode was applied to the sample. Experiments were performed from 50 to 400^{o}C at the frequency of 10rad/s with 5^{o}C/min heating rate. From the DMA spectra, change in storage modulus, G', as a function of temperature was obtained. Tg was determined as the temperature at which maximum drop of G' occurs.

Thermal gravimetric analyzer, TA Q500, was used to investigate the thermal and oxidative stability of cured BMPM/DABPA/DCP thermosets. All the experiments were conducted from room temperature to 500^{o}C with a heating rate of 20^{o}C/min. The onset degradation temperature was determined as the temperature at 5wt% weight loss occurs.

Moisture absorption was also under investigation in this study. Before the test, all specimens were dried at 80°C in a convention air oven until no weight change observed. The moisture absorption was conducted by submerging the specimens in 50°C and 80°C de-ionized water baths. The water absorption was monitored gravimetrically according to the following equation:

$$M_t = \left(\frac{W - W_i}{W_i} \right) \times 100$$

where M_t is the weight gain percentage at time t, W_i represents the initial weight (dry weight) at time zero and W is the weight of the specimen at time t.

Before recording the moisture uptake of the specimen, the specimens were gently wiped with lint-free paper towels to remove excess water. A Mettler balance with 0.1mg precision was utilized to record the weight change.

2.3 Results and Discussion

2.3.1 Effect of DCP on reaction mechanism in Bismaleimide network

2.3.1.1 Cure reaction by DSC study

The cure reaction of Bismaleimide (BMI) thermoset consisted by BMPM and DABPA have been studied for decades by a number of researchers [6-11]. Three principal reaction temperature regimes were established in BMI thermoset, 100-200°C, 200-300°C and 300-350°C respectively. In the 100 to 200°C temperature region, BMPM and DABPA monomers will form “ene” molecules through the Alder-ene reaction. In this ene molecule, there existed three kinds of C=C bond which were allyl bond, propenyl bond and imide bond respectively. In the

200-300^{o}C region, these C=C bonds will undergo free radical polymerization, such as BMPM homopolymerization and copolymerization with DABPA. However, these reactions will not occur at a significant rate until the temperature is above 200^{o}C [11].

Typical DSC scan of BMI, as shown in Figure 2.2, an exothermic curve ranging from 160^{o}C to 300^{o}C representing the crosslink reaction was observed. Principal reaction peak was centered at 250^{o}C. This high curing temperature was due to the fact that maleimide would not form free radicals by itself below 200^{o}C. In 300 to 350^{o}C region, reaction become diffusion control as the temperature was around the glass transition temperature of BMI thermoset. Reactions were principally dehydration reaction of hydroxyl groups from DABPA, followed by complex dissociation of ether linkage in this high temperature range. Comparing to the major free radical crosslink reaction, these reactions had very little heat evolved [10].

To investigate effect of DCP on cure reaction of BMI, several DCP weight percentage were selected, which were 0.5, 1, 2 and 4wt% respectively. DSC scans were shown in Figure 2.3. From Figure 2.3, three effects of DCP on BMI were observed. Firstly, maximum temperature of the principle reaction peak was shifted to much lower temperature, from 250^{o}C to 170 ^{o}C. Secondly, rate of reaction in BMI cured with DCP was higher than the control system, this effect was more pronounced with higher amount of DCP. Finally, the minor secondary reaction peak centered at 250^{o}C was the same as the principle reaction peak in the control system and it was gradually eliminated by increased amount of DCP.

The main results from DSC analysis were reported in Table 2.1. The existence of two reaction peaks in BMI-DCP system was not surprising. The half-life time of DCP was about 6min at 150°C, which was around the onset temperature of the first reaction peak. Thus, it was not hard to understand that the principle reaction peak was shifted to much lower temperature. In order to understand what kind of reaction was going on underneath the first peak, reaction of BMPM and DABPA with 0.5wt% DCP was investigated respectively, as shown in Figure 2.4 and 2.5. For BMPM itself, an endothermic peak was observed which corresponding to the melting of BMPM, followed by an exothermic peak that represented the homopolymerization of the imide double bonds. When BMPM was mixed with 0.5wt% DCP, no more melting peak was observed. Instead, a sharp reaction peak showed right above the original melting peak. This indicated that BMPM was ready to react upon receiving free radicals from DCP. On the other hand, in DABPA-0.5wt% DCP system, an exothermic peak centered on 350°C was observed. It was out of the reaction temperature range in BMI-DCP system. The activation energy for DCP forming free radical was 152kJ/mol while the activation energy for BMPM was 288kJ/mol [9]. The rate of DCP giving out free radicals must be much higher than BMPM itself. Hence, the reaction underneath the first peak of BMI-DCP would consisted mainly by the homopolymerization of the imide bonds accompanied with some copolymerization of imide bonds to allyl bonds.

As the DCP amount increased, this phenomenon was more pronounced. Otherwise the rate of reaction would not be increased but stayed the same. For the second reaction peak of

BMI-DCP, as we know, it was similar to the primary reaction peak in the control system. Thus, reaction underneath this minor secondary peak should be able to form much more uniform network than the reaction underneath the first peak. As shown in Table 2.1, degree of cure at the end of first reaction was significantly increased with higher DCP concentration. It was determined by heat of reaction underneath the first peak over the overall heat of reaction. The secondary reaction peak was gradually eliminated by higher DCP in the system. As a result, the final network would be less uniform due to the rapid low temperature reaction underneath the first reaction peak. In order to obtain the most uniform network structure of BMI-DCP system, only a minor amount of DCP, 0.5wt% was needed to initiate low temperature cure reaction.

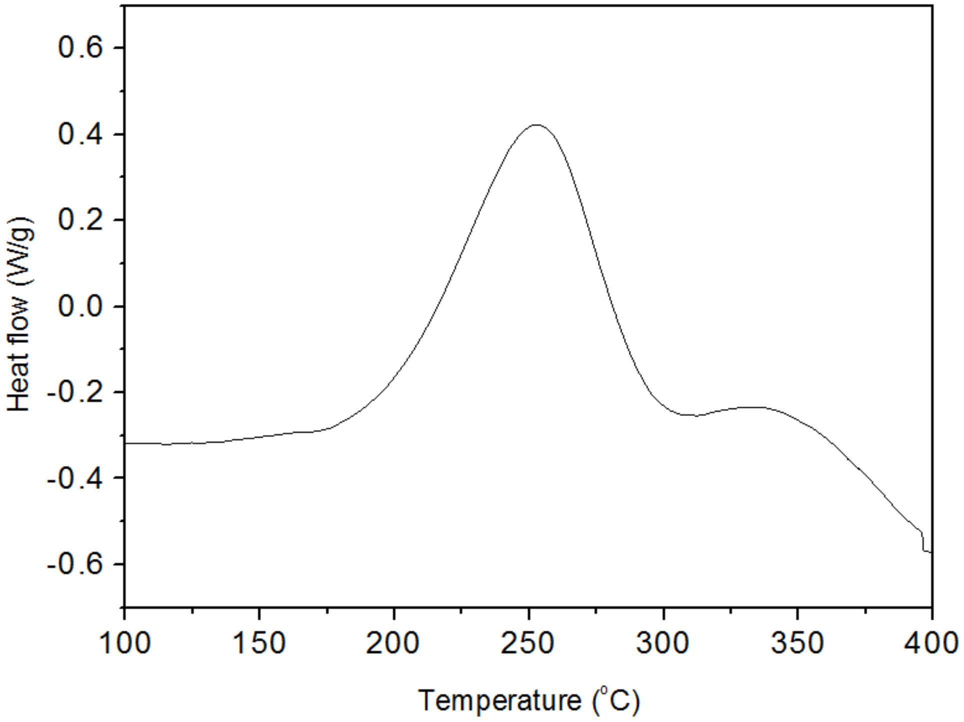

Figure 2.2: Dynamic DSC curve of BMPM/DABPA with a heating rate of 10^{o}C/min

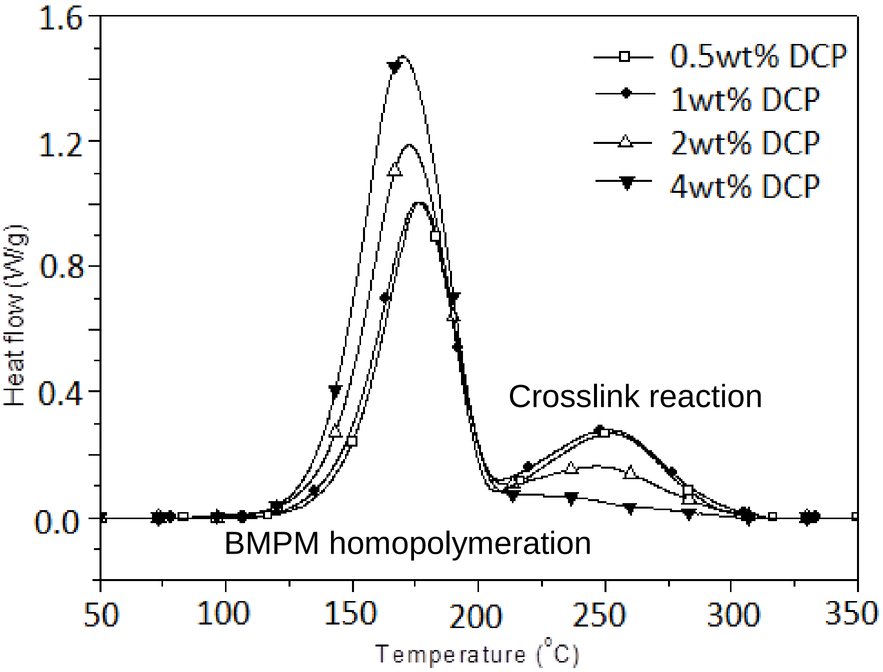

Figure 2.3: Dynamic DSC curves of BMPM/DABPA with different amount of DCP at 10°C/min heating rate

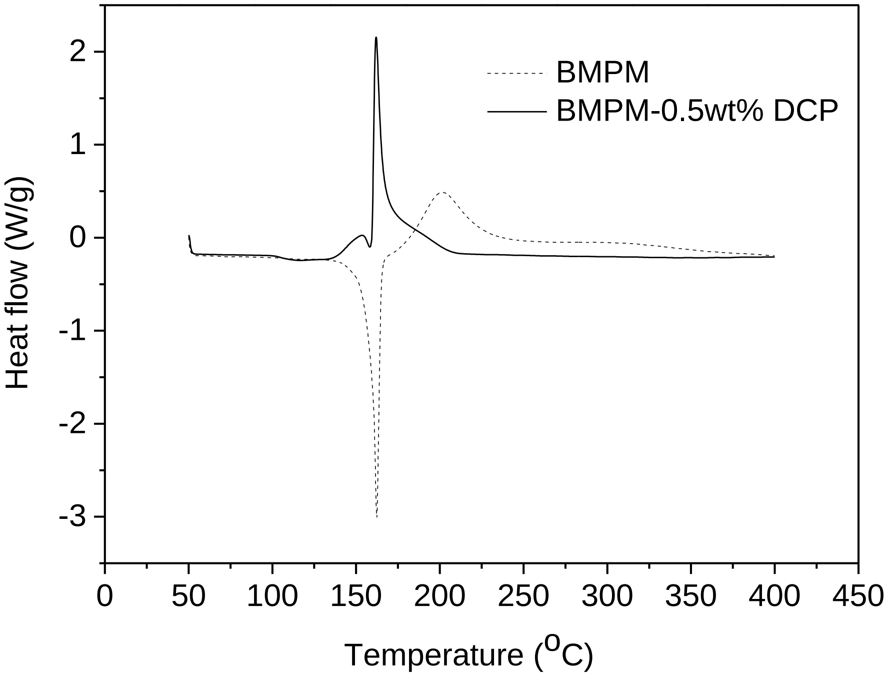

Figure 2.4: Curing profiles of BMPM (dashed line) and BMPM with 0.5wt% DCP (solid line) with a heating rate of 10°C/min

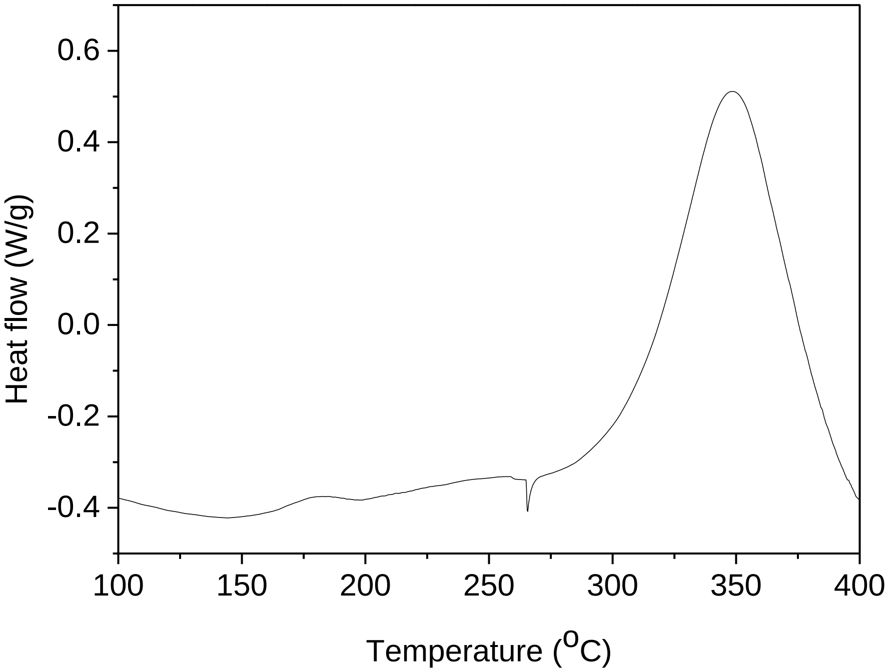

Figure 2.5: Dynamic DSC curve of DABAP with 0.5wt% DCP with a heating rate of 10°C/min

Table 2.1: Maximum temperatures, heat of polymerization determined from DSC analysis for the polymerization of BMI with various amount of DCP

Initiator	wt%	Tp(°C)	ΔHp* (J/g)	α (%)
DCP	0.5	177	213	56
	1	176	233	68
	2	173	291	81
	4	170	330	94

*Principle reaction peak in BMI and BMI with DCP are different from each other, α represents the percent of cure at the end of first reaction peak.

2.3.1.2 Cure cycle determination

The standard curing cycle of BMPM/DABPA was 180^{o}C for 1h, 200^{o}C for 2h and 250^{o}C for 6h. Different type of reaction at different temperature was the rules of choosing these temperature and time. At 180^{o}C, the reaction was mostly “Ene” reaction. When raising the temperature to 200^{o}C, BMPM will form free radicals from the imide bonds dissociation. The homopolymerization of BMPM, copolymerization of DABPA with BMPM occurred at this temperature rage. Curing at 250^{o}C was to complete the crosslink reaction after the system reach gel state.

As learned from the DSC analysis, DCP can initiate the free radical polymerization at much lower temperature as compared to control system. The onset reaction temperature of BMI/DCP systems was chose as the first curing step temperature. Since when preparing the sample, system was heated at 150^{o}C for 30min, “Ene” reaction was mostly completed. Besides, the onset temperature was lower than 180^{o}C, thus the first step of 180^{o}C for 1h to complete “Ene” reaction was eliminated for BMI/DCP systems.

The curing cycle chose for BMI/DCP was 150^{o}C for 2h and 250^{o}C for 6h. The lower curing temperature was to mimic the reaction of control BMI system cured at 200^{o}C. After the major crosslink reaction, the left over reaction at 250^{o}C was the same as control system, thus the same cure temperature and time was chose as the control system.

2.3.2 Effect of DCP content on glass transition temperature of Bismaleimide network

From DSC analysis, the samples were cured at respective onset reaction temperature for 2h and all post cured at 250°C for 6h to obtain samples for DMA tests. Representative DMA results for BMI cured with different content of DCP were shown in Figure 2.6. Tanδ of BMI/DCP system did not show up completely under the test temperature range. Since it was very difficult to determine Tg from the tanδ curve, the onset temperature where G' begins to drop from its glassy state was chose as Tg. However, we still can obtain information from the tanδ curves. The significant decrease and shift of tanδ peak to higher temperature in BMI/DCP system clearly implied that system with DCP had higher crosslink density than control system. Besides, the transition slope of G' decreased and it was independent of initiator concentration. It also implied that crosslink density of BMI/DCP was higher than control one.

Glass transition temperatures of BMI/DCP systems were shown in Table 2.2. An increase of 90°C for sample cured by only 0.5wt% DCP was observed. With higher DCP concentration, Tg was 100°C higher for 1wt% DCP system. However, with higher content of DCP in the system, Tg started to drop slight. When 4wt% DCP was added into the BMI system, Tg was dropped to a value even slightly lower than 0.5wt% DCP system. This may due to the chain transfer or termination of DCP initiator when there was too much free radical in the system because the possibility of chain with free radical combining with each other and terminating the polymerization was increased. As a result, the network crosslink density could be decreased. Nonetheless, this much higher Tg was another confirmation of rapid homopolymerization of imide bonds at the low temperature, which gave the network a tighter crosslink network. As we know that BMPM when cured by itself without any co-reactants would result with much higher Tg around 400°C [11]. Moreover, the storage modulus (G') was always higher for BMI-DCP system compared with the control network, which was also an indication of a stiffer network.

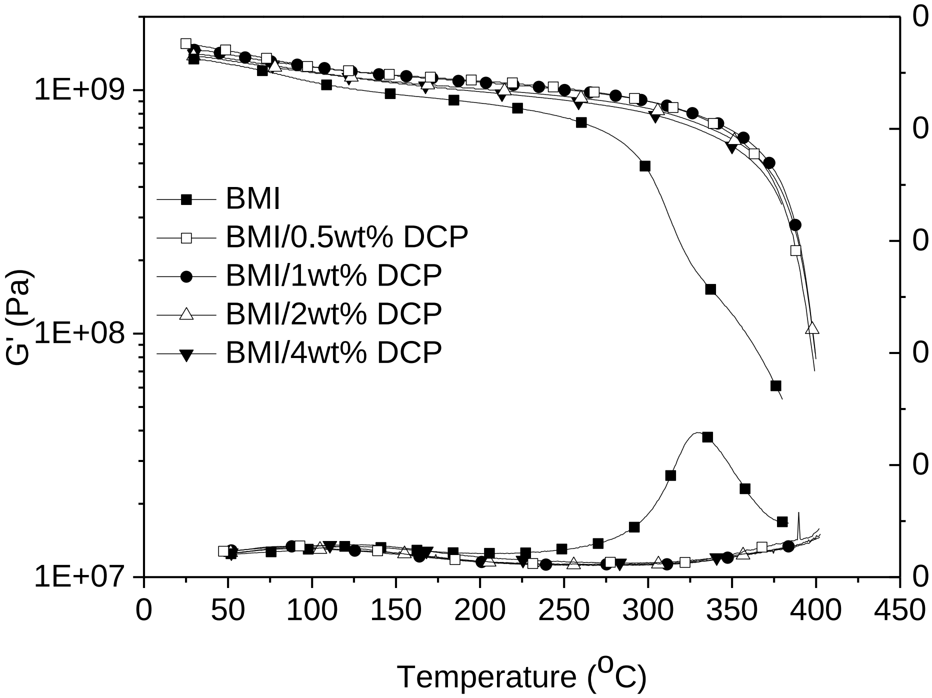

Figure 2.6: Shear modulus (G') and tanδ versus temperature for BMI control system, BMI with 0.5, 1, 2 and 4wt% DCP

Table 2.2: Glass transition temperatures of BMI control system and BMI with 0.5, 1, 2 and 4wt% DCP

System	Initiator content wt%	Tg (ºC)
Control	0	280
With DCP	0.5	373
	1	380
	2	377
	4	368

2.3.3 Effect of DCP on thermal stability of Bismaleimide network

Figure 2.7 showed TGA curves of BMI cured with 0.5, 1, 2 and 4wt% DCP. In all cases, single-step decomposition was observed. This implied that curing with initiator did not change the decomposition mechanism. The thermal degradation temperatures at different values of weight loss are listed in Table 2.3. T_{d1}, T_{d2}, T_{d3} and T_{d4} are defined as the temperature at 5, 10, 15 and 20% weight loss, respectively. Thermal stability of the BMI network cured with DCP is independent of the initiator content. Figure 2.8 shows derivative of TGA weight loss versus temperature. The slope of the curve indicates weight loss rate of the system and the peak value of the curve represents the maximum weight loss rate in the system. At the very beginning of degradation, the rate of degradation for BMI cured with initiator was lower than the control system. However, when temperature reaches the onset degradation temperature that is 430°C, the weight loss rate as well as maximum weight loss rate of BMI cured with initiator was mostly higher than control system. Again, weight loss rate was independent of the amount of initiator in the system. This phenomenon also implied that the crosslink density of BMI cure with DCP was higher than the control system, which gave the system higher onset degradation temperature and lower weight loss rate at lower temperature. However, with initiator addition, fast polymerization of maleimide made the system crosslink junctions not as uniform as the control one. As a result, degradation of BMI cured with initiator occurs much more rapidly upon heating.

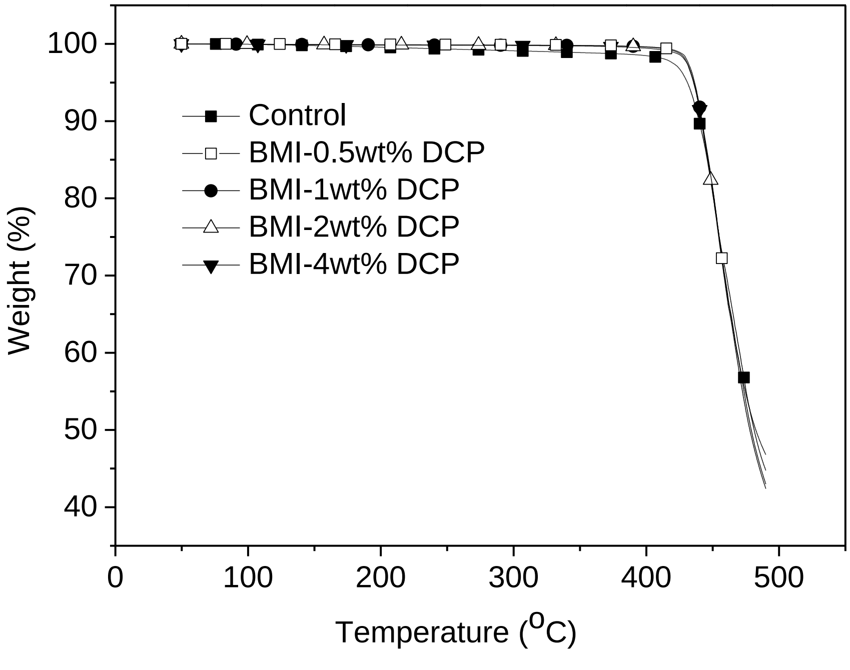

Figure 2.7: TGA profiles of BMI control and BMI with 0.5, 1, 2 and 4wt% DCP

Table 2.3: Degradation temperatures of cured BMI with DCP system at different values of weight loss

DCP (wt%)	T_{d1}(°C)	T_{d2}(°C)	T_{d3}(°C)	T_{d4}(°C)
0	431	439	445	450
0.5	435	441	446	451
1	436	442	447	451
2	435	441	446	451
4	436	442	447	451

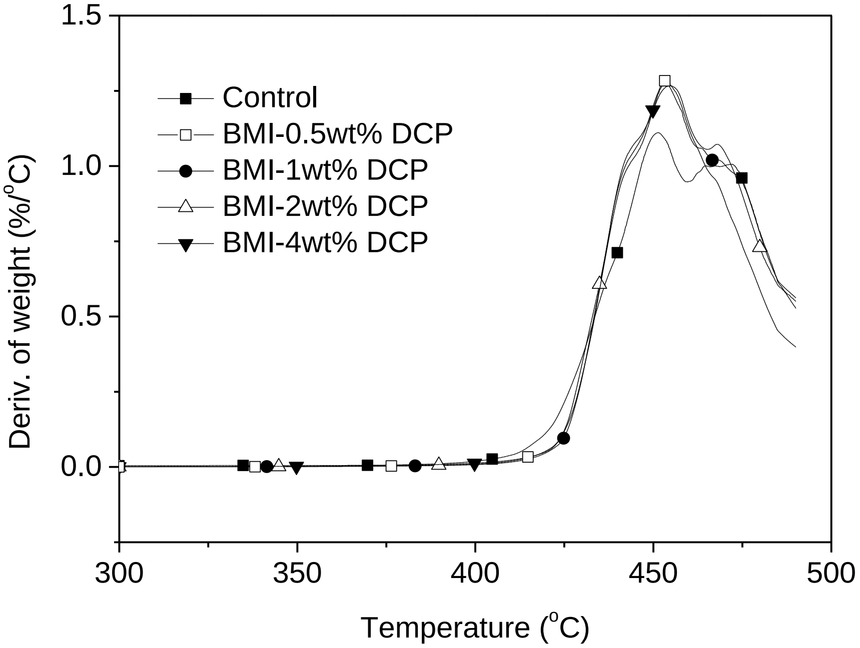

Figure 2.8: Derivative of TGA curves of BMI cured with 0.5, 1, 2 and 4wt% DCP

2.3.4 Effect of DCP on moisture absorption of Bismaleimide network

Moisture uptake into a polymer matrix can give indicative information about the network structure characteristic. Studies have been shown that thermosets with lower crosslink density will absorb less moisture as compared to higher crosslink network [13-14]. As from the above thermal mechanical analysis, BMI cured with 0.5wt% DCP were chosen as representative networks for moisture uptake study. Figure 2.9 display water uptake curves as a function of the square root of time normalized to the specimen thickness. The equilibrium moisture content of control system is higher than system cured with initiator. This result is contradictory to previous studies that network with higher crosslink density will absorb more moisture. Our postulation for this phenomenon is that when BMI cured with initiator, fast polymerization of maleimide make the system crosslink junctions not as uniform as the control one. Thus some area in the network is highly crosslinked while some area is less crosslinked. As a result, water molecules will not be all trapped or locked into molecular cages and can diffuse out of the system from less crosslinked area. This is very important to composite materials which upper service temperature will reduce significantly when moisture locked in.

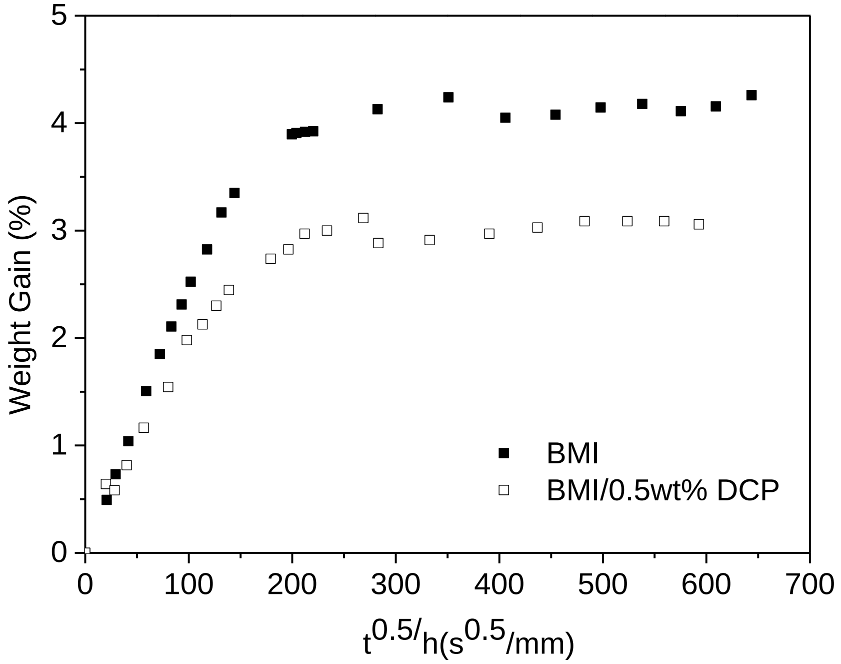

Figure 2.9: Moisture absorption curves of BMI control system and BMI with 0.5wt% DCP

2.3.5 Molar ratio effect of BMPM to DABPA on Bismaleimide cured with DCP

2.3.5.1 Cure reaction of BMPM/DABPA with off stoichiometric ratio by DSC study

In order to further understand the reaction mechanism of BMI with DCP initiator, different BMPM to DABPA molar ratio system was prepared. The hypothesis of the research was that if the first reaction peak was mostly related with BMPM, then the rate and heat of reaction for the first primary reaction peak would be affected. With more BMPM in the system, more imide bonds were available for homopolymerization. As seen in Fig 2.4, BMPM self-polymerization showed a very sharp reaction peak. Thus, the rate of polymerization of BMPM rich system should be faster than the control system that is 1 to 1 molar ratio system. On the other side, when more DABPA was in the system, the first peak reaction should not be affected since it mostly concerns with BMPM. Dynamic DSC runs of these off stoichiometric ratio system were shown in Figure 2.10. Heat of reaction and first reaction peak temperature were summarized in Table 2.4. Higher heat of reaction and degree of cure for BMPM rich system was observed which was expected. However, the degree of cure at the end of first peak was slightly higher in DABPA rich system than 1 to 1 molar ratio system. Although the first reaction was mostly concerned with BMPM, crosslink reaction of BMPM to DABPA will also occur at certain degree. The left over DABPA and BMPM will undergo the secondary reaction peak. Under this peak, the source of free radical was no longer coming from DCP. It was self-polymerization by BMPM. Thus, the secondary reaction peak temperature was the same as BMPM-DABPA control system. As a result, higher amount of DABPA gave the opportunity to incorporate more DABPA into the network other than allowing BMPM fast homopolymerization with DCP addition. So, higher amount of DABPA in the system ideally would give the BMI/DCP system better homogenous network than control system.

Table 2.4: Maximum temperatures, heat of polymerization determined from DSC analysis for the polymerization of BMI with 0.5w% DCP and different molar ratio of BMPM to DABPA

BMPM to DABPA	Tp(°C)	ΔHp* (J/g)	α* (%)
1 to 1	181	130	56
1.5 to 1	179	169	68
1 to 1.5	180	128	63

*α represents the percent of cure at the end of first reaction peak

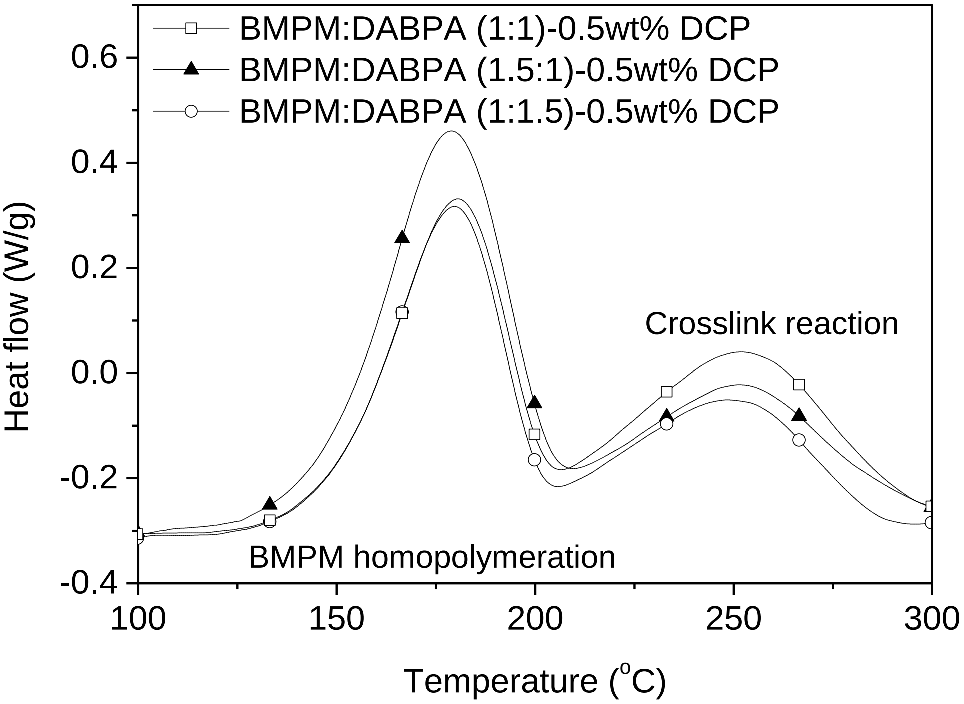

Figure 2.10: Dynamic DSC curves of BMPM to DABPA molar ratio at (1 to 1, 1 to 1.5 and 1.5 to 1) with 0.5wt% DCP at heating rate of 10°C/min

2.3.5.2 Glass transition temperature affected by molar ratio change

DMA of different BMPM to DABPA molar ratio system with 0.5wt% DCP was also investigated, as shown in Figure 2.11. It was obviously that BMPM rich system had relatively higher Tg than control system while DAPBA rich system showed lower Tg as determined from G’ curve. This was under expectation that when BMPM rich in the system, the final network should have higher crosslink density as validated by previous researchers that BMPM self-polymerization would result in very high crosslinked and brittle network as well as high Tg around 400^{o}C. From the tand curve, one broad peak was observed in DABPA rich system with a peak temperature around 200^{o}C. This could be due to the unreacted DABPA in the network since 1 to 1.5 molar ratio of BMPM to DABPA was much higher than previous researcher and industrial’s investigation of 1 to 1.15. Glass transition temperature of these three systems was shown in Table 2.5. With result again confirmed the hypothesis that with more BMPM in the system, higher crosslink density should be and 10^{o}C higher Tg was observed also. When DAPBA was rich in the system, about 10^{o}C lower Tg was observed when compared with 1 to 1 molar ratio system. This result also confirmed the hypothesis that the higher amount of DABPA gave the opportunity to incorporate more DABPA into the network other than allowing BMPM fast homopolymerization with DCP addition. So, higher amount of DABPA in the system ideally would give the BMI/DCP system better homogenous network than control system.

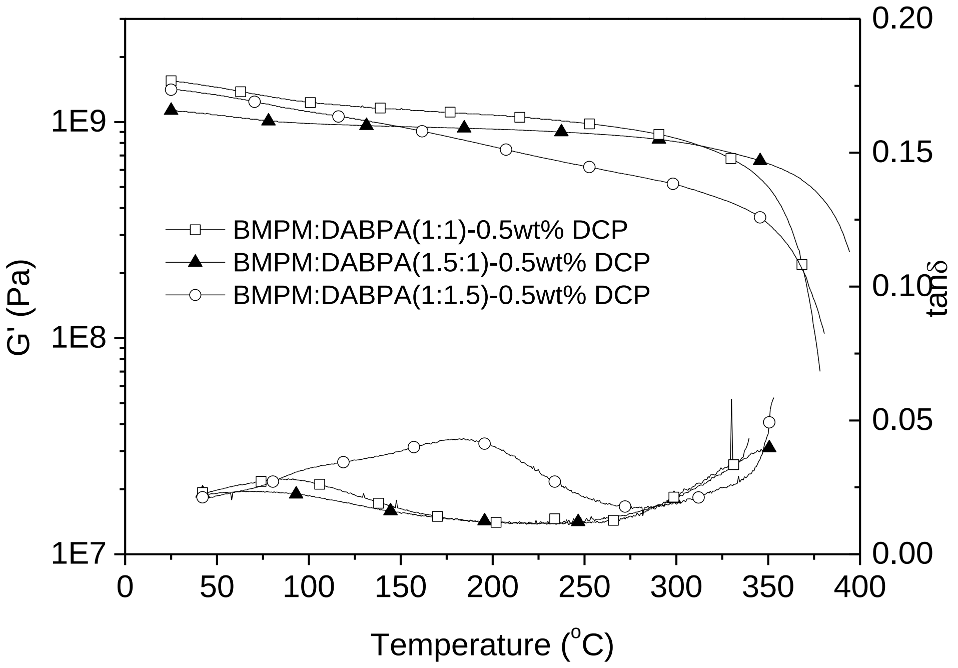

Figure 2.11: Shear modulus (G') and tanδ versus temperature for BMI with 0.5wt% DCP varying in BMPM to DABPA molar ratio

Table 2.5: Glass transition temperature of BMI with 0.5wt% DCP varying in BMPM to DABPA molar ratio

BMPM-DABPA-0.5wt% DCP	Tg (°C)
1:1	373
1.5:1	383
1:1.5	364

2.3.5.3 Thermal stability affected by molar ratio change

Effect of resin molar ratio on degradation of BMI network was shown in Figure 2.12. In all cases, single-step decomposition was observed. This implied that changing resin molar ratio did not change the decomposition mechanism. The thermal degradation temperatures at different values of weight loss are listed in Table 2.6. T_{d1}, T_{d2}, T_{d3} and T_{d4} are defined as the temperature at 5, 10, 15 and 20% weight loss, respectively. As can be seen from the figure and table, the degradation temperature of BMPM rich system showed relatively higher onset of degradation temperature as well as higher char yield at the end of the experiment. The higher content of BMPM will give the network high degree of crosslink density. As a result, the polymer chain was relatively stable at the onset of degradation.

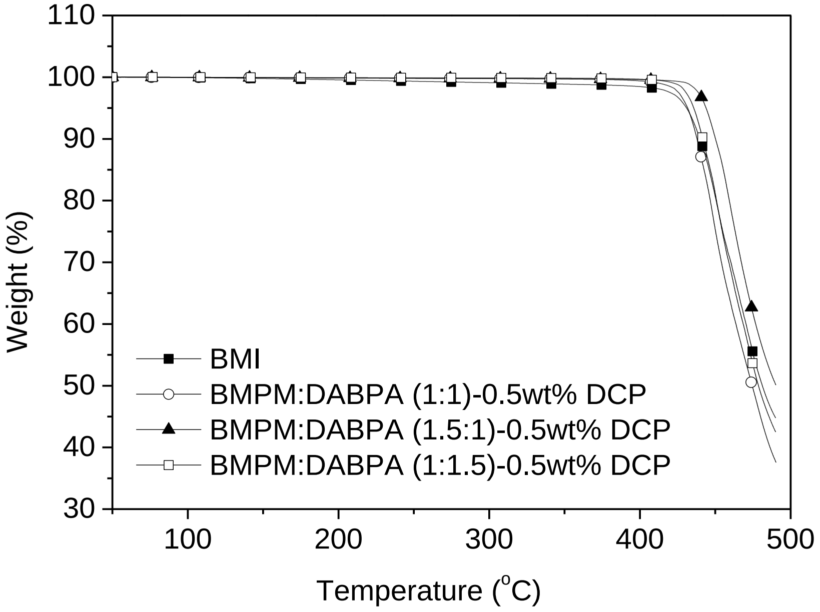

Figure 2.5: TGA profiles of BMI with 0.5wt% DCP varying in BMPM to DABPA molar ratio

Table 2.6: Degradation temperatures of cured BMI/DCP network at different temperatures of weight loss

BMI/0.5wt% DCP	T_{d1}(°C)	T_{d2}(°C)	T_{d3}(°C)	T_{d4}(°C)
1:1	435	441	446	451
1:1.5	432	438	442	446
1.5:1	443	450	455	459

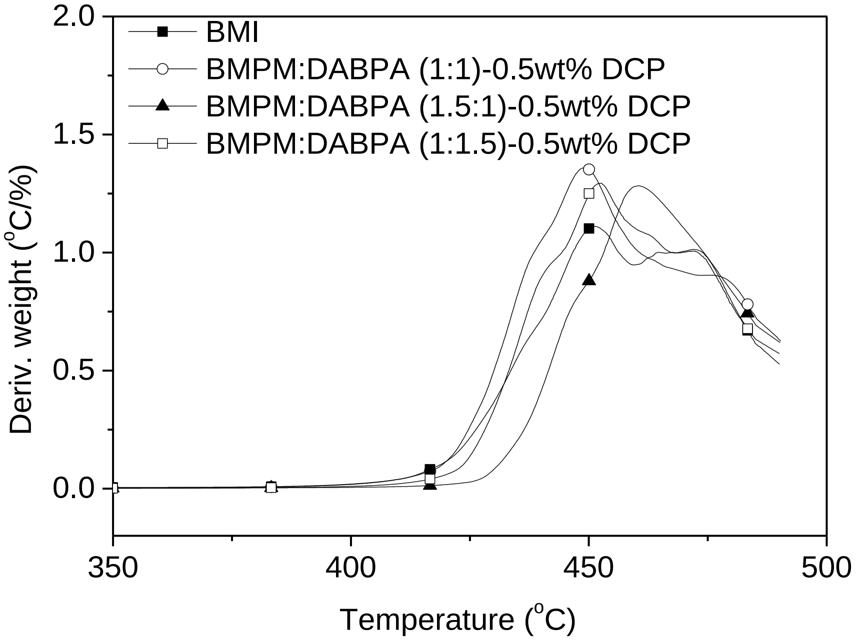

Figure 2.6: Derivative of TGA curves for BMI with 0.5wt% DCP varying in BMPM to DABPA molar ratio

The derivative of degradation curves of BMI system varying BMPM to DABPA molar ratio with 0.5wt% DCP were shown in Figure 2.13. The slope of the derivative curve represents the rate of degradation over temperature. It can be seen from the figure that DABPA rich system showed relatively higher rate of degradation than the other systems. This was possibly due to the left over unreacted DABPA in the system. As learned from above DMA study that, the DABPA rich system showed a tanδ peak around 200^{o}C, which also indicated the dangling chain of DABPA in the network without crosslinked into the system. On the other hand, BMPM rich system had higher onset degradation temperature than the other three systems. This was due to the reason that DCP favors BMPM homopolymerization that gave the system higher degree of crosslink density.

2.4 Conclusions

A series of BMI network catalyzed by DCP were studied to determine the effect of DCP and DCP concentration on the cure reaction and thermal characteristics of BMPM/DABPA based thermosets. It was shown that the addition of DCP significantly lowered the onset cure temperature of BMI network up to 50^{o}C. The rate of curing was much faster when the system was initiated by DCP. This phenomenon indicated that fast crosslink reaction might be introduced by the addition of DCP. With higher amount of DCP, more chemical reaction occurred at the lower temperature range, 150-200^{o}C, while reaction at higher temperature, 200-300^{o}C, was inhibited. This implied that DCP favors BMPM crosslink reaction and the etherification of DABPA was inhibited also. DMA analysis shows that shear modulus and crosslink density of BMI cured by DCP was significantly higher than control system. Tg was significantly increased even with only 0.5wt% initiator in the system. Thermal stability of BMI was independent of the DCP concentration. Although onset of degradation temperature of initiator system was slightly higher than the control, the degradation rate was mostly higher than the control. This might be due to the un-homogeneity of network by DCP addition. As for moisture uptake, it was significantly lower for BMI/DCP system, which was also related with the un-homogeneity of the network. The water molecular can move out of the system rather than locked in the network. Overall, thermal properties of BMI were enhanced with DCP addition. A minor amount of initiator is sufficient for improving the thermal and moisture uptake properties of BMI network.

When BMI system was BMPM rich, the glass transition temperature and degradation behavior was further enhanced as compared to BMPM to DABPA stoichiometric ratio with 0.5wt% DCP network. It was again due to the amount of crosslink reaction initiated by DCP was higher when more BMPM was rich in the system. When DABPA was rich in the system, both DMA and TGA data showed that BMI network had deteriorated thermal property. To sum up, DCP can efficiently initiate the crosslink reaction in BMI thermoset. With more BMPM in the system, higher crosslink density would be achieved, thus result in enhanced thermal properties.

REFERENCES

REFERENCES

1. Ghosh, M.K. and Mittal, K.L. Polyimides: Fundamentals and applications. New York: Marcel Dekker, Inc., 1996.

2. Wilson, D, Stenzenberger, H.D and Hergenrother, P.M., Polyimides. New York: Chapman and Hall Inc., 1990.

3. Lin, S.C. Pearce, E.M. High performance thermosets. New York: Hanser Publishers, 1993.

4. Seris, A., Feve, M., Mechin, F. and Pascault, J.P. Thermally and anionically initiated cure of bismaleimide monomers, Journal of applied polymer science, vol. 48, pp257-269, 1993.

5. Boris, A.R., Emma, A.D., Roger, J.M. and Eugene, E.S. The polyaddition, chain and polycondensation mechanisms of formation of networks based on bismaleimides, Macromolecular symposia, vol.171, pp87-96, 2001.

6. Boris, A.R, Emma, A.D., Roger, J.M. and Eugene, E.S. High-performance bismaleimide matrices: cure kinetics and mechanism, Polymers for advanced technologies, vol.13, pp837-844, 2002.

7. Thomas, M.D. and David, R. Relationships in a bismaleimide resin system. Part I: cure mechanisms, Polymer engineering and science, vol.32, pp409-414, 1992.

8. David, B.C., Brett, A.C. and James, M.C. Cure reaction pathways of bismaleimide polymers: a solid state NMR investigation, Macromolecules, vol.31, pp6776-6782, 1998.

9. Mijovic, J. and Andjelic, S. Study of the mechanism and rate of bismaleimide cure by remote in-situ real time fiber optic near-infrared spectroscopy, Macromolecules, vol.29, pp239-246, 1996.

10. Roger, J.M., Eugene, E.S. and Jason, E.L. Thermal properties of high temperature polymer matrix fibrous composites, Handbook of thermal analysis and calorimetry. Ed. Cheng S.Z.D. Vol 3. Elsevier science, 2002.

11. Boey, F., Xiong, Y., Rath, S. K. Glass transition temperature in the curing process of bismaleimide modified with diallyl bisphenol A, Journal of applied polymer science, vol.91, pp3244-3247, 2004.

12. Venditti, R.A and Gillham, J.K. A relationship between the glass transition temperature (Tg) and fractional conversion for thermosetting systems, Journal of Applied Polymer Science, vo.l64, pp3-14, 1998.

13. Morgan, R.J., Kong, F.M. and Walkup, C.M., Structure-property relations of polyether-triamine-cured bisphenol-A-diglycidyl ether epoxy, Polymer, vol. 25, pp375-386, 1984.

14. Barton, J.M., Effect of absorbed water on the thermal relaxation of biaxially stretched-crosslinked Poly (methyl methacrylate), Polymer, vol.20, pp8-1024, 1979.

15. Stenzenberger H., Polyimides in structural adhesives, A. J. Kinloch, Ed., Elsevier, London, 1986.

16. Varma, I.K., Gupta, S.P., and Varma, D.S., Effect of triallyl cyanurate on the properties of bismaleimide, Journal of applied polymer science, vol.33, pp151-164, 1987.

17. Kwiatkowski, G.T., Robeson, L.M. and Bedwin, A.W., Thermosetting diphenyl sulfone -based maleimides, Journal of polymer science: polymer chemistry edition, vol.13, pp961-972, 1975.

18. Acevedo, M., Abajo, J.D. and Campa, J.G., Kinetic study of the crosslinking reaction of flexible bismaleimides, Polymer, vol.31, pp1955-1959, 1990.

CHAPTER 3: CURING AND THERMAL PROPERTIES OF 4, 4'-BIS-MALEIMIDODIPHENYLMETHANE AND O, O'-DIALLYL BISPHENOL A BASED BISAMLEIMIDE NETWORK ASSISTED BY TRIGONOX PEROXIDES

3.1 Introduction

Heat resistant bismaleimide resin has been widely used in circuit board, aerospace application as polymer matrix for composite materials [1-12]. The crosslink reactions of bismaleimide resin generally need high temperature above 200°C [13, 14]. Network formed by pure maleimide is very brittle. As a result, co-reactants are usually used to modify bismaleimide. Generally, aromatic diamine or diallyl compounds can react with bismaleimide ending with chain extensions that can reduce crosslink density of the network.

The effect on obtaining a curing agent serving as initiator for free radical polymerization of high performance polymers has been research since the 1970s [15-20]. The choosing of initiator depends on decomposition rate of peroxides that is the primary factor during application. Generally, the initiator should be dispersed into the polymer before the final processing stage. Then the system goes through thermal cure to crosslink the polymer. As for the initiator, it should produce free radicals without the generation of volatiles. It also should be compatible with the polymer in order to molecular dispersed into the network. At last, it should be stable at room temperature for easy storage and handling.

Typically, two-step decomposition process will occur in peroxides with the formation of strong abreacting alkoxy radical. Dicumyl Peroxides (DCP) discussed in Chapter 2 was a commonly used initiator in free radical initiated polymerization system. However, when used in bismaleimide thermosets, it tends to increase the crosslink density of the network due to fast homopolymerization of BMPM [16]. Thus, it was critical to find a initiator that can initiate the reaction at low temperature while do not intend to create high crosslink density in the thermoset. Several researchers have investigated Trigonox initiator in polyethylene and polypropylene. It was found that besides free radical initiation step, 2,5-Dimethyl- 2,5-di(tert-butylperoxyl) hexane (Trigonox® 101) and 3,6,9-Triethyl-3,6,9,- Tri-methyl-1,4,7-triperoxonane (Trigonox®301) have also been shown its ability in abstract H bonds on polymer backbone and inducing branching in polymer chain or possible crosslinking reaction [21-23]. Thus, it is possible that Trigonox®101 and 301 can abstract H bonds in DABPA, incorporating more DABPA into the network as compared to other free radical initiators, such as dicumyl peroxide. In this work, we will evaluate the influence of Trigonox®101 and 301 on the reaction as well as thermal and mechanical properties of final Bismaleimide Thermoset. Resin ratio was changed from 1 to 1 stoichiometric molar ratio to BMPM rich or DABPA rich system to study the reaction and properties in these systems with Trigonox®101. This kind of study was an important step for process optimization as well as for the understanding of structure-property relations in the final network. The primary objective of this chapter study was to understand the effect of Trigonox initiators on curing kinetic of BMI. As a result, how this different curing process as compared to the original BMI system affected the final network.

3.2 Experimental Techniques

3.2.1 Materials

The Bismaleimide resin (BMI) utilized was the Matrimid®5292 system (Huntsman Co.) consisted by 4, 4'- Bismaleimidodiphenyl Methane (BMPM) and O, O'- Diallyl Bisphenol A (DABPA) monomers at controlled stoichiometric molar ratio of 1 to 1. 2,5-Dimethyl-2,5-di(tert-butylperoxyl) hexane (Trigonox®101) and 3,6,9-Triethyl-3,6,9,-trimethyl-1,4,7-triperoxonane (Trigonox®301) (AkzoNobel Co.) were added into the BMI thermoset respectively. Besides, off stoichiometric molar ratio of BMPM to DABPA was investigated with fixed amount of TrigonoX®101 and 301. The amount was controlled at 0.3wt% for Trigonox®101 and 0.2wt% for 301, while the molar ratio of BMPM to DABPA was chose at 1 to 0.87 and 0.87 to 1, which represented BMPM rich and DABPA rich system. All chemical compounds were used as received with no further purification. A schematic drawing of these components was depicted in Figure 3.1.

3.2.2 Sample preparation

The amber viscous liquid of DABPA monomers was poured into a glass beaker with magnetic stir bar. It was heated on a hot plate at 150°C until the viscosity decreased. Corresponding amount of yellow crystalline BMPM powder was then added in slowly stirred for about 30min until a homogenous solution was obtained. The mixture was cooled down to 100°C, Trigonox initiator was added and quickly stirred in until dissolved. Finally, BMI resin panels were prepared by pouring the mixture into aluminum round disk. All panels containing were cured in a convention air oven at 150^{o}C for 2h and 230^{o}C for 6h while samples containing 301 were cured at 170^{o}C for 2h and 230^{o}C for 6h.

A diamond saw was utilized to cut cured BMI resin panel into desired size. Surface oxidation and porosity on the resin were removed by polishing with grit paper. The final specimen thickness was around 1.5mm. All samples were then cleaned with de-ionized water, followed by drying in a convention air oven at 80^{o}C until no weight change.

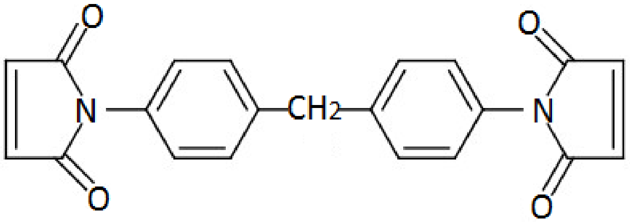

4,4’-bismaleimidodiphenylmethane (BMPM)

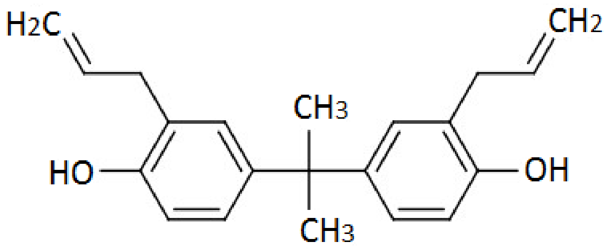

O, O’-diallyl bisphenol A (DABPA)

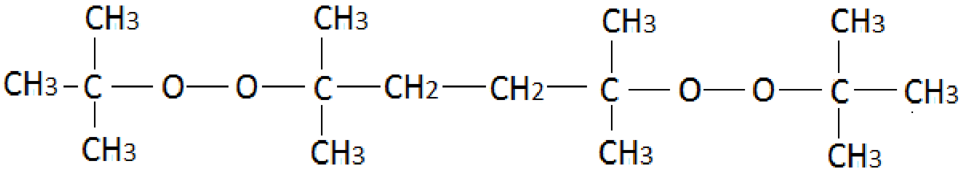

2,5-Dimethyl-2,5-di(tert-butylperoxyl) hexane (Trigonox$^{®}$101)

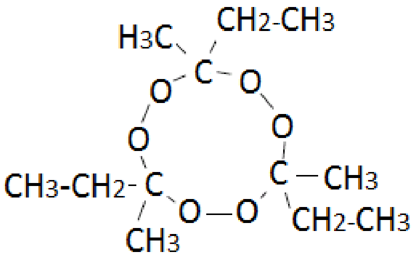

3,6,9-Triethyl-3,6,9,-trimethyl-1,4,7-triperoxonane (Trigonox$^{®}$301)

Figure 3.1: Schematic structure of BMPM, DABPA, Trigonox$^{®}$101 and 301

3.2.3 Characterization Techniques

Differential Scanning Calorimetry (DSC) analysis was studied using around 10mg mixture in a Mettler Toledo DSC-1. Dynamic heating rates of 10°C/min were used to determine the heat of reaction during curing process. The heating range was from 50-350°C with nitrogen gas at a flow of 50ml/min. The assumption of DSC analysis was that the area underneath the curves is proportional to the extent of reaction. The extent of cure α at any time was defined as

$$\alpha = \frac{\Delta H}{\Delta Hr}$$

where ΔH is the partial heat of reaction at any determined time while ΔH_r is the overall heat of reaction.

Dynamic Mechanical Analysis (DMA) was carried out on a Rheometric Solid Analyzer III with a 350g transducer. Cured samples were cut into rectangular bars with a width of 5mm and thickness of 1.5mm. Torsion mode was applied to the sample. Experiments were performed from 50 to 400°C at the frequency of 10rad/s with 5°C/min heating rate. From the DMA spectra, change in shear modulus, G’, as a function of temperature can be obtained. Tg was determined as the temperature when maximum drop of G’ occurs.

Thermal gravimetric analyzer, TA Q500, was used to investigate the thermal and oxidative stability of the BMPM/DABPA/DCP thermosets. All the thermal analysis was conducted from room temperature to 500°C at a heating rate of 20°C/min. The onset degradation temperature was determined as the temperature at 5wt% weight loss.

Moisture uptake of the network was also under investigation. Before moisture absorption test, all specimens were dried at 80°C in a convention air oven until no weight change observed. The moisture absorption was conducted by submerging the specimens in 50°C and 80°C de-ionized water baths. The water absorption was monitored gravimetrically according to the following equation:

$$M_t = \left(\frac{W - W_i}{W_i} \right) \times 100$$

where M_t is the weight gain percentage at time t, W_i represents the initial weight (dry weight) at time zero and W is the weight of the specimen at time t.

Before record the moisture uptake of the specimen, the specimens were gently wiped with lint-free paper towels to remove excess water. A Mettler balance with 0.1mg precision was utilized to record the weight change.

3.3 Results and Discussion

3.3.1 Effect of Trigonox® 101 and 301 on reaction mechanism in Bismaleimide network

3.3.1.1 Cure reaction of Bismaleimide with Trigonox® 101 and 301 by DSC study

As discussed in the last chapter with the DCP system, only a minor amount of initiator would be enough for initiating the cure reaction of BMI thermoset. Thus, 0.3wt% Trigonox® 101 and 0.2wt% Trigonox® 301were added into BMI resin in order to maintain the same molar ratio of free radicals as the system cured with 0.5wt% DCP. The reaction profile of BMI with

Trigonox®101 and 301 was shown in Figure 3.2. The detailed reaction data was summarized in Table 3.1.

For Trigonox®101, two major reaction peaks were observed. The first peak of Trigonox® 101 was centered at 187°C. Similar to the reaction in BMI-DCP system, the reaction under this first peak should be mostly related with the homopolymerization imide bonds of BMPM. It was obviously that the rate of reaction for the first peak was much lower than BMI-DCP system. This would be due to the efficiency of Trigonox®101 radicals transferring to imide bonds. Since Trigonox®101 has two possible free radical formation sites. The Trigonox®101 free radicals may not all decomposed and transferred to the imide bonds. Besides, due to the hydrogen abstracting nature of the Trigonox®101, it was postulated that Trigonox®101 can abstract hydrogen from the allyl bond leading to crosslink reaction of allyl to imide bonds. All of these factors could be contributing to the slowed down homopolymerization of BMPM. The second reaction peak of BMI-Trigonox®101 system was centered at the same temperature as the control system. Besides, an overlapping of the first and second reaction peaks was observed. Moreover, the heat of reaction underneath the second peak was even higher than the first one. This again indicated that the crosslinking reaction initiated by Trigonox®101 did not involve too much rapid homopolymerization of imide bonds, otherwise there would not exist that this even higher secondary reaction peak under which the reaction was initiated by imide bond itself.

For BMI with Trigonox®301 system, three reaction peaks were observed. The first peak of Trigonox®301 was centered at 202°C, which was higher than both DCP and Trigonox®101. This was due to the fact that the initiation temperature of Trigonox®301 was the highest among these three initiators. The second reaction peak of Trigonox®301 system was again centered at the same temperature as the control system. Beside, a more pronounced overlapping of the first two peaks was observed. This indicated that Trigonox®301 was most mild initiator in this study. It did not efficiently initiate homopolymerization of imide bonds. Thus, quite a few imide bonds were leftover to react at higher temperature. Last but not the least was the third reaction peak which was centered the same as the secondary peak of the control system. This occurrence of third peak was not surprising since Trigonox®301 did not efficiently initiate the first reaction, the left over reaction should follow the reaction route of the control system. For the reaction underneath the third peak, it was principally etherification reaction of hydroxyl groups from DABPA. As with BMI thermosets, this further crosslink reaction was not favored since it would create a higher crosslink density of the network resulting with brittle mechanic properties [11].

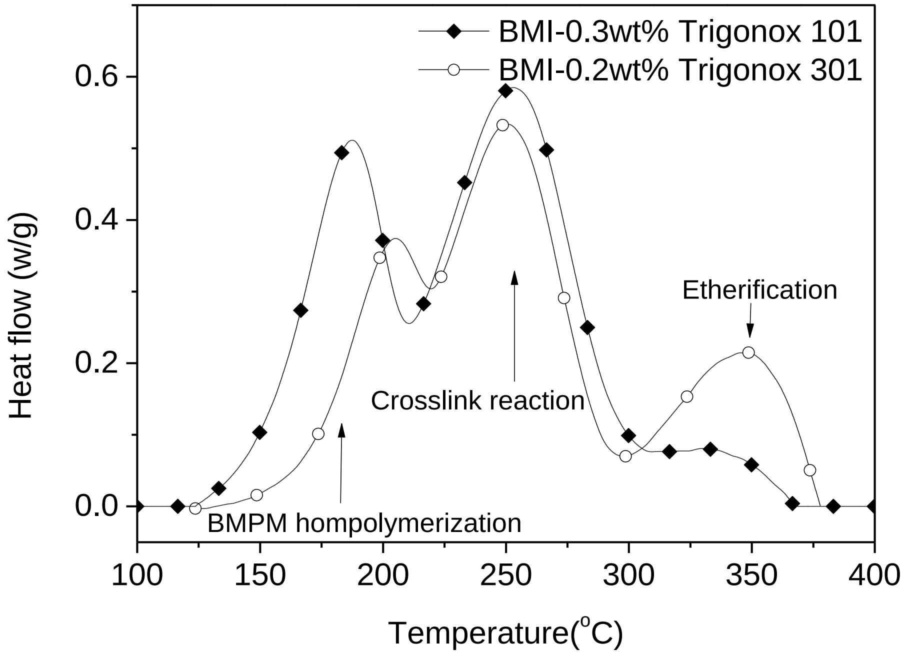

Figure 3.2: Reaction DSC profile of BMI-0.2wt% Trigonox®301 and 0.3wt% Trigonox®101 with a heating rate of 10°C/min

Table 3.1: Maximum temperatures, heat of polymerization determined from DSC analysis for the polymerization of BMI with Trigonox®101 and 301

Initiator	wt%	Tp(°C)	ΔHp* (J/g)	α (%)
Trigonox®101	0.3	188	124	37
Trigonox®301	0.2	203	159	33

*Principle reaction peak in BMI with Trigonox®101 and 301 are different from each other,

α represents the percent of cure at the end of first reaction peak.

3.3.1.2 Reaction affected by the amount of Trigonox® 101 and 301 in Bismaleimide network

Higher amount of Trigonox initiators was investigated with BMI in order to further understand the reaction mechanism. For both Trigonox® 101 and 301 systems, 2wt% initiators were added into the resin. Although the molar ratio of initiators might be a little different between these two systems, it still can give information about the reaction affected by the amount of initiators in the system. Dynamic DSC curve of BMI with 2wt% Trigonox® 101 and 301 was shown in Figure 3.3. Two reaction peaks were shown in both initiator systems.

For Trigonox® 101, the first reaction peak was much higher than the secondary reaction peak. This phenomenon was about the same as BMI with 0.5wt% DCP. As discussed above, Trigonox® 101 initiated the first reaction peak and leftover unreacted imide bonds of BMPM initiated the secondary reaction peak. When higher amount of Trigonox® 101 in the system, there were enough free radical provided by the initiators to initiate the crosslink reaction, thus less BMPM was left for the second reaction to move on. Although Trigonox® 101 can abstract H from allyl, homopolymerization of imide bonds would be favored. The higher rate of reaction was also an indication of faster polymerization rate. As discussed before, this high degree of polymerization by initiator will result in much higher crosslink density that is not necessary the best way for thermoset system design.

For BMI/Trigonox® 301 system, the third reaction peak was eliminated when higher amount of initiator was in the network. This was clearly due to the sufficient amount of initiator in the system. Although the reaction peak was eliminated, the rate of polymerization was still lower than Trigonox®101 when comparing the first reaction peak. Besides, the reaction peak temperature was higher than BMI/Trigonox®101 system as well. This was due to the fact that Trigonox®301 has relatively higher degradation temperature than Trigonox®101. As a result, the onset reaction temperature was also higher than BMI initiated by Trigonox®101. In general, Trigonox®301 was a mild initiator when compared to Trigonox®101. However, when using only a minor amount of initiator in BMI, Trigonox®301 was too mild that it was not efficiently initiating the reaction. Thus, Trigonox®101 was selected as the main initiator to study in this chapter.

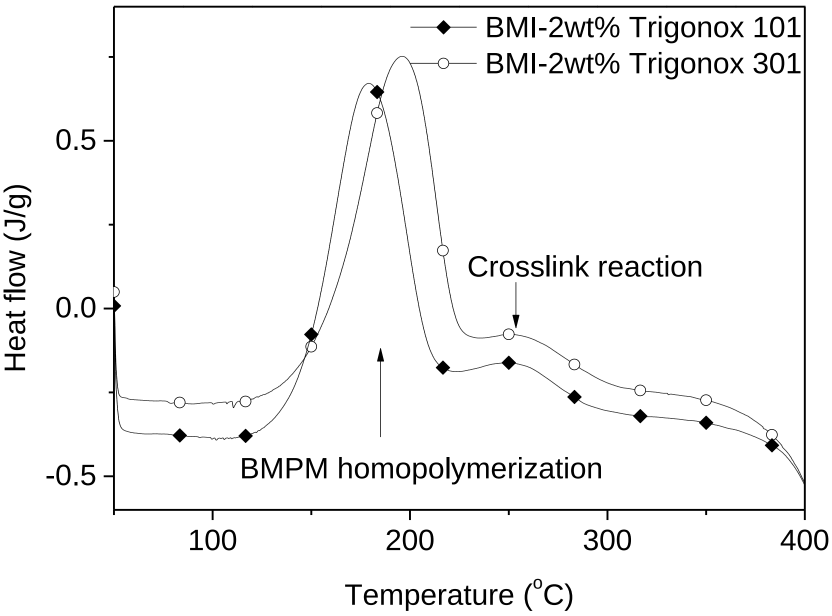

Figure 3.3: Reaction DSC profile of BMI-2wt% Trigonox®301 and 101 with a heating rate of 10^{o}C/min

3.3.1.3 Cure cycle determination

The standard curing cycle of BMPM-DABPA was 180^{o}C for 1h, 200^{o}C for 2h and 250^{o}C for 6h. Different type of reaction at different temperature was the rules of choosing these temperature and time. At 180^{o}C, the reaction was mostly “Ene” reaction. When raising the temperature to 200^{o}C, BMPM will begin to produce free radicals from the imide bonds dissociation. The homopolymerization of BMPM, copolymerization of DABPA with BMPM occurred at this temperature rage. Curing at 250^{o}C was to complete the crosslink reaction after the system reach gel state [6].

As learned from the DSC analysis, Trigonox®101 and 301 can initiate the free radical polymerization at lower temperature as compared to control system. The onset reaction temperature of BMI-Trigonox®101 and 301 systems was chose as the first curing step temperature. Since when preparing the sample, system was heated at 150^{o}C for 30min, “Ene” reaction was mostly completed. Besides, the onset temperature was lower than 180^{o}C, thus the first step of 180^{o}C for 1h to complete “Ene” reaction was eliminated for Trigonox initiator systems.

The curing cycle chose for Trigonox®101 was 150^{o}C for 2h and 250^{o}C for 6h. For Trigonox®301 system, the cure cycle was 170^{o}C for 2h and 250^{o}C for 6h. The lower curing temperature was to mimic the reaction of control BMI system cured at 200^{o}C. After the major crosslink reaction, the left over reaction at 250^{o}C is the same as control system, thus we chose the same cure temperature and time as the control system.

3.3.2 Effect of Trigonox®101 and 301 on glass transition temperature of BMI network

DMA curves of BMI cured with Trigonox®101 and 301 were shown in Figure 3.4. Glass transition temperatures of these systems were summarized in Table 3.2. Tg of BMI-Trigonox®101 was significantly higher than control system while BMI-Trigonox®301 had the relatively lowest Tg as determined from the G' curve. The tanδ curves of BMI-Trigonox®101 and 301 were not complete under the experiment data range. When compared with control system, BMI-Trigonox®101 and 301 had about the same G' modulus at the beginning. This indicated that Trigonox initiators were relatively mild initiators when comparing with DCP from the second chapter study. These observations implied that the final network structure of BMI cured by different initiator were quite different from each other. When BMI cured by DCP, the rapid homopolymerization of imide bonds gave the system a much tighter network. Thus the storage modulus as well as Tg was the highest among the three initiators. When BMI cured by Trigonox®301, some reaction happed at lower temperature, but most reaction was following the control system. Thus, it had the lowest Tg among the initiator system. For BMI with Trigonox®101, it had the compromised results that were between DCP and Trigonox®301.

Table 3.2: Glass transition temperatures of BMI control system and BMI/ Trigonox® 101 and 301 systems

System	Initiator content wt%	Tg (°C)
BMI	0	280
BMI/Trigonox® 101	0.3	372
BMI/Trigonox® 301	0.2	355

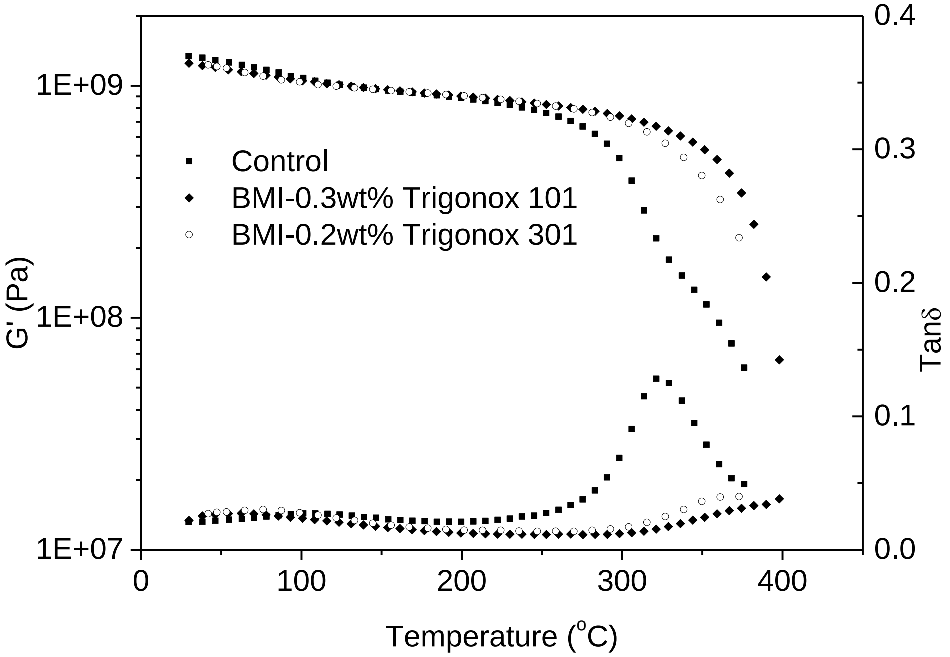

Figure 3.4: Shear modulus (G') and tanδ versus temperature for BMI control system, BMI with 0.3wt% Trigonox® 101 and BMI with 0.2wt% Trigonox® 301

Although BMI with 0.3wt% Trigonox® 101 system showed the same glass transition temperature as BMI with 0.5wt% DCP, the modulus of BMI with DCP was higher than BMI with Trigonox® 301. It has been shown by previous researchers that system with higher crosslink density would show higher modulus before as well as above Tg [24]. Since under experiment range, BMI with initiator system did no show rubbery plateau, it was hard to determine the exact crosslink density. However, it still can give information that BMI with DCP did have higher crosslink density than BMI with Trigonox® 101 and 301 systems.

3.3.3 Effect of Trigonox® 101 and 301 on thermal stability of Bismaleimide network

Figure 3.5 shows TGA curves of BMI cured with 0.3wt% Trigonox® 101 and 0.2wt% Trigonox® 301. In all cases, single-step decomposition was observed. This implied that curing with initiator did not change the decomposition mechanism. The thermal degradation temperatures at different values of weight loss are listed in Table 3.3. T_{d1}, T_{d2}, T_{d3} and T_{d4} are defined as the temperature at 5, 10, 15 and 20% weight loss, respectively. Slight and similar increase of degradation temperatures for BMI system cured with Trigonox® 101 and 301 is observed. Figure 3.6 shows derivative of TGA weight loss versus temperature. The slope of the curve indicates weight loss rate of the system and the peak value of the curve represents the maximum weight loss rate in the system. At the very beginning of degradation, the rate of degradation for BMI cured with initiator was lower than the control system. However, when temperature reaches the onset degradation temperature, which was 430°C, the weight loss rate as well as maximum weight loss rate of BMI cured with initiator, is mostly higher than control system. This phenomenon also implies that the crosslink density of BMI cure with Trigonox initiators is higher than the control system, which gives the system higher onset degradation temperature and lower weight loss rate at lower temperature. However, with initiator addition, fast polymerization of maleimide make the system crosslink junctions not as uniform as the control one. Thus, degradation of BMI cured with initiator occurs much more rapidly.

Table 3.3: Degradation temperatures of cured BMI with 0.3wt% Trigonox®101 and 0.2wt% Trigonox®301

Initiator	T_{d1}(°C)	T_{d2}(°C)	T_{d3}(°C)	T_{d4}(°C)
Trigonox®101	436	442	447	451
Trigonox®301	436	442	447	451
Control	431	439	445	450

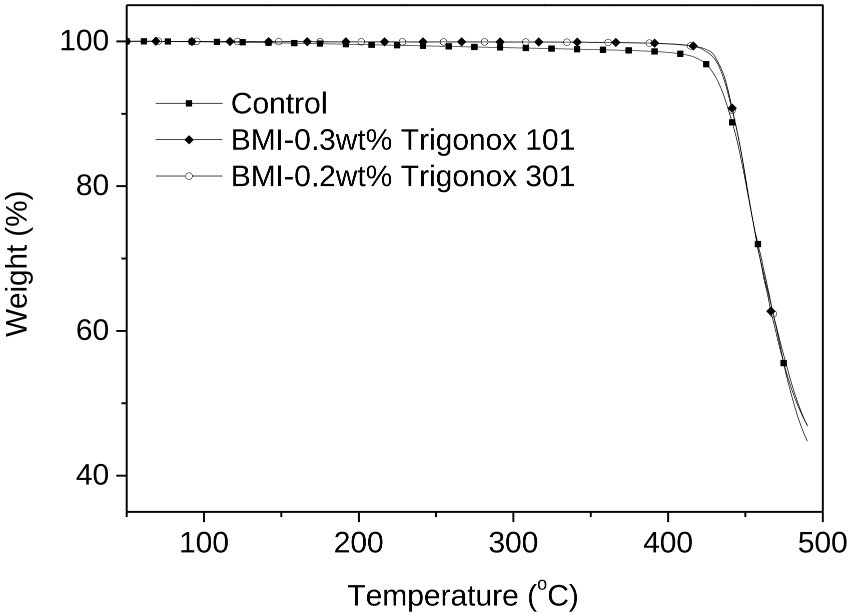

Figure 3.5: TGA profiles of BMI cure with 0.3wt% Trigonox® 101 and BMI with 0.2wt% Trigonox® 301

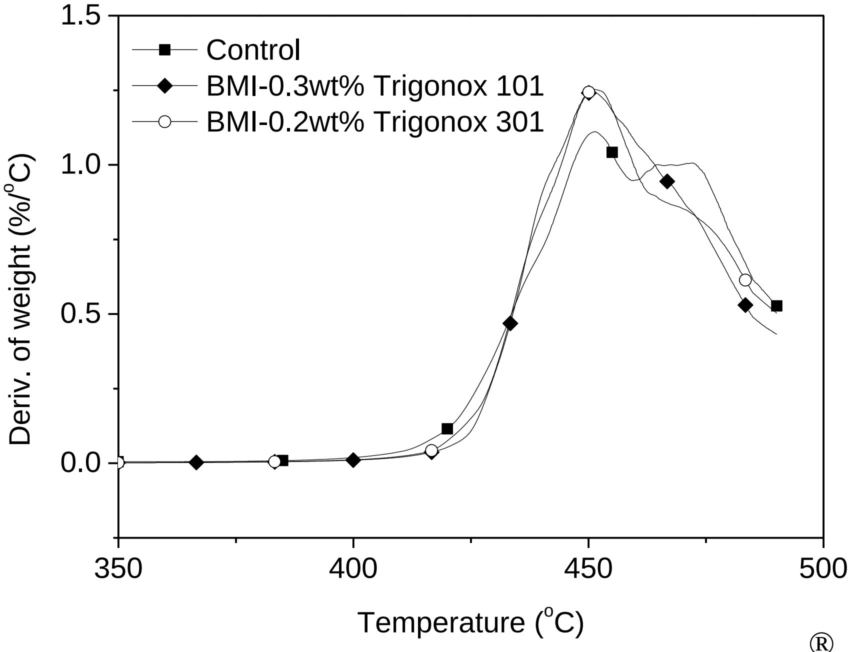

Figure 3.6: Derivative of TGA curves for BMI cured with 0.3wt% Trigonox® 101 and BMI with 0.2wt% Trigonox® 301

3.3.4 Effect of Trigonox® 101 and 301 on moisture absorption of Bismaleimide network

Low water absorption is very important to structural materials like Bismaleimide thermosets that were required to have stable high performance. The absorbed water molecules usually act as a plasticizer. It tends to reduce the thermal mechanical properties of polymer resulting detrimental effect on dielectric properties. As a result, water absorption is regarded as one of key properties that should be investigated with any new materials for structural application.

Moisture uptake into a polymer matrix can give indicative information about the network structure characteristic. Studies have been shown that thermosets with lower crosslink density will absorb less moisture as compared to higher crosslink network [11]. As from the above thermal mechanical analysis, BMI cured with 0.5wt% DCP were chosen to compare with Trigonox initiator system. Figure 3.7 displayed water uptake curves as a function of the square root of time normalized to the specimen thickness. The equilibrium moisture content of control system was higher than system cured with initiator. This result was contradictory to previous studies that network with higher crosslink density will absorb more moisture. Our postulation for this phenomenon is that when BMI cured with initiator, fast polymerization of maleimide make the system crosslink junctions not as uniform as the control one. Thus some area in the network was highly cross-linked while some area was less cross-linked. As a result, water molecules will not be all trapped or locked into molecular cages and can diffuse out of the system from less cross-linked area. This is very important to composite materials which upper service temperature will reduce significantly when moisture locked in.

When comparing these three initiators system with control no initiator system, apparently, the control system has much higher weight gain and fast water absorption at the very beginning of the experiment. First of all, the control system has lower crosslink density than the initiator systems. Thus, water molecular can diffuse into the control system easier than the initiators ones. Secondly, since the crosslink reaction was initiated by BMPM itself, the formation of network structure was more homogenous as compared to the rapid homopolymerization of BMPM by initiators. As a result, although control system had lower crosslink density, its homogenous network would lock the water molecule in the system.

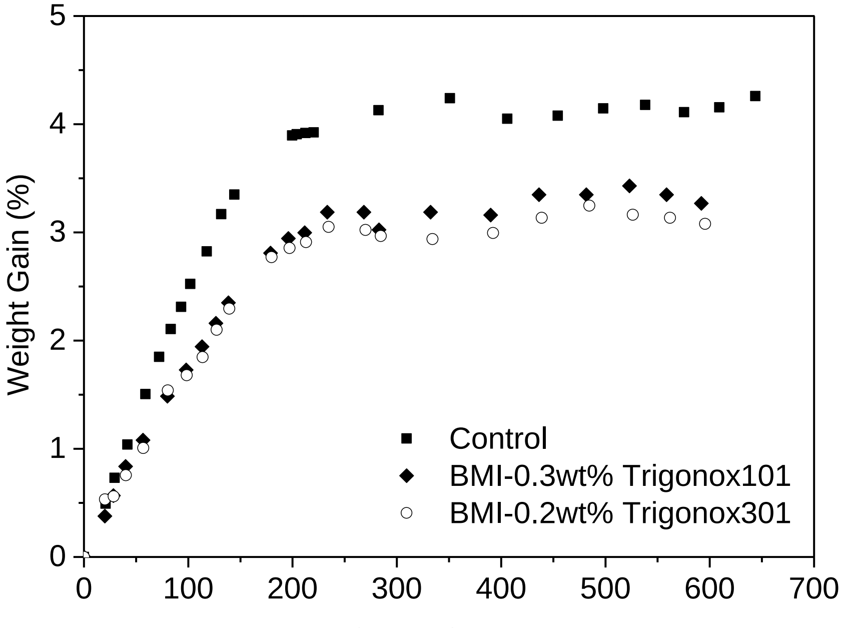

Figure 3.7: Moisture absorption curves of BMI control system and BMI with 0.3wt% Trigonox®101 and 0.2wt% Trigonox®301

When comparing BMI/Trigonox®101, BMI/Trigonox®301 with BMI/DCP system, the initial linear slope of weight gain was almost the identical among the systems. The final moisture uptake was slight higher for BMI/ BMI/Trigonox®101 system. As discussed before that Trigonox®101was a relatively mild initiator as compared to DCP, thus it would give the network less rapid free radical polymerization rate under low cure temperature and result in a relatively homogenous network as compared to BMI/DCP. From the previous research that the water uptake for the control BMI system was higher than BMI/DCP system, thus it is safe to say that BMI/ Trigonox®101 system has better network homogeneity as compared to BMI/DCP system.

As for BMI/ Trigonox®301system, it showed about the same moisture uptake as BMI/DCP network. From previous DSC study that Trigonox®301 did not efficiently initiate the low temperature cure reaction of BMI. Most of the crosslink reaction was further carried on when the system was heated to higher temperature following the same trend as the control system that BMPM form free radicals by heating. Although it also has been shown in DMA study that BMI/ Trigonox®301 system did have higher Tg than the control system that is an indication of higher crosslink density in the network.

3.3.5 Molar ratio effect of BMPM to DABPA on Bismaleimide thermoset cured with

3.3.5.1 Cure reaction of BMPM/DABPA with off stoichiometric ratio by DSC Study

As initiator was introduced into the BMI system, fast free radical homopolymerization of BMPM will result in high crosslink density. Although Trigonox system was relatively mild initiators as compared to DCP, it was still giving the system higher crosslink density as compare to the control system. The advantage of Trigonox initiator was not only slower initiation rate as compared to DCP, it also has the possibility of abstract H from allyl group in DABPA which gives the system more possibility of cross-linking between DABPA and BMPM besides the fast homopolymerization of BMPM.

Off ratio of BMPM to DAPBA system was investigated with Trigonox®101. The aim of this study was to further understand the reaction mechanism of crosslink reaction initiated by Trigonox initiators. The hypothesis was that if Trigonox®101 can abstract H from DABPA, with more DABPA than BMPM in the system, more DABPA can be incorporated into the network during the first free radical reaction step. The off ratio was chose as BMPM to DAPBA at 1 to 0.87 as the BMPM rich system and 0.87 to 1 as the DAPBA rich system. All systems were cured with 0.3wt% Trigonox®101. Dynamic DSC curves of all systems were shown in Figure 3.8.

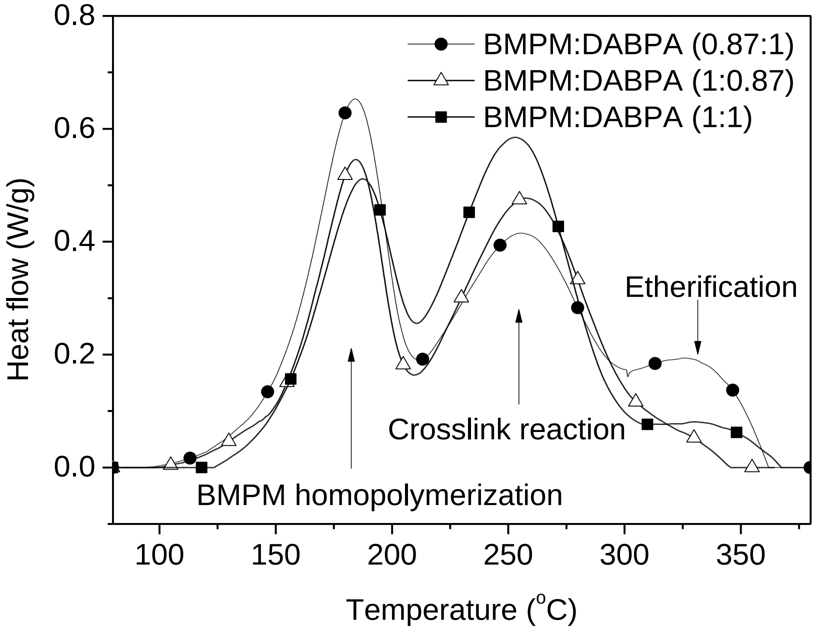

Figure 3.8: Reaction DSC profile of BMPM to DABPA at 1 to 1, 1 to 0.87 and 0.87 to 1 with 0.3wt% Trigonox® 101 with a heating rate of 10°C/min

As shown in the DSC curves, when BMPM was rich in the system, two major peaks were observed. When comparing with control system, the BMPM rich system missing the third small peak which is designated as the DABPA etherification peak. This indicated that when BMPM was rich in the system, the fast homopolymerization of BMPM would give the system higher crosslink density and restrict the movement molecule. Thus, the higher temperature reaction of DABPA was eliminated. On the other side, when DABPA was rich system, this third reaction peak was the most pronounced among these three systems. This also indicated that DABPA rich system the crosslink density should be lower than both the control system and the BMPM rich system. But, it also indicated that there might be few DABPA was not incorporated into the cross-linked network.

3.3.5.2 Glass transition temperature affected by molar ratio change

As learned from the above DSC study, in BMPM rich system, the system would result in a higher crosslink density than 1 to 1 molar ratio system. On the other side, the DABPA rich system had either etherification at higher temperature or left over unreacted DABPA in the network. The glass transition temperature and the tand curve of these systems could reveal some information about the network structure that was resulted from the different reactions in the system as initiated by Trigonox initiator. Dynamic DMA runs of stoichiometric system, BMPM rich and DABPA rich systems were shown in Figure 3.9.

As can be seen in the figure, the control BMI system has the highest tand peak value that indicated that control system has the lowest crosslink density among all these systems. Again, system with initiator, no matter it's off ratio or not, the tand peak did not show up completely within the experiment temperature range. The glass transition temperature here was again determined from the G' shear storage curve. The slope of G' curve at the end is an indication of the crosslink density of the thermosets. Steeper slope indicated that the system has lower crosslink density. From this, it is obviously, again, control system has the lowest crosslink density. When comparing the initiator system, stoichiometric and BMPM rich systems had about the same Tg and slope rate at the end. The DABPA rich system, on the other side, storage modulus started to drop significantly from 200°C. This could be due to the unreacted DABPA dangling on the backbone of the BMPM polymer chain. If observe carefully, the slope slowed down around 300°C which is the onset of etherification. The slope followed about the same rate as stoichiometric and BMPM rich system around 350°C again, which was the end of etherification temperature. This slightly increase of slope drop rate was due to the further etherification of DABPA that increase the local crosslink density of the network. However, this high temperature etherification reaction was not always wanted in industrial application because it will decrease the toughness of the system.

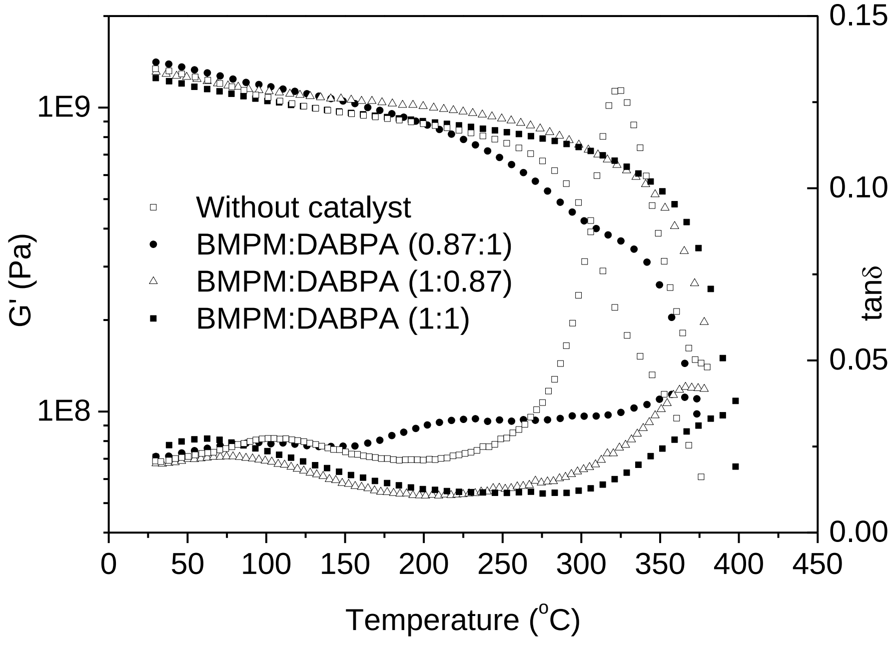

Figure 3.9: Shear storage modulus (G') and tanδ versus temperature of off molar ratio of BMI system with 0.3wt% Trigonox® 101

3.3.5.3 Thermal stability affected by molar ratio change

Degradation of BMI off ratio system cured with Trigonox® 101 was shown in Figure 3.10. The degradation temperatures of each system were summarized in Table 3.4. T_{d1}, T_{d2}, T_{d3} and T_{d4} are defined as the temperature at 5, 10, 15 and 20% weight loss, respectively. The temperatures at 5wt% weight loss can be considered as initial decompose temperature. As can be seen in Table 3.4, the onset decomposition temperature decreased in off molar ratio systems. When comparing the two off molar ratio system, DABPA rich system had relatively lower onset degradation temperature. Besides that, char yield at the end of the experiment was shown in Table 3.4 also. DAPBA rich system also had the lowest weight retention at the end. The derivative TGA curves were shown in Figure 3.11. The curve shape of BMI control 1 to 1 molar ratio system and BMPM rich system were similar to each other besides the BMPM rich system has lower onset degradation temperature and lower peak value of maximum weight loss rate. This indicated that when BMPM was rich in the system, the final network was less homogenous as the control one, thus link between crosslink junctions was relatively weak, resulting lower onset degradation temperature.

On the other side, the derivative TGA curve of DABPA rich system was different from the other two. It contained two major peaks and one was centered at the same temperature as the other two systems at 450^{o}C. The other peak centered on 475^{o}C that also showed up in BMI control system without initiator. The comparison of DAPBA rich system and BMI control system without initiators was shown in Figure 3.12. The similarity between DABPA rich system with

Trigonox and BMI control system without initiator suggested that when DAPBA was rich in the network, the possibility of Trigonox abstract hydrogen from DABPA helped to incorporate more DABPA into the network with BMPM. As a result, some similarity between the networks might be the major factor contributed to the same degradation mechanism

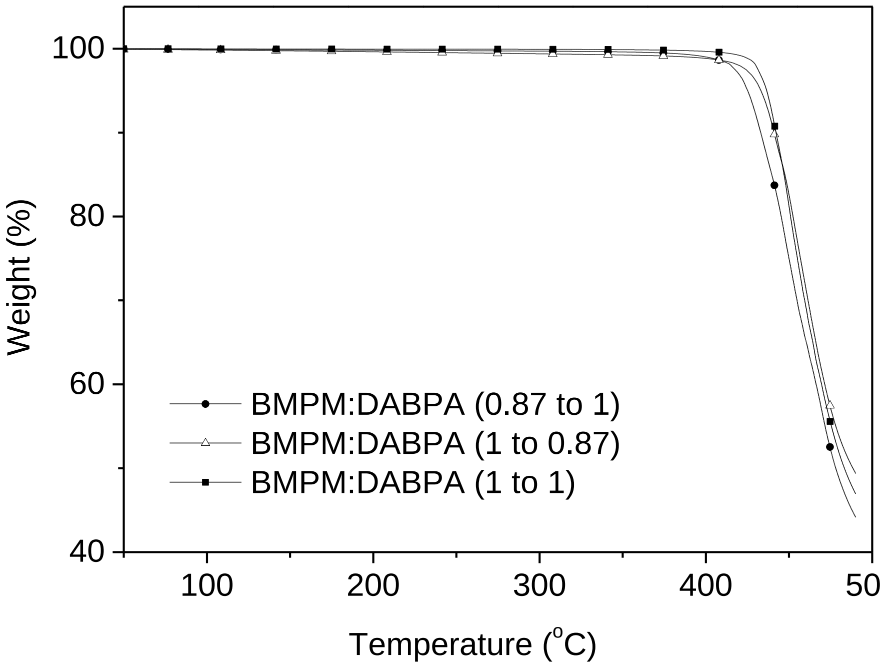

Figure 3.10: TGA profiles of BMI/0.3wt% Trigonox® 101with different BMPM to DABPA molar ratio in N_2

Table 3.4: Degradation temperatures of cured BMI/ Trigonox® 101 with different BMPM to DABPA molar ratio

BMPM to DABPA	T_{d1}(°C)	T_{d2}(°C)	T_{d3}(°C)	T_{d4}(°C)	Char Yield(%)
1 to 1	436	442	447	451	47
1 to 0.87	429	437	444	449	48
0.87 to 1	425	433	440	445	44

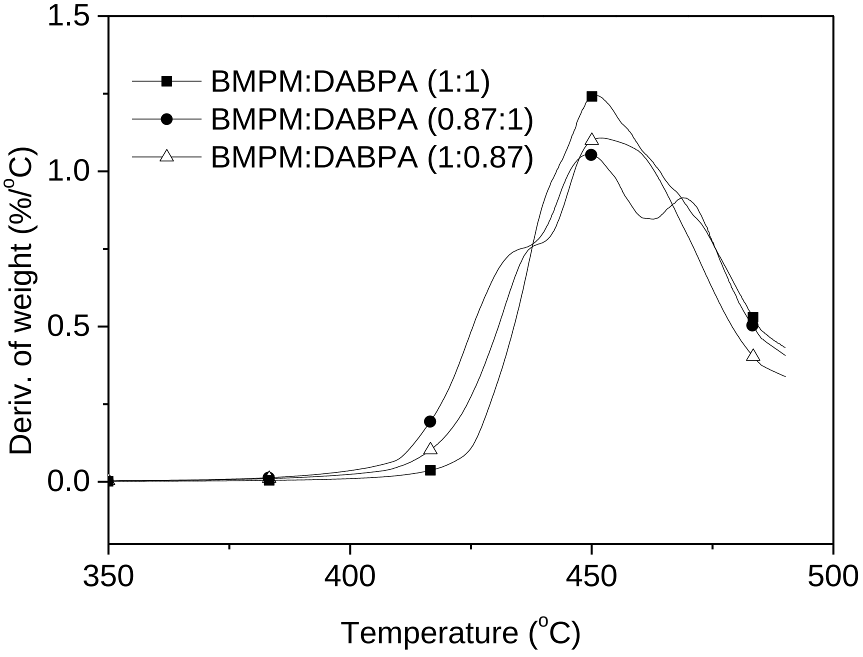

Figure 3.11: Derivative of TGA curves for BMI with 0.3wt% Trigonox® 101 with different BMPM to DABPA molar ratio

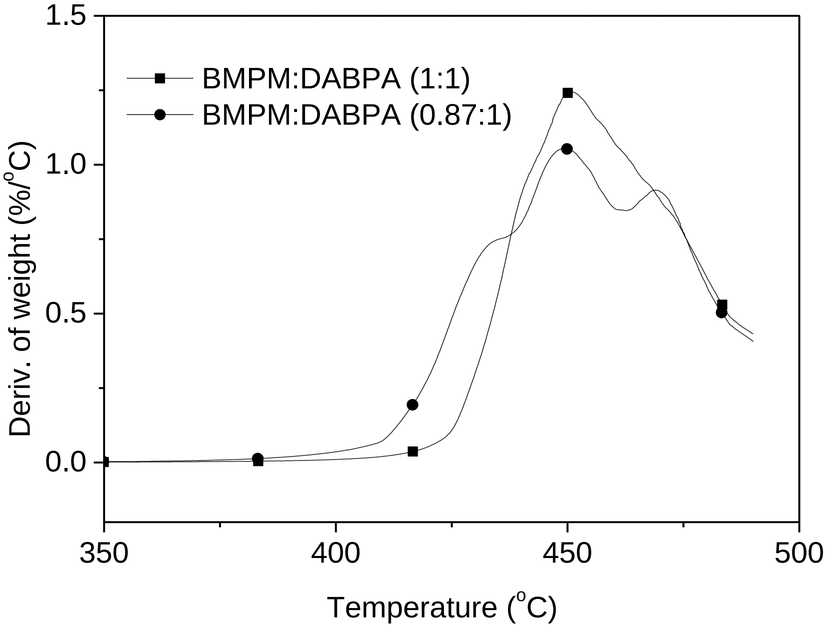

Figure 3.12: Derivative of TGA curves for BMPM: DABPA (0.87:1) with 0.3wt% Trigonox® 101 and BMI control system without initiator

3.4 Conclusions

A series of BMI catalyzed by Trigonox initiators were studied to determine the effect of initiator type and initiator concentration on the cure reaction and thermal characteristics of BMPM-DABPA based BMI Thermoset. It was shown that the addition of Trigonox® 101 and 301 can significantly lowered the onset cure temperature of BMI up to 50°C. Both initiator systems showed two reaction peaks during DSC analysis. The rate of curing was more efficient for BMI cured by Trigonox® 101 compared with system cured by Trigonox® 301. With higher amount of Trigonox initiators, more chemical reaction occurred at the lower temperature range while reaction at higher temperature was inhibited. From DSC study, the lower temperature initiation of initiator can efficiently initiate the polymerization of BMI system. However, the reaction of the lower temperature reaction was mainly concerned with BMPM homopolymerization. Thus, the higher temperature reaction that was similar to the BMI control system was considered a beneficial reaction to the BMI network. From there, only a small amount of initiator was enough for the network. Since Trigonox®301 showed a third reaction peak that was not a beneficial reaction to the network and it also had higher initiation temperature than Trigonox®101, Trigonox®101 was considered as a better initiator to efficiently initiate the BMI crosslink reaction at lower temperature.

DMA analysis showed that storage modulus and crosslink density of BMI cured by both initiators was significantly higher than control system. Tg was increased with both Trigonox initiators while Trigonox®301 system had slightly lower Tg than Trigonox®101's. This was due to the inefficient initiation of Trigonox®301. It initiated some part of BMPM homopolymerization and crosslink reaction under low temperature, however, it still left over quite a few BMPM unreacted and followed the control system reaction path when temperature was raised.

Thermal stability of BMI was slightly enhanced also by initiator addition. Although the onset degradation temperature of initiator system was slightly higher than the control, the degradation rate was also mostly higher than the control system. This may be caused by the un-homogeneity of network due to initiator addition. Both Trigonox initiators showed the same degradation temperature at different weight loss. The derivative curves of both Trigonox systems were similar to each other, indicating the same degradation mechanism. And the network degradation was not significantly affected by different reaction path introduced by initiators. Moisture uptake was significantly less for initiator system as compared to the control network, which was also related with the un-homogeneity of the network. This lower degree of moisture uptake was beneficial for structural application.

For off ratio study, thermal mechanical properties of BMI were clearly affected by different molar ratio of BMPM to DABPA. The DSC study showed that Trigonox®101 did give the system higher heat of reaction when DAPBA was rich in the system. This indicated that the hypothesis of hydrogen abstraction by Trigonox®101 could be true. However, thermal mechanical property of DAPBA rich system was not very promising showing a much lower Tg than the 1 to 1 molar ratio control system with initiator. This indicated that this off ratio might be too much, that some part of DABPA was left over and unreacted. On the other side, thermal resistance study showed that DABPA rich network had the most similar degradation curve as the control system without any initiator. This might be another indication of network similarity.

In general, the addition of Trigonox®101 can effectively initiate the cure reaction at much lower temperature than control system. Trigonox®101 enhanced the thermal mechanical and moisture uptake of BMI cured with Trigonox®101. A minor amount of initiator is sufficient for improving the thermal and moisture uptake properties of BMI network. A slight off ratio network with DAPBA rich in the system, might contribute to the BMI final network better homogeneity in the end.

REFERENCES

REFERENCES

1. Stenzenberger, H.D., Addition polyimides, High performance polymers, Advances in polymer science, vol.17, pp165-220, 1994.

2. Morgan, R.J., Jurek, R.J. and Larive, D.E., Structure property relations of high temperature composites polymer matrices, Advances in chemistry series, vol.233, pp493-506, 1993.

3. Kenny, J.M., Trivisano, A. and Nicolais, L., Thermal characterization of the cure kinetics of advanced matrices for high performance composites, Advances in chemistry series, vol.233, 539-557, 1993.

4. Denny, L.R., Goldfarb, I.J, and Farr, M.P., Characterization of bisbenzocyclobutene high temperature resin and bisbenzocyclobutene blended with a compatible bismaleimide resin, ACS symposium series, vol.367, pp366-378, 1988.

5. Chandra, R., Rajabi, L., Recent advances in bismaleimides and epoxy-imide/bismaleimide formulations and composites, Jouranl of macromolecular science-reviews in macromolecular chemistry and physics, vol.c37, pp61-69, 1997.

6. Morgan, R.J., Shin, E.E., and Rosenberg, B., Characterization of the cure reactions of bismaleimide composite matrices, Polymer, vol.38, pp639-646, 1997.

7. Mijovic, J. and Andjelic, S., Study of the mechanism and rate of bismaleimide cure by remote in-situ real time fiber optic near-infrared spectroscopy, Macromolecules, vol.29, pp239-246, 1996.

8. Morgan, R.J., Jurek, R.J. and Yen, A., Toughening procedures, processing and performance of bismaleimide carbon fiber composites, vol.34, pp835-842, 1993.

9. Yan, Y.H., Shi, X.M. and Liu, J.G, Thermosetting resin system based on novolak and bismaleimide for resin transfer molding, Journal of applied polymer science, vol.83, pp1651-1657, 2002.

10. Bao, L.R. and Yee, A.F., Moisture absorption and hygrothermal aging in a bismaleimide resin, Polymer, vol.42, pp7327-7333, 2001.

11. Cheng, Q.F., Bao, J.W. and Park, J.G., High mechanical performance composite conductor:

multi-walled carbon nanotube sheet/bismaleimide nanocomposites, Advanced functional materials, vol.19, pp3219-3225, 2009.

12. Nair, C.P.R. and Francis, T., Blends of bisphenol A based cyanate ester and bismaleimide: cure and thermal characteristics, Journal of applied polymer science, vol.74, pp3365-3375, 1999.

13. Seris, A., Feve, M., Mechin, F. and Pascault, J.P. Thermally and anionically initiated cure of bismaleimide monomers, Journal of applied polymer science, vol. 48, pp257-269, 1993.

14. Kwiatkowski, G.T., Robeson, L.M. and Bedwin, A.W., Thermosetting diphenyl sulfone based maleimides, Journal of polymer science, polymer chemistry edition, vol.13, pp961-972, 1975.

15. Iwata. K. and Stille, J.K. Higher molecular weight phenylated free radical curing agents: 4,4’-oxybis(triphenylmethyl hydroperoxide, Journal of polymer science, polymer chemistry edition, vol.14, pp2841-2843, 1976.

16. Takashi, E., Toshiro, T. and Keiichiro I., Effects of initiators on the model reactions of several maleimide resin systems-(I) amine modified maleimide, High performance polymer, vol.6, pp385-393, 1994.

17. H. Stenzenberger, Structural Adhesives, A. J. Kinloch, Ed., Elsevier, London, 1986.

18. I. K. Varma, S. P. Gupta, and D. S. Varma, Effect of triallyl cyanurate on the properties of bismaleimide resin, Journal of applied polymer science, vol.33, pp151-164, 1987.

19. Acevedo, M., Abajo, J.D. and Campa, J.G.D., Kinetic study of the crosslinking reaction of flexible bismaleimide, Polymer, vol.31, pp1955-1959, 1990.

20. Seris, A., Feve, M. and Pascault, J.P., Thermally and anionically initiated cure of bismaleimide monomers, Journal of applied polymer science, vol.48, pp257-269, 1993.

21. Syed, M.S.J., Azlan, M.R.N and Ishiaku, U.S., Quantitative analysis on the grafting of an aromatic group on polypropylene in melt by FTIR technique, Polymer testing, vol.19, pp635-642, 2000.

22. Valeria, D.R., Helson, M.C., Marisa, C.G.R. and Ailtion S.G., Study of different peroxide types on the modification of LLDPE. Part 1. Factorial experimental design and thermal properties, Polymer testing, vol.25, pp306-312, 2006.

23. Hamerton, I., Howlin, B. J., Klewpatinond, P. and Takeda, S., Conformational studies of polycyanurates: a study of internal stress versus molecular structure, Polymer, vol.43, pp4599-4604, 2002.

24. Xia, S., Jong, K.L. and Michael, R.K., Influence of cross-link density on the properties of ROMP thermosets, Polymer, vol.50, pp1264-1269, 2009.

CHAPTER 4: CURING AND THERMAL PROPERTIES OF 4, 4’-BIS-MALEIMIDODIPHENYLMETHANE AND O, O’-DIALLYL BISPHENOL A BASED BISAMLEIMIDE NETWORK WITH POLYHEDRAL OLIGOMERIC SILSESQUIOXANE

4.1 Introduction

The stability of polymer determines its usage and reliability during application. In the case of higher temperature performance polymer, it requires very good thermal and dimensional stability. However, most polymers cannot meet these requirements on themselves [1-6]. In recent years, nanocomposites made from the combination of polymer matrix and nano inorganic fillers have been proven to exhibit excellent property and performance [7-9]. The nano-sized inorganic fillers often exhibit dramatic physical and chemical properties that are superior to their micro-phase counterpart. Polyhedral Oligomeric Silsesquioxane (POSS), has received a lot of attention in recent years due to its uniformly porous in nanometer-size nature and its combination of an inorganic core covered with organic shell. POSS itself has been labeled as the smallest organic-inorganic hybrid [10]. POSS molecules with organic functional groups have great compatibility with polymers and thus provide vast possibilities for designing new hybrid materials with well-defined dimensions and nano-phase behavior [11]. POSS containing one or more reactive functional groups have been synthesized and studied. It can be prepared via grafting, surface bonding, transformation or polymerization. Large-scale process for POSS monomer synthesis has already developed in the early 2000. The incorporation of POSS into polymers can always lead to significant improvement of polymer properties including both mechanical and physical properties, such as extended temperature range of polymer, reductions in flammability [12-16].

In this study, Octastyrenyl POSS (OSTS) and N-Phenylaminopropyl (APS) were investigated with BMPM/DABPA based bismaleimide network. The unsaturated C=C bonds of OSTS between benzene and the POSS cage made its reactivity lower than styrene group, but it still has possibility to react with the BMI resin through free radical polymerization. For system with APS, the secondary amine could react with BMPM through Michael addition reaction. Both POSS can be incorporated into the system by convent bonding. However, the different reaction mechanism between resin and POSS molecule will affect the thermal properties of BMI differently. The objective study of this chapter research was to study the thermal properties of BMI/POSS nanocomposites, understanding the structure-property relationships of POSS modified thermoset network and optimize the best performance for BMI/POSS nanocomposites.

4.2 Experimental Techniques

4.2.1 Materials

Bismaleimide resin (BMI) in this study was consisted by 4, 4'- bisamleimidodiphenyl methane (BMPM) and O, O'-Diallyl Bisphenol A (DABPA) (Huntsman Co.) mixed together with 1:1 molar ratio. Additional Octastyrenyl POSS (OSTS) and N-Phenylaminopropyl POSS (APS) (Hybrid Plastic Co.) was mixed into the BMI resin at 2, 5 and 10wt%. For BMI/APS system, off stoichiometric BMPM to DABPA ratio was investigated with 2 and 10wt% APS addition. All components were used as received with no further purification. The structures of these components were shown in Figure 4.1.

4.2.2 Sample Preparation

For system with additional 2wt% OSTS, two kinds of BMI nanocomposites were prepared to study the mixing sequence of OSTS into BMI system, System A and System B. System A was prepared by mixing DABPA with additional 2wt% OSTS first at 150^oC for 20min until OSTS was completely dissolved into DABPA. BMPM was then added into the mixture and stirred for another 30min until a clear solution was obtained. System B was prepared by mixing DABPA and BMPM first for 30min at 150^oC for 30min. Then additional 2wt% OSTS was added in and stirred for additional 20mins. Control system was also prepared by mixing BMPM and DABPA at 150^oC for 30min. For system with additional 5 and 10wt% OSTS, preparation step followed the System A method. Each system was then placed into a conventional oven and cured under standard cure cycle, which was 180^oC for 1h, 200^oC for 2h and 250^oC for 6h. Cured samples were collected for further properties analysis. To compare with OSTS system, additional 2, 5 and 10wt% APS was added into the system following System A method by mixing DABPA with APS first at 150^oC for 20min until APS was completely dissolved into DABPA. BMPM was then added into the mixture and stirred for another 30min until a clear solution was obtained. The molar ratio of BMPM to DAPBA was controlled at 1 to 1 stoichiometric molar ratio.

In order to investigate the effect of APS reaction with BMPM on the thermal properties of the cured network, careful calculation of 2 and 10wt% APS was added into the system while maintain the reaction groups from APS plus DABPA was the same as reaction groups in BMPM. Ideally, if all APS react with BMPM, the left over BMPM to DAPBA molar ratio would still be 1 to 1. If not, the BMI/APS system will be slightly BMPM rich.

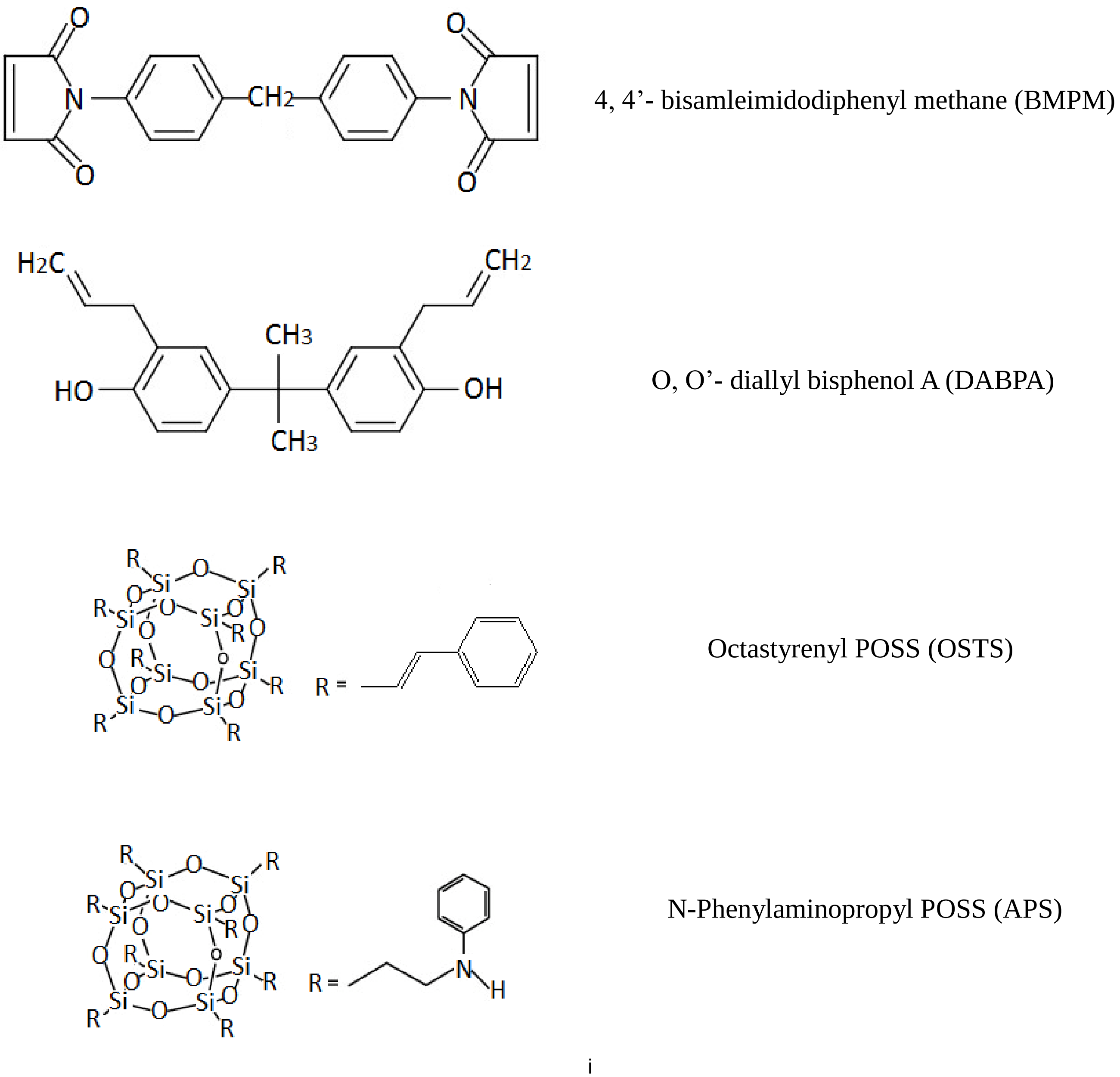

Figure 4.1: Schematic structure of BMPM, DABPA, OSTS and APS

4.2.3 Characterization Techniques

DSC analysis was studied using around 10mg mixture in a Mettler Toledo DSC-1. Dynamic heating rates of 10°C/min were used to determine the heat of reaction during curing process. The heating range was from 50-350°C with nitrogen gas at a flow of 50ml/min. The assumption of DSC analysis was that the area underneath the curves is proportional to the extent of reaction. The extent of cure α at any time was defined as

$$\alpha = \frac{\Delta H}{\Delta Hr}$$

where ΔH is the partial heat of reaction at any determined time while ΔH_r is the overall heat of reaction.

XRD measurements were performed at room temperature on a Schintag XDS 2000 diffractometer with Cu Kα radiation (λ=0.154nm). Samples were scanned from 5 to 30° with a scan speed of 0.5°/min. The X-ray intensity was recorded as a functional of diffraction angle 2θ. From X-ray diffraction patterns, possible POSS crystallite formation in the BMI matrix can be characterized.

Glass transition study by Dynamic Mechanical Analysis(DMA) was carried out on a Rheometric Solid Analyzer III with a 350g transducer operated using the torsion rectangular fixture. All measurements were performed from 30 to 400°C at the frequency of 10rad/s and outer tensional strain amplitude of 0.05%. In this study, the glass transition temperature was referred as the temperature when the shear modulus begins to drop significantly.

Thermal gravimetric analyzer, TA Q500, was used to investigate the thermal and oxidative stability of the BMI/POSS thermosets. All the thermal analysis was conducted from room temperature to 500^{o}C at a heating rate of 20^{o}C/min. The onset degradation temperature was determined as the temperature at 5wt% weight loss.

For moisture uptake study, specimens were dried at 80^{o}C for 72h. The moisture absorption was determined by submerging the samples (50mm radius x 1.5mm) in de-ionized water bath of 80^{o}C and monitoring water uptake gravimetrically. Samples were removed from the water bath and excess water was removed gently with lint-free cloth. Weight was recorded to 0.1mg precision on a Mettler balance. The water absorption was monitored gravimetrically according to the following equation:

$$M_t = \left(\frac{W - W_i}{W_i} \right) \times 100$$

Where M_t is the weight gain percentage at time t, W_i represents the initial weight (dry weight) at time zero and W is the weight of the specimen at time t.

4.3 Results and Discussion

4.3.1 Bismaleimide/OCTASTYRENYL POSS (OSTS) System

The reaction of BMPM and DABPA has been well studied by previous researches [17-19]. The following reaction types have been proposed and accepted by most researchers: “Ene”, Diels-Alder, homopolymerization of BMPM and alternating copolymerization of BMPM and DABPA. Around 150^{o}C, the BMPM and DABPA monomers react forming “Ene” molecule which contains three active C=C double bonds. Above 200^{o}C, these three sites will undergo crosslinking reaction [20-22].

In this study, whether Octastyrenyl POSS (OSTS) can react with BMI resin was investigated at the first place. The possible reactive group of OSTS was the styrenyl double bond. Due to the spatial position of the carbon double bond was between the benzene ring and the POSS cage, OSTS was assumed to be nonreactive by itself. Figure 4.2 showed a typical single dynamic DSC curve of OSTS heated up to 350^{o}C. Only a melting peak was observed, which confirmed that OSTS couldn’t polymerize by itself. DABPA was also known cannot undergo self-polymerization. The only possible reaction left would be between BMPM and OSTS.

BMPM can form free radicals by itself when it was heated up to 200^{o}C, thus it was possible that radicals can transfer from the imide bonds of BMPM to styrenyl C=C bonds of OSTS. Single dynamic DSC curves of pure BMPM and BMPM/33wt% OSTS mixture heated up to 400^{o}C at 10^{o}C/min was shown in Figure 4.3. Melting and reaction peaks were observed in both systems. Reaction peak temperature was shifted to higher temperature by OSTS addition. Reaction rate that was related with the slope of DSC reaction curve was decreased when OSTS was in the system. These changes all indicated that OSTS was reacted with BMPM. Due to the bulky cage of OSTS, the reactivity of BMPM was lowered. As a result, the reaction peak temperature shifted to higher range.

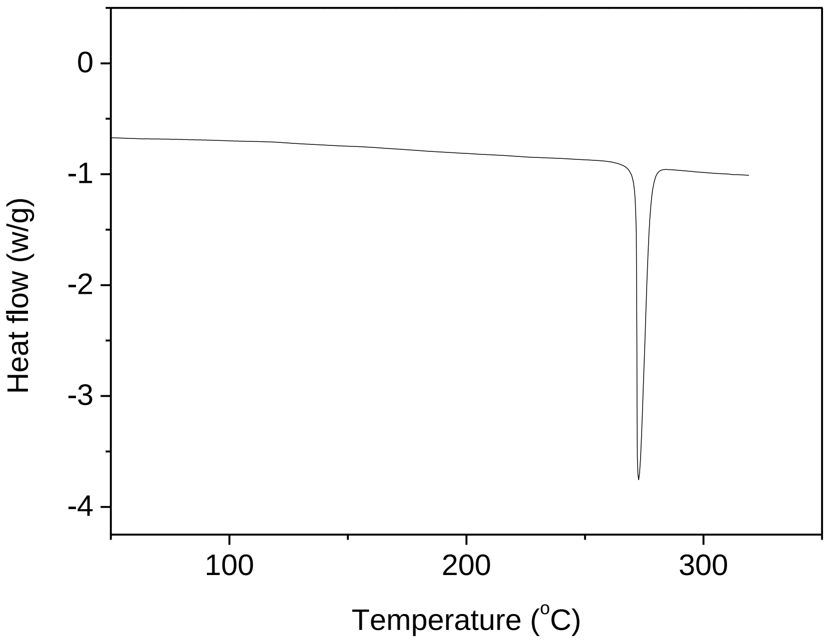

Figure 4.2: Single dynamic DSC curve of OSTS at 20^{o}C/min heating rate

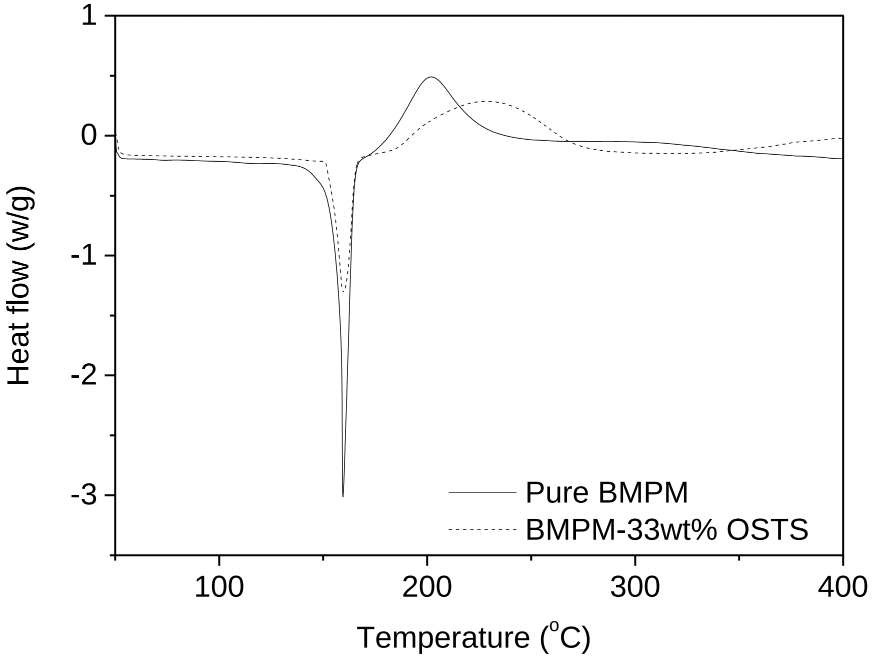

Figure 4.3: Dynamic DSC curves of pure BMPM and BMPM with 33wt% OSTS at 10^{o}C/min heating rate

4.3.1.1 Mixing sequence effect of OSTS into Bismaleimide system by DSC

By elucidating the reaction between OSTS and BMI, the continued study was effect of mixing sequence on properties of BMI/OSTS nanocomposites. Single dynamic DSC curves of System A, B and Control system were shown in Figure 4.4. Major exothermic curing was observed in the temperature range of 160-300^{o}C. Since only 2wt% OSTS was added into the system, most of the crosslinking reactions in the system were still between BMPM and DABPA. The onset and peak temperature of the reaction was not significantly affected, which indicated that OSTS did not alter the crosslinking reactions of BMI resin.

Heat of reaction for the major curing process was determined by integrating the area underneath the exothermic peak, results were shown in Table 4.1. It was clear that the sequence of adding OSTS into BMI system had a significant effect on the heat of reaction. The heat of reaction for System A was slightly lower than the control system while System B was significantly lower than the control system. For System A, the addition of OSTS first into DABPA during mixing might interfere the ene reaction of BMPM to DABPA. As a result, there was some Ene reaction left over during crosslinking reaction during DSC running process. Furthermore, when OSTS react with BMPM, the crosslinking reaction rate would be slowed down which also contributed to the lower heat of reaction. On the other side, the significant lower heat of reaction in System B compared to control system, which would be mostly due to slowed down crosslink reaction rate by POSS addition onto the BMI polymer chain.

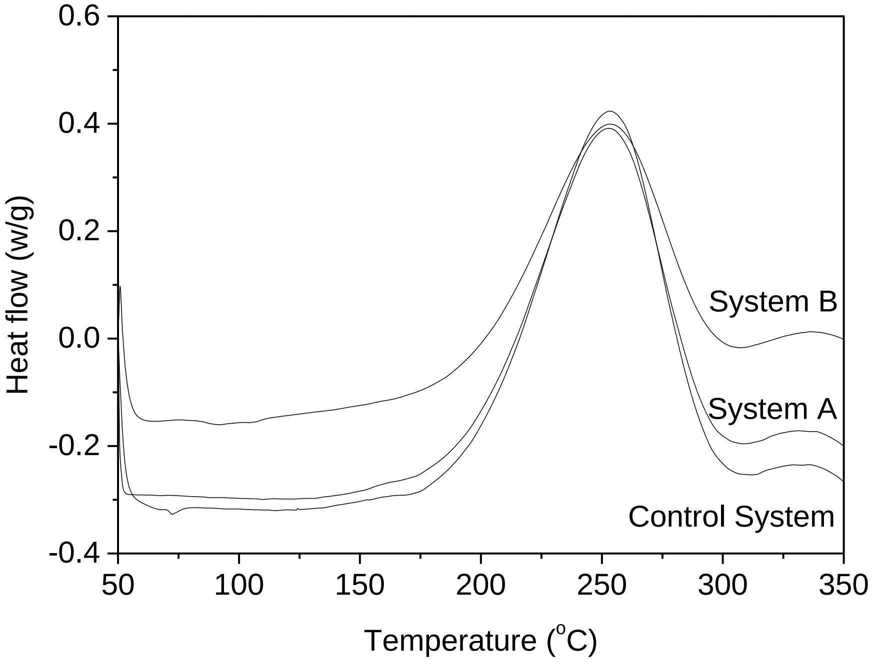

Figure 4.4: Dynamic DSC curves of System A, B and control system at 10^{o}C/min heating rate

Table 4.1: Maximum temperatures, heat of polymerization determined from DSC analysis for the polymerization of BMI with OSTS

System	OSTS(wt%)	Tp(^{o}C)	ΔHp* (J/g)	α (%)
Control	0	252	269	92
System A	2	253	266	84
System B	2	253	180	68

*α represents the percent of cure at the end of first reaction peak.

4.3.1.2 Effect of OSTS content on reaction in Bismaleimide network

Dynamic DSC curves of all the systems running at 10^{o}C/min were shown in Figure 4.5. Heat of the cure reaction can be obtained by integrating the area underneath the peak. The results were shown in Table 4.2. The heat of reaction decreases with the increase of OSTS content in the BMI matrix. When 10wt% OSTS was added in the BMI system, the heat of reaction was decreased up to 30% as compared to the control system. This again indicated that OSTS POSS did react with BMPM and slow down the crosslink reaction rate. With more OSTS in the BMI network, the crosslink reaction was further retarded by OSTS. As a result, heat of reaction was significantly lower when higher content of OSTS was added into the system.

Beside decreased heat of reaction, rate of reaction was also decreased by OSTS. When 10wt% OSTS was added into BMI network, the slope of first reaction peak was clearly less steep than BMI with lower amount of OSTS. Moreover, the peak position was decreased which also indicated a less rapid chemical reaction. This all can be explained by the reaction of OSTS onto BMI polymer chain. The reaction of OSTS with BMPM free radical may terminate free radical transfer, thus decrease the amount of crosslink reaction.

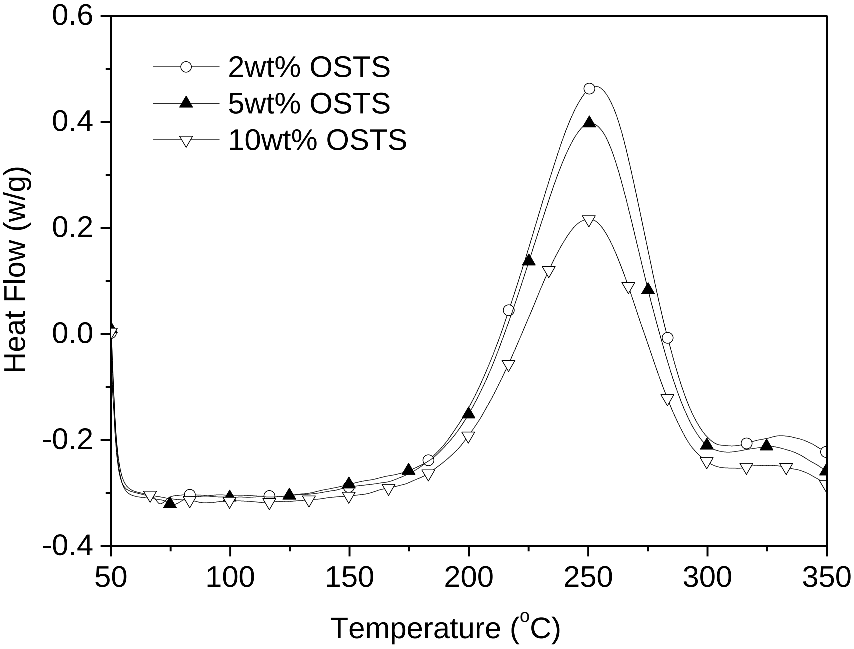

Figure 4.5: Dynamic DSC curves of BMI systems with different OSTS content at 10°C/min heating rate

Table 4.2: Maximum temperatures, heat of polymerization determined from DSC analysis for the polymerization of BMI with different amount of OSTS

System	Tp(°C)	ΔHp* (J/g)	α (%)
Control	252	269	92
2wt%	253	266	84
5wt%	251	231	82
10wt%	251	178	82

*α represents the percent of cure at the end of first reaction peak

4.3.1.3 Morphology of Bismaleimide/OSTS network

The morphology of the BMI/OSTS cured network was investigated by XRD. X-ray diffraction patterns for all BMI system with OSTS POSS content up to 10wt% were shown in Figure 4.6. As can be seen in the XRD profiles of OSTS, there were several distinctive peaks from 2θ=5° to 10°. These peaks were caused by the crystal structure of OSTS POSS. The neat BMPM-DABPA resin was responsible for the amorphous peak at 17.5° in these systems. All hybrid systems had similar XRD spectra as that of the amorphous halo of BMI control system. Moreover, the characteristic diffraction peak of OSTS was not observed in the hybrid system. All the XRD information implied that the OSTS in these BMI systems was homogeneously dispersed into the network at molecular level without the formation of dissociative OSTS crystallites.

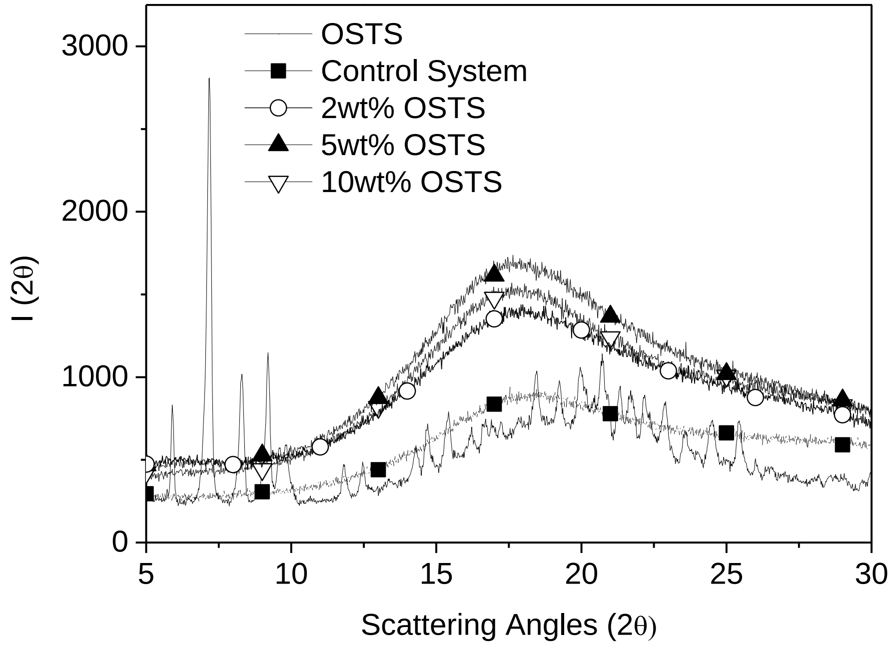

Figure 4.6: XRD patterns of BMI systems with different content of OSTS

4.3.1.4 Effect of OSTS on glass transition temperature of BMI network

Glass transition temperatures of the BMI composites were determined by DMA analysis. DMA was performed on Control System, System A and B as a function of temperature. Storage modulus of these systems was shown in Figure 4.7 and glass transition temperature was shown in Table 4.3, which was determined as the temperature when storage modulus begins to drop sharply. The glass transition temperature of System A and B was clearly shifted to higher temperature, about 10^{o}C higher than the Control System. The addition of OSTS could retard the chain mobility of the network, thus improve the T_g of BMPM thermosets. For System A and B, POSS addition sequence did not make a significant difference on the T_g since the systems undergo the same cure cycle. Thus, the overall crosslink reaction could undergo to completion for both System. For System B, it is possible that less amount of OSTS molecules could be covalently attached to the network. However, the existence of OSTS molecules around the matrix can affect the mobility of the chain too. Besides, since only 2wt% OSTS was added into the system, the overall effect of retarding the chain mobility might not be significantly different from each other.

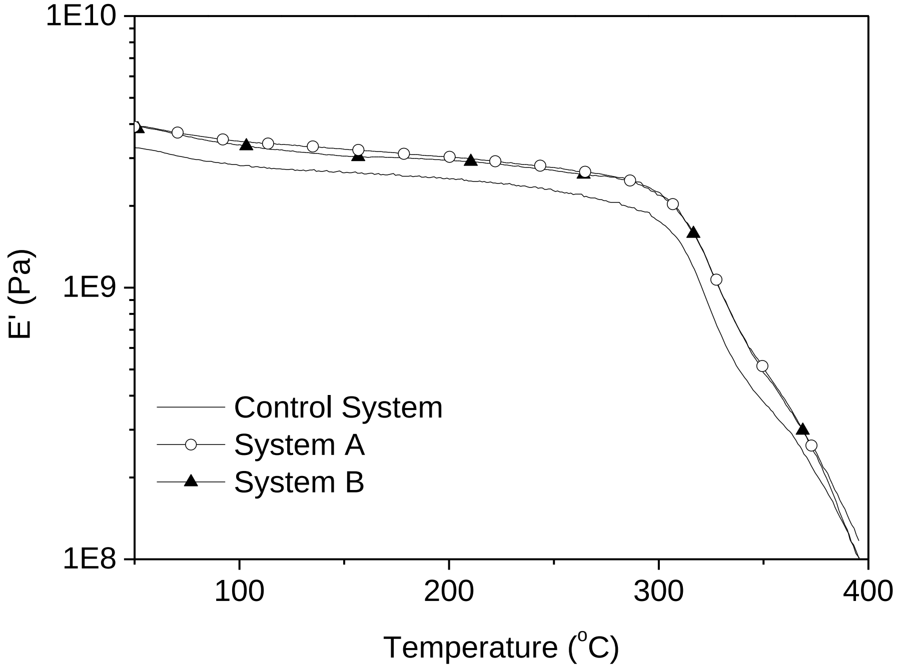

Figure 4.7: Storage modulus and tanδ vs. temperature of Control System, System A and B

Table 4.3: Glass transition temperature of cured Control System, System A and B

System	Tg(°C)
Control	300
System A	305
System B	303

DMA curve of G’ for all the systems were shown in Figure 4.8. From the curve, it was clear that with the increase of OSTS content in the BMI resin, the glass transition temperature of the systems shifted to higher range. With10wt% OSTS in the network, glass transition temperature was increased from 300^{o}C to 320^{o}C. Glass transition temperature of all systems was shown Table 4.4. When OSTS molecules were covalently bonded to the BMI network, the chain mobility was further retarded with higher content of OSTS in the system. As a result, the increase in glass transition temperature was expected with the increase of OSTS content in the network. Besides, the addition of OSTS also damped and broadened the tand peak of BMI. This was again due to the incorporation of OSTS in BMI that affected the chain mobility.

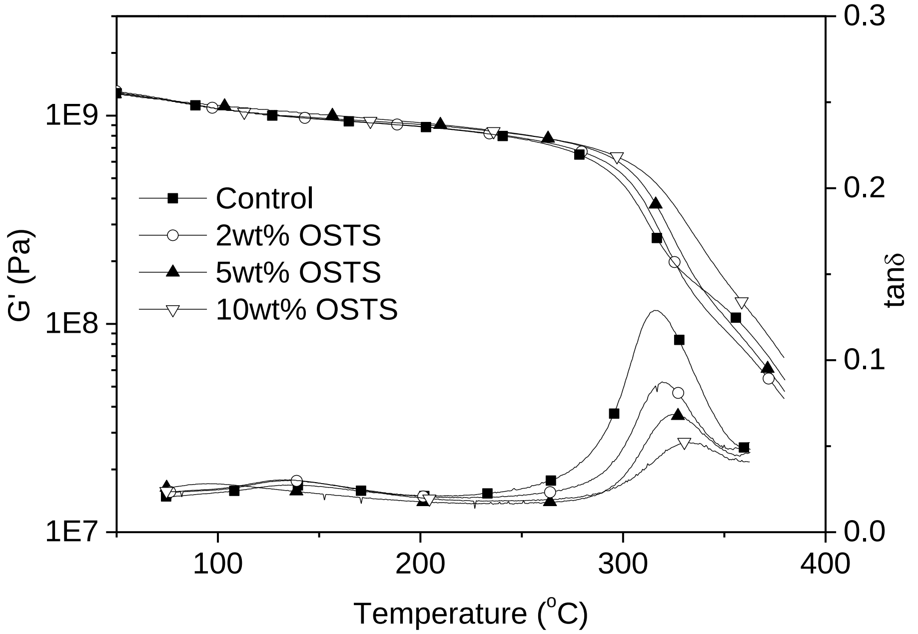

Figure 4.8: Shear modulus and tanδ vs. temperature of BMI composites with different OSTS content

Table 4.4: Glass transition temperatures of BMI/OSTS with different OSTS content

System	Tg (^oC)
Control	300
2wt%	305
5wt%	308
10wt%	320

4.3.1.5 Effect of OSTS on thermal stability properties of Bismaleimide network

Thermal stability of BMI/OSTS system was investigated by TGA. Typical dynamic TGA curves were shown in Figure 4.9, single step decomposition was observed, which indicated that OSTS does not alter the decomposition mechanism of the BMI system. As can be seen from the degradation curves, thermal stability of the network was enhanced by OSTS addition in both systems. Decomposition of System A and B were similar with each other. For the Control System, the char yield at 500^oC was 36.84%. However, with only 2wt% OSTS addition, the char yield of System A and B was both improved, which were 42% and 41.95% respectively. This improvement in thermal stability should be ascribed to the POSS inorganic cage structure. This inorganic nature of POSS could stabilize the bulk material against thermal degradation by providing additional heat capacity.

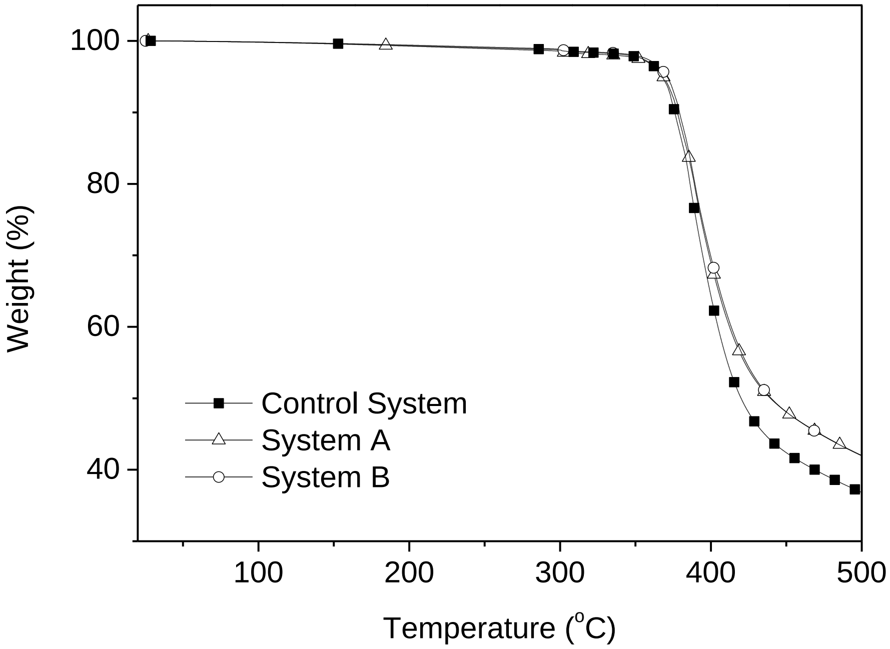

Figure 4.9: TGA curves of the cured BMI, System A and B under nitrogen atmosphere with a heating rate of 20°C/min

TGA diagram of BMI system with different OSTS content in nitrogen atmosphere are shown Figure 4.10. The weight loss of the nanocomposites was in one stage. The temperature for 5wt% weight loss and residual weight at 500°C were summarized in Table 4.5. The onset degradation temperature increased with the increase of OSTS content in the BMI resin. Residual weight was also higher for system with more POSS addition. It was again due to the fact that with more inorganic phase introduction, thermal stability of the BMI nanocomposites was enhanced.

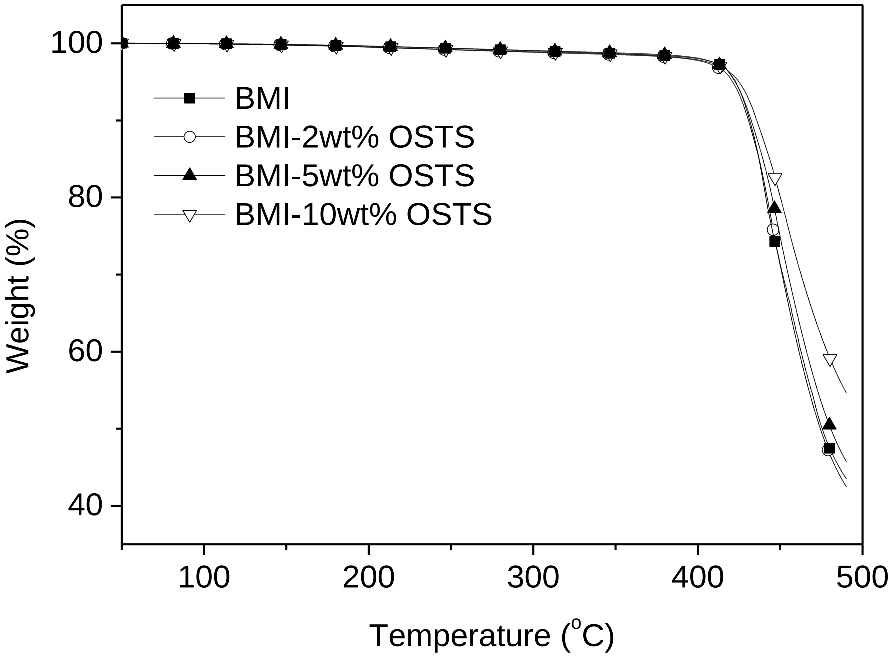

Figure 4.10: TGA curves of BMI systems with different OSTS content under nitrogen atmosphere at 20^{o}C/min heating rate

Table 4.5: Thermal resistance of BMI with different OSTS content under 20^{o}C/min heating rate in nitrogen

System	T_{d1}(^{o}C)	T_{d2}(^{o}C)	T_{d3}(^{o}C)	T_{d4}(^{o}C)	Char Yield (%)
BMI	427	431	437	441	43
2wt % OSTS	421	431	437	442	42
5wt% OSTS	423	432	439	445	46
10wt% OSTS	425	436	443	450	55

TGA analyses in air of BMI/OSTS systems were shown in Figure 4.11 and Table 4.6. Thermal decomposition of C-N bond took place at first in the heating process. Therefore, the onset of degradation does not change much with the increase of OSTS content in the system. However, char yield increased significantly with the incensement in OSTS content. This was due to the formation of SiO_2 at high temperature that can further protect the system from degradation. BMI system with OSTS has very good thermal and oxidative resistance with 10wt% OSTS addition. This was also shown in the derivative curve of TGA, Figure 4.11, BMI with more OSTS in the network, the rate of degradation was slowed down.

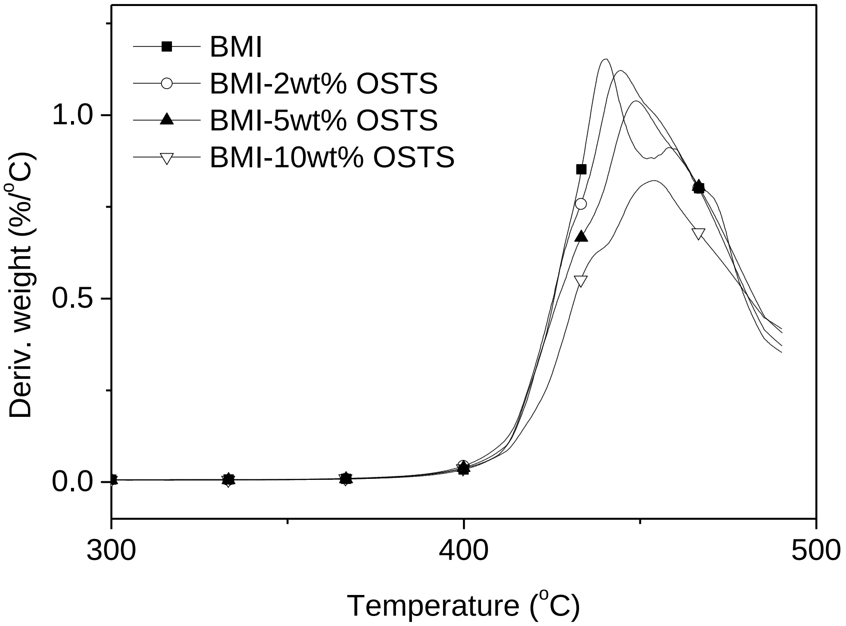

Figure 4.11: Derivative of TGA curves for BMI with different OSTS content under nitrogen atmosphere at 20°C/min heating rate

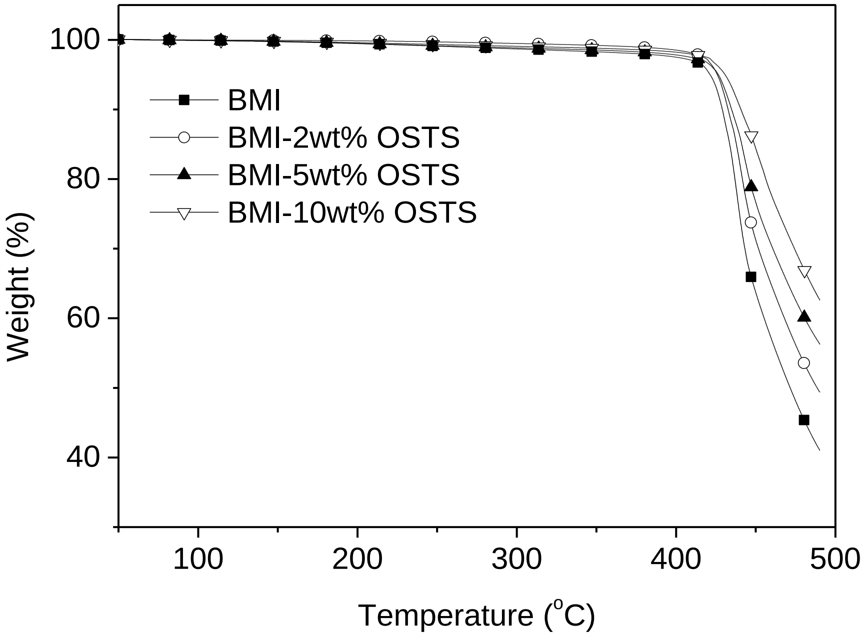

Figure 4.12: TGA curves of BMI with different OSTS content under air atmosphere at 20°C/min heating rate

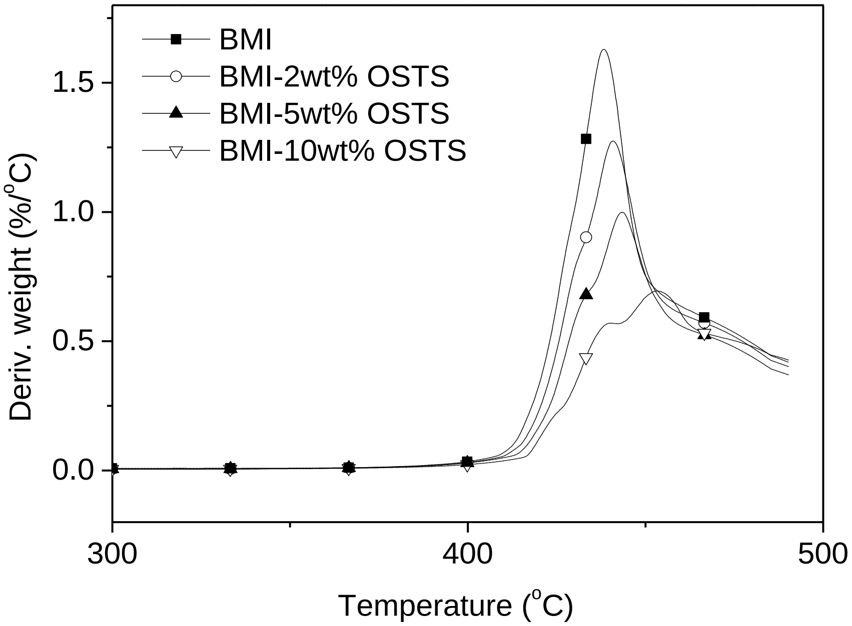

Figure 4.13: Derivative of TGA curves for BMI with different OSTS content under air atmosphere at 20°C/min heating rate

Table 4.6: Oxidative resistance of BMI with different OSTS content under 20°C/min heating rate in air

System	T_{d1}(°C)	T_{d2}(°C)	T_{d3}(°C)	T_{d4}(°C)	Char Yield (%)
BMI	427	431	437	441	43
2wt % OSTS	426	433	437	442	49
5wt% OSTS	426	434	441	446	56
10wt% OSTS	430	440	449	456	62

4.3.1.6 Effect of OSTS on moisture absorption of Bismaleimide network

Moisture uptake of polymer can give indicative information about the network structure characteristics. Studies have been shown that thermosets with lower crosslink density will absorb less moisture as compared to higher crosslink network [23-26]. Water uptake curves as a function of the square root of time normalized to the specimen thickness was shown in Figure 4.14. The equilibrium moisture content of control system was higher than BMI with OSTS. Our postulation for this phenomenon was that when BMI cured with OSTS, dangling chain of OSTS in the network made the network structure less close-packed than control network. As a result, water molecules will not be all trapped or locked into molecular cages and can diffuse out of the system from less close-packed area. This was very important to composite materials which upper service temperature will reduce significantly the moisture locked in.

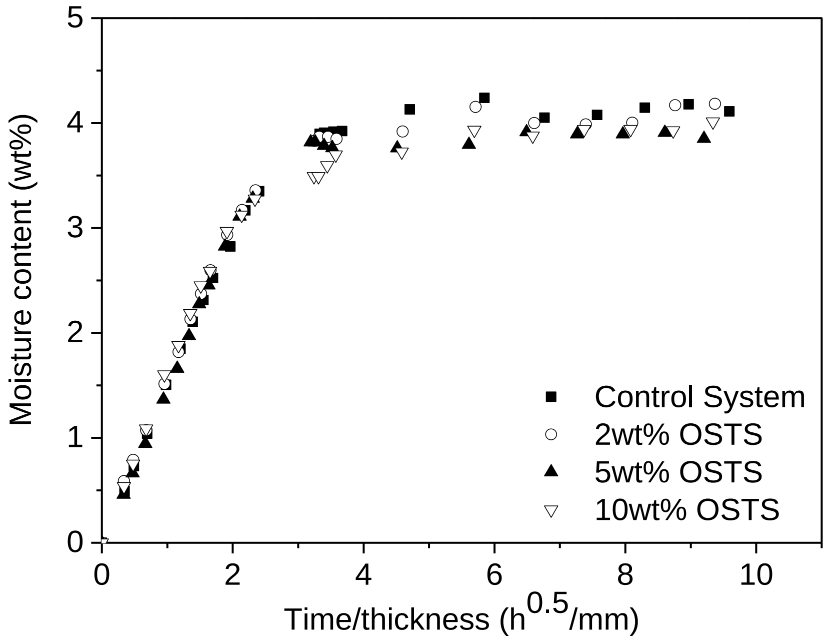

Figure 4.14: Moisture absorption curves of BMI with different OSTS content at 80^{o}C

4.3.2 BMI/N-Phenylaminopropyl POSS (APS) system

4.3.2.1 BMPM/DABPA stoichiometric ratio with additional APS

4.3.2.1.1 DSC study of BMPM/DABPA stoichiometric ratio with additional APS

N-Phenylaminopropyl POSS (APS) contains functional groups of secondary amine. It was known from previous researches that there is Michael addition reaction between maleimide and primary amine groups [27]. Commercial application of diamine modified bismaleimide resin has already been developed [28-30]. The reaction of secondary amine with biamaleimide could happen only under certain conditions [31].

As compared with Octastyrenyl POSS, APS POSS was consisted by a mixture of octa-functional POSS and deca-functional POSS. APS POSS at room temperature was a viscous solution that can be mixed easily with BMI resin during sample preparation stage. The first study of APS POSS with BMI was to find out if it will react with BMI or not. The only possible reaction between APS and BMI is the amine addition to the imide bonds.

APS POSS was mixed with BMPM in acetone and then evaporated in vented hood overnight to obtain a homogenous mixture of BMPM and APS POSS. In order to compare with OSTS POSS, the same weight amount of APS POSS that was 33wt% in BMPM was also used. Dynamic DSC curves of BMPM-33wt% APS was shown in Figure 4.15. As seen in the figure, both APS and OSTS POSS addition will increase the reaction peak temperature. The reaction peak temperature of pure BMPM was 210^{o}C while BMPM with APS and OSTS POSS centered on 240^{o}C. Besides, the reaction rate was significantly decreased by POSS addition. All these information indicated that both APS and OSTS POSS reacted with BMPM and restrain the chain mobility.

Besides the information obtained from the reaction peak, melting peak of BMPM also can tell some information about the effect of POSS on the resin. It was found that melting peak was obviously affected by POSS since it was less as sharp as the pure BMPM. If observe carefully, the onset of melting of BMPM-APS POSS was lower than BMPM-OSTS POSS. This can be explained by the Michael addition of BMPM to APS at lower temperature around 150^{o}C. The reaction between BMPM and APS POSS affected the crystalline structure of BMPM, thus the melting start at lower temperature and finish at lower temperature also. Thus, from all the analysis above, APS POSS is more reactive than OSTS POSS. The reaction mechanism of APS with BMPM was different also. The reaction mechanism of BMPM and POSS was amine addition for BMPM-APS system while it was free radical polymerization for BMPM-OSTS system.

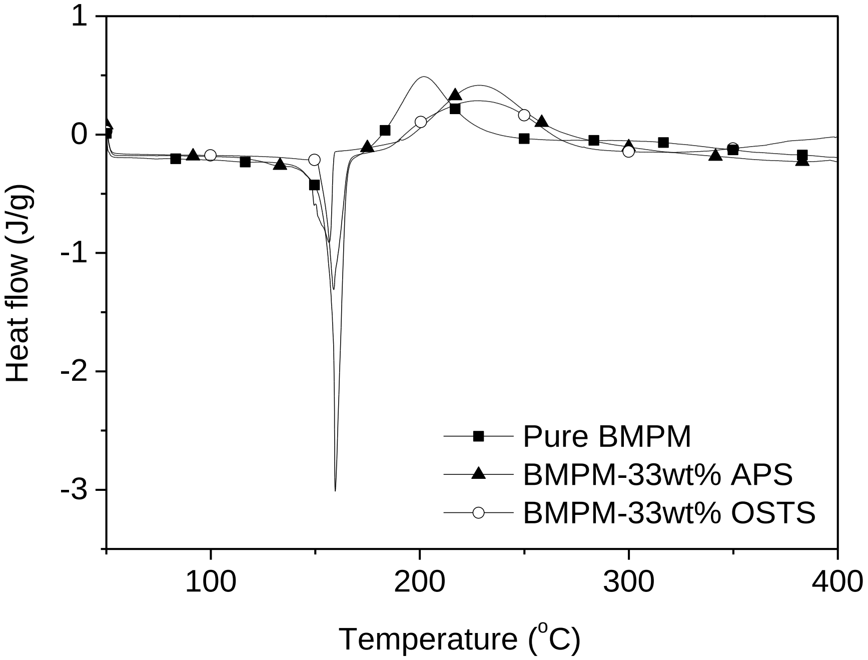

Figure 4.15: Dynamic DSC curves of pure BMPM and BMPM with 33wt% APS, OSTS respectively at 10^{o}C/min heating rate under nitrogen atmosphere

In order to compare the effect of POSS on the thermal properties of BMI resin, 2, 5 and 10wt% additional APS was added into the network. DSC curves of these samples were shown in Figure 4.16. Heat of reaction was obtained by integrating the area underneath the curve. The heat of reaction of these systems was summarized in Table 4.7. It can be seen in the DSC curves that curing peak temperature was slightly increased in BMI-APS systems. With higher content of APS added into BMI resin, the percentage of cure for the first reaction peak was decreased subsequently. This was due to the fact that reaction of APS and BMPM will consume some BMPM for crosslink reaction with DABPA. Besides, Michael reaction between APS and BMPM would restrain the chain mobility especially when the network was consisted by aromatic rings. As a result, the crosslink reaction between BMPM and DABPA may be hindered.

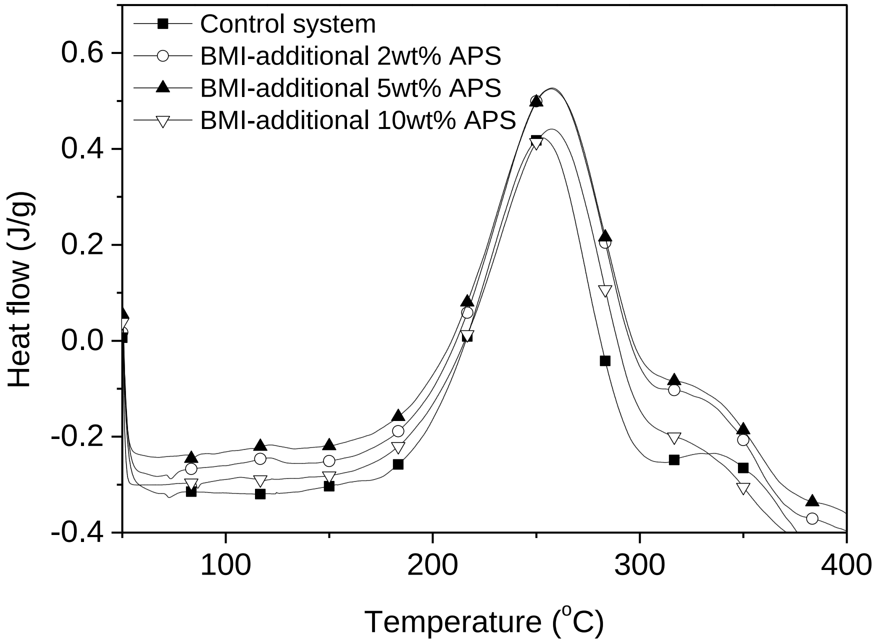

Figure 4.16: Dynamic DSC curves of BMPM: DABPA (1:1 molar ratio) with additional 2, 5 and 10wt% APS at 10°C/min heating rate

Table 4.7: Heat of reaction for BMPM: DABPA (1:1 molar ratio) with additional 2, 5 and 10wt% APS

System	Overall (J/g)	First peak (J/g)	α (%)
Control	368	339	92
2wt% APS	365	329	90
5wt% APS	343	313	91
10wt% APS	379	333	88

*α represents the percent of cure at the end of first reaction peak

4.3.2.1.2 DMA study of BMPM/DABPA stoichiometric ratio with additional APS

Dynamic DMA was performed BMI/additional APS systems as a function of temperature. Storage modulus of BMI resin with additional APS POSS was shown in Figure 4.17 and glass transition temperature was shown in Table 4.8, which was determined as the onset temperature when storage modulus begins to drop. It was noted that all BMI/APS hybrids had higher Tg values than BMPM/DABPA resin. This indicated that with APS added into the resin, thermal resistance of BMI resin was significantly improved. The control BMPM/DAPBA resin was different from the resin used for BMI-OSTS POSS system due to different batch of BMPM received from the company. The glass transition temperature of this control system was lower than previous study. The Tg value of BMI-APS POSS was significantly higher than the control network when 5wt% POSS was added into the network. When 10wt% APS POSS was added into the resin, the Tg was decreased again as compared to BMI-5wt% APS POSS. This result can be attributed to the effect of APS POSS on the crosslinked structure.

As discussed in the above DSC study, there was Michael reaction between –NH groups in the APS molecule and double bonds in imide rings of BMPM. This reaction in one way can effectively contribute to the homogenous dispersion of APS POSS in BMI resin. However, on the other side, it would inhibit some segmental motion in the BMI resin due to the high rigidity of APS POSS and thus lead to higher Tg values. Besides this, Michael addition also restrains the chain mobility, especially in network formed by aromatic rings. However, it also would show up the negative role on reducing the Tg values of the resultant curing network. With increased amount of APS POSS introduced into the network, the reaction between APS POSS and BMPM made the system DABPA rich and also hinder the further stage of curing reaction between BMPM and DABPA. Similar phenomenon was also reported by other researchers [32,22]. The tand curve also provides information about the network. When inorganic particles were added into polymer system, the tand peak would be suppressed. The continuous drop of tand peak value in BMI-APS POSS system when more APS POSS added into the network was observed. The peak shape also became broader with increased POSS amount. Although BMI-10wt% APS had lower Tg than BMI-5wt% APS, its peak was broader. All the information indicated that APS POSS inhibited the chain movement.

When comparing BMI-APS POSS system with BMI-OSTS POSS system, it can be seen that OSTS POSS continuously increase the Tg of the resin and depress the tand peak value with higher amount of OSTS POSS addition. Besides, the incensement in Tg was slower than the BMI-APS POSS system. These indicated that OSTS POSS was not as reactive as APS POSS. The incorporation of OSTS POSS may not all be the reaction incorporation. Thus, the chain movement might be inhibited by decreased free volume in the system other than the chemical bonds between the POSS molecule and BMI resin.

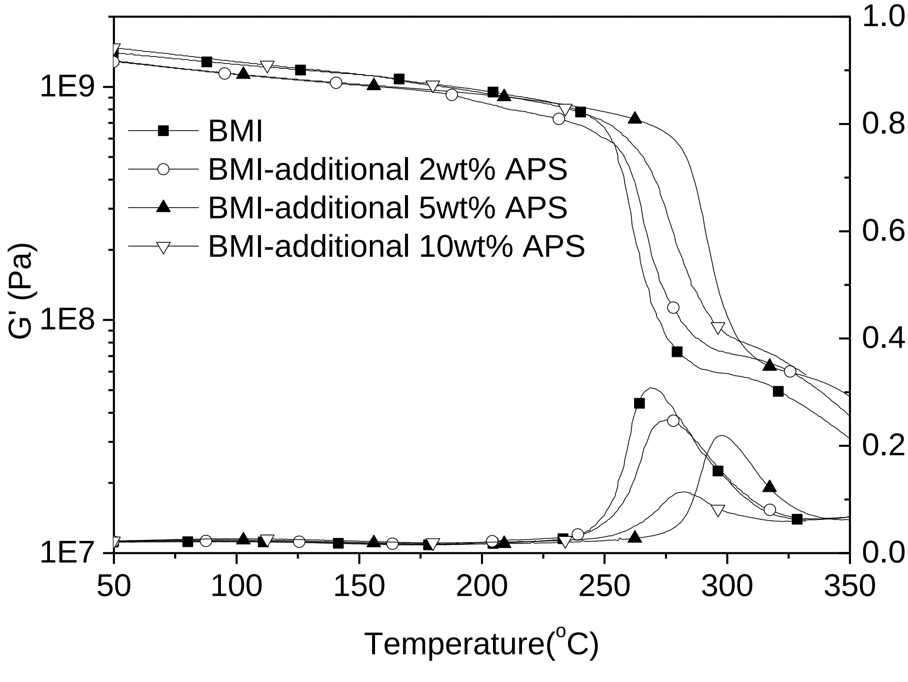

Figure 4.17: Shear modulus and tanδ vs. temperature of BMPM: DABPA (1:1 molar ratio) with additional 2, 5 and 10wt% APS

Table 4.8: Glass transition temperature of cured BMPM: DABPA (1:1 molar ratio) with additional APS

System	Tg (^oC)
Control	255
2wt% APS	261
5wt% APS	284
10wt% APS	265

4.3.2.1.3 Thermal resistance of cured BMPM/DABPA stoichiometric ratio with additional APS

The degradation behavior of cured BMPM/DABPA resin and BMPM/DABPA/APS composites were investigated by TGA analysis under N_2 atmosphere. TGA curves of these systems were shown in Figure 4.18. The typical data, T_{d1}, T_{d2}, T_{d3} and T_{d4}, temperature at 5, 10, 15 and 20% weight loss were summarized in Table 4.9. Single step decomposition was observed, which indicated that APS does not alter the decomposition mechanism of the BMI system. It can be seen that all composites have similar decomposition temperature values that also indicated that similar degradation mechanism. Interesting, compared with BMPM/DABPA resin, resin with 5wt% APS has slightly increased char yield value. This was different from BMI with OSTS system. The char yield values of BMI-OSTS constantly increased with the increased content of OSTS. The high yield value was mainly attributed to the high char yield value of OSTS.

This difference between BMI-OSTS and BMI-APS system was mostly due to the different reaction mechanism of incorporating these two different kinds of POSS into the BMI resin. For BMI-APS system, Michael addition between imide bonds and –NH groups of APS can happen at lower temperature range and it deprived some BMPM for further curing reaction with DABPA. As a result, the resultant network crosslink density might be lower when higher amount of APS was added into the system. This can explain the lowered char yield value of BMI-10wt% APS system than BMI-5wt% APS. On the other side, the reaction between OSTS and BMPM cannot happen until BMPM self-generate free radical above 200°C. It would a competition reaction between BMPM to DABPA and BMPM to OSTS. Besides, the double bonds of OSTS had steric hindrance that would make the reaction between BMPM and OSTS difficult.

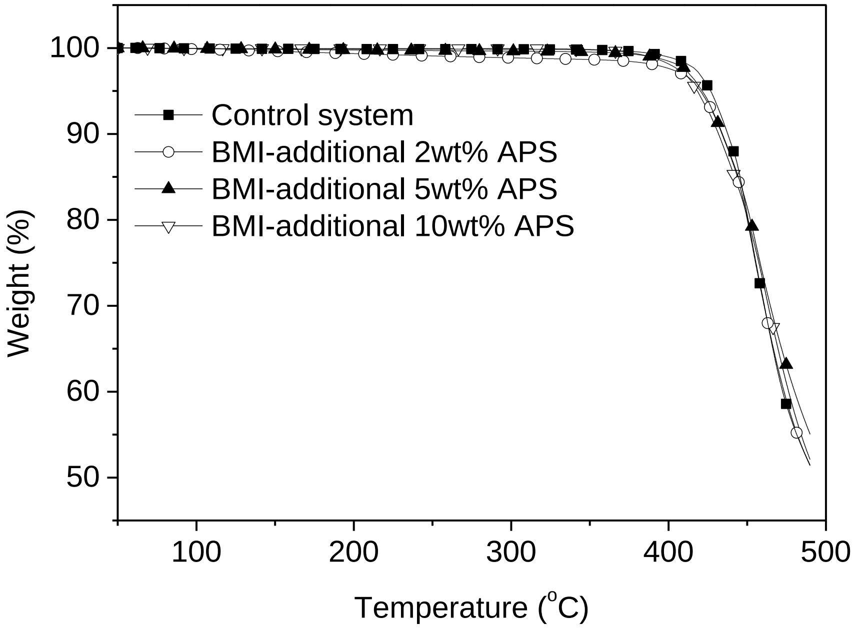

Figure 4.18: TGA profiles of cured BMPM: DABPA (1:1 molar ratio) with additional 2, 5 and 10wt% APS

Table 4.9: Degradation temperatures of cured BMPM: DABPA (1:1 molar ratio) resin with additional APS

System	T_{d1}(°C)	T_{d2}(°C)	T_{d3}(°C)	T_{d4}(°C)	Char Yield (%)
BMI	427	436	445	451	51
2wt % APS	420	434	444	450	51
5wt% APS	421	434	444	452	55
10wt% APS	418	432	442	451	52

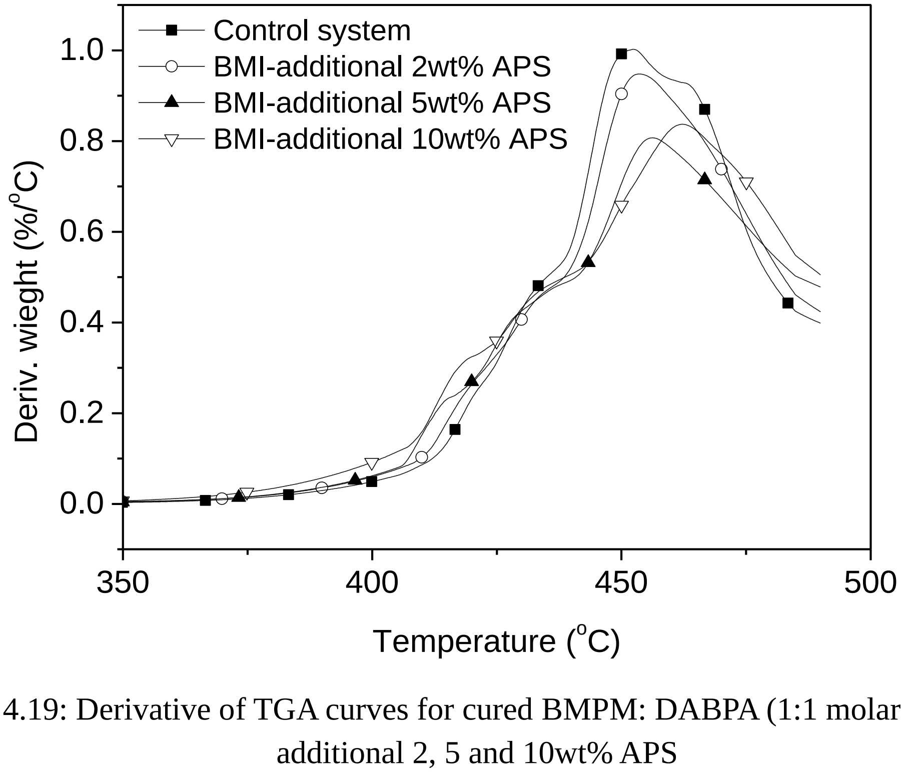

Figure 4.19: Derivative of TGA curves for cured BMPM: DABPA (1:1 molar ratio) with additional 2, 5 and 10wt% APS

Derivative degradation curves of BMI-APS system were shown Figure 4.19. The slope of the curve indicates weight loss rate of the system and the peak value of the curve represents the maximum weight loss rate in the system. It can be seen from the curve that when APS was added into the system, the maximum weight loss rate was suppressed. This was due to the protection of POSS that was inorganic in nature. Besides, the peak temperature also shifted to higher range with increased amount of APS in the system. Again, with 10wt% APS in the system, maximum weight loss rate was higher than BMI resin with 5wt% APS although the peak temperature was shifted to slightly higher range. There was competition between the effect of APS protecting the network and the hindrance of APS on further cure reaction of BMPM and DAPBA.

4.3.2.1.4 Moisture uptake of cured BMPM/DABPA stoichiometric ratio with additional APS

Moisture uptake of polymer can give indicative information about the network structure characteristics. Although studies have been shown that thermoset with lower crosslink density will absorb less moisture as compared to higher crosslink network [23-26], our research on BMI/DCP system showed that when the network has high crosslink density but un-homogenous network, water molecule will not all be trapped into the network. It can move in and out of the network from relatively less crosslinked area. Water uptake curves as a function of the square root of time normalized to the specimen thickness was shown in Figure 4.20. The equilibrium moisture content of BMI with additional 2 and 5wt% APS was consistently decreased with higher content of APS. This phenomenon was in the same trend as the glass transition temperature enhancement by APS to the network. Our postulation for this phenomenon was that when BMI react with APS, some localized crosslink density was enhanced. However, free volume around APS would be larger than the control system. As a result, water molecules will not be all trapped or locked into molecular cages and can diffuse out of the system from higher free volume area. This was very important to composite materials which upper service temperature will reduce significantly the moisture locked in. For BMI with 10w% additional APS which showed higher equilibrium moisture uptake than the control system, it might be due to fact that over amount of APS made the system DABPA rich, some localized crosslink density maybe enhanced by APS addition, but the DABPA rich made the system in general less crosslinked compared with control network.

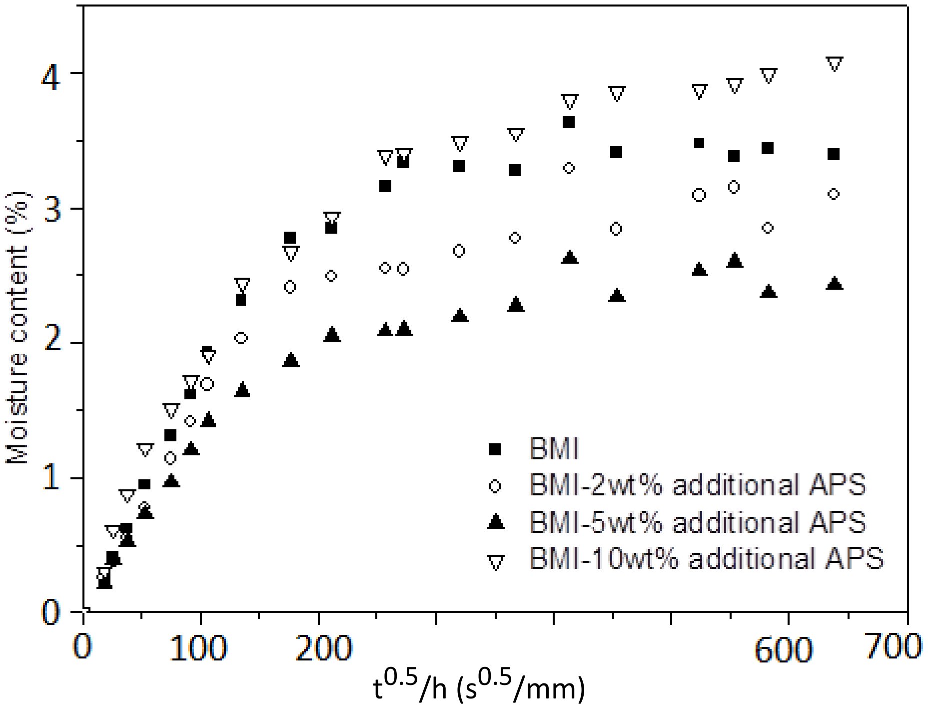

Figure 4.20: Moisture absorption curves of cured BMI consisted by BMPM: DABPA (1:1 molar ratio) with additional 2, 5 and 10wt% APS at 80°C

4.3.2.2 Non-stoichiometric ratio of BMPM/DABPA resin with APS

4.3.2.2.1 DSC study of BMPM/DABPA non-stoichiometric ratio with APS

Due to the reaction between APS and BMPM, higher amount of APS would make the molar ratio of BMPM to DAPBA off stoichiometric. In other words, system studied above might be DABPA rich. In industry application, DABPA rich was not preferred because it will decrease the thermal resistance of the resin. Thus, it is necessary to find out how the thermal properties of BMI-APS system would be changed or possible further enhanced if the amount of reaction groups in APS plus DABPA were the same as reaction groups in BMPM. To investigate this, BMPM/DABPA with 2, 5 and 10wt% APS was again chose to added into the BMI resin. If reaction groups from APS were not all reacted with BMPM, the system would be slightly BMPM rich. As a result of that, Tg of network would be higher due to higher BMPM to DAPBA ratio in the system.

Dynamic DSC curves of BMPM/DABPA non-stoichiometric system with APS were shown in Figure 4.21. As compared to control system, the secondary reaction peak of BMI/APS system was suppressed, especially when 10wt% APS was added into the resin. This was due to the fact that the system was slightly BMPM rich as compared to the control system. The reaction peak temperature was also shifted to higher values with APS addition, which was due to the Michael addition reaction between APS and BMPM. The bulky cage of APS would restrain the chain movement, thus the reaction was shifted to higher temperature range. Heat of reaction was summarized in Table 4.10. Percent of cure after the first reaction peak was summarized in the table also. Reaction underneath the first peak represents major crosslink reaction in the network. The second reaction peak that was due to the etherification of –OH groups in DABPA. The suppression of second reaction peak in BMI-additional 10wt% APS was about the same as BMI-10wt% APS. This indicated that the reaction of APS and BMPM would inhibit crosslink reaction at higher temperature whether the BMPM to DAPBA molar ratio off stoichiometric or not.

Table 4.10: Heat of reaction of non-stoichiometric ratio BMPM/DABPA resin with APS

System	Overall (J/g)	First peak (J/g)	Percentage of cure (%)
Control	368	339	92
2wt% APS	402	357	89
5wt% APS	401	353	88
10wt% APS	390	353	91

*α represents the percent of cure at the end of first reaction peak

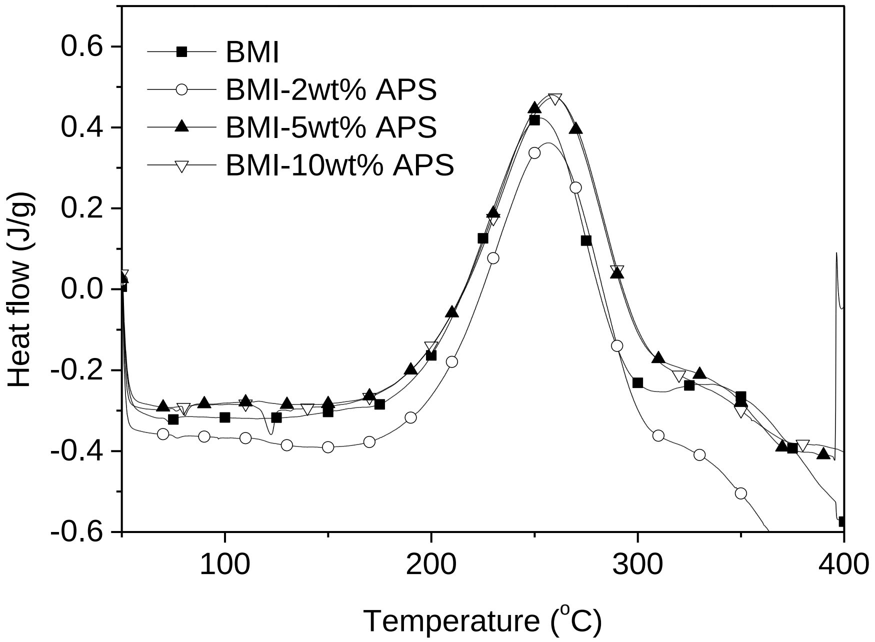

Figure 4.21: Dynamic DSC curves of non-stoichiometric ratio of BMPM/DABPA resin with APS

4.3.2.2.2 DMA study of BMPM/DABPA non-stoichiometric ratio with APS

Dynamic DMA was performed on BMPM/DABPA non-stoichiometric ratio with APS systems as a function of temperature. Storage modulus of BMI resin with additional APS POSS was shown in Figure 4.22 and glass transition temperature was shown in Table 4.11, which was determined as the onset temperature when storage modulus begins to drop. It was noted that all BMI/APS hybrids had higher Tg values than BMPM/DABPA resin. This indicated that with APS added into the resin, thermal resistance of BMI resin was significantly improved.

The hypothesis of this study was to investigate the off stoichiometric ratio of BMPM to DAPBA effect on the Tg of BMI-APS network. This off stoichiometric molar ratio was that BMPM was slightly richer than DABPA to compensate the amount of BMPM reacted with APS. The molar ratio of BMPM to DABPA will return to stoichiometric molar ratio if all reaction groups from APS react with BMPM. If so, the Tg of this BMI/APS system should be higher than previous BMI with additional APS systems since those systems were sligtly DABPA rich. However, as can be seen in Table 4.11, Tg was almost the same as the BMI with addition APS. Beside, system with 5wt% APS did showed a significantly increasement in Tg as the previously studied BMI with additional 5wt% APS system. This might be due to the effect of Michael reaction between APS and BMPM. The further reaction between BMPM and DABPA might be inhibited due to APS addition. This phenomenon also indicated that Tg of BMI-APS system was more depend on the amount of APS in the resin other than the molar ratio between BMPM and DABPA.

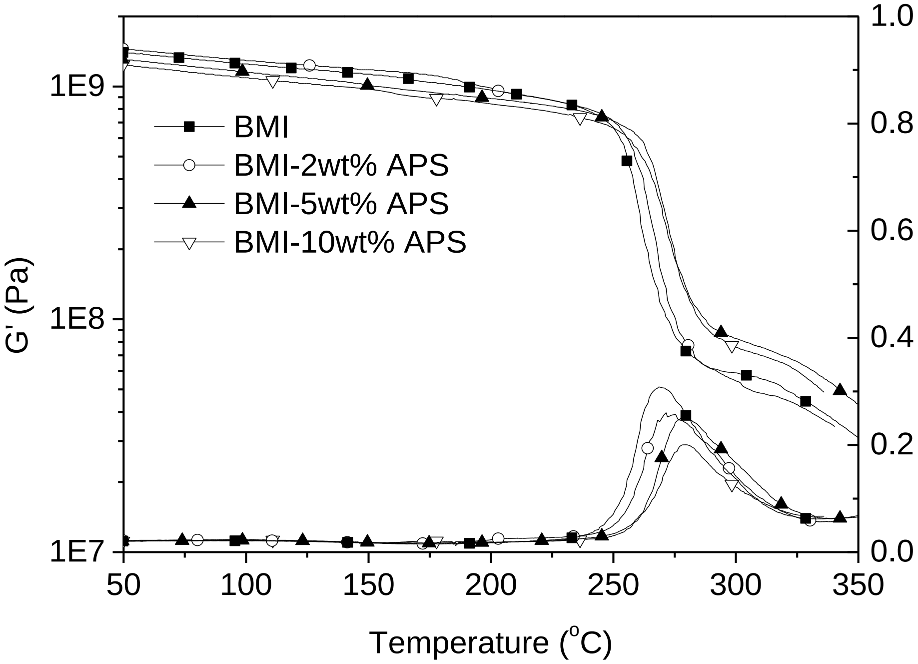

Figure 4.22: Shear modulus and tanδ vs. temperature of BMPM/DABPA non-stoichiometric ratio with APS

Table 4.11: Glass transition temperature of BMPM/DABPA non-stoichiometric ratio with APS

System	Tg (°C)
Control	255
2wt% APS	260
5wt% APS	265
10wt% APS	264

4.3.2.2.3 TGA study of BMPM/DABPA non-stoichiometric ratio with APS

The degradation behavior of cured BMPM/DABPA resin and BMI with APS composites were investigated by TGA analysis under N_2 atmosphere. TGA curves of these systems were shown in Figure 4.23. The typical data, T_{d1}, T_{d2}, T_{d3} and T_{d4}, temperature at 5, 10, 15 and 20% weight loss were summarized in Table 4.12. Single step decomposition was observed, which indicated that APS does not alter the decomposition mechanism of the BMI system. It can be seen that all composites have similar decomposition temperature values that also indicated that similar degradation mechanism. Onset degradation temperature was slightly higher in BMI-APS system. Besides, the char yield of BMI/APS at the end was higher in BMI-additional APS system. Especially for BMI-10wt% APS, char yield increased about 6% than BMI-additional10wt% APS. This enhancement in thermal stability was due to actual higher weight content of APS in the system. The APS POSS cage can protect the system from degradation and char yield should be higher since the POSS cage will be preserved. On the other hand, BMI-additional APS system was in fact DABPA rich due to the consumed BMPM by APS. As a result, any unreacted DABPA molecules will contribute to the weight loss at the end.

Derivative degradation curves of BMI-APS system were shown Figure 4.24. The slope of the curve indicates weight loss rate of the system and the peak value of the curve represents the maximum weight loss rate in the system. It can be seen from the curve that when APS was added into the system, the maximum weight loss rate was suppressed. This was due to the protection of POSS that was inorganic in nature. Besides, the peak temperature also shifted to higher range with increased amount of APS in the system. Again, with 10wt% APS in the system, maximum weight loss rate was lower than BMI-additional 10wt% APS system.

Table 4.12: Degradation temperatures of BMPM/DABPA non-stoichiometric ratio with APS

System	T_{d1}(°C)	T_{d2}(°C)	T_{d3}(°C)	T_{d4}(°C)	Char Yield (%)
Control	427	436	445	451	51
2wt % APS	423	435	444	450	53
5wt% APS	422	435	445	452	50
10wt% APS	421	435	446	455	58

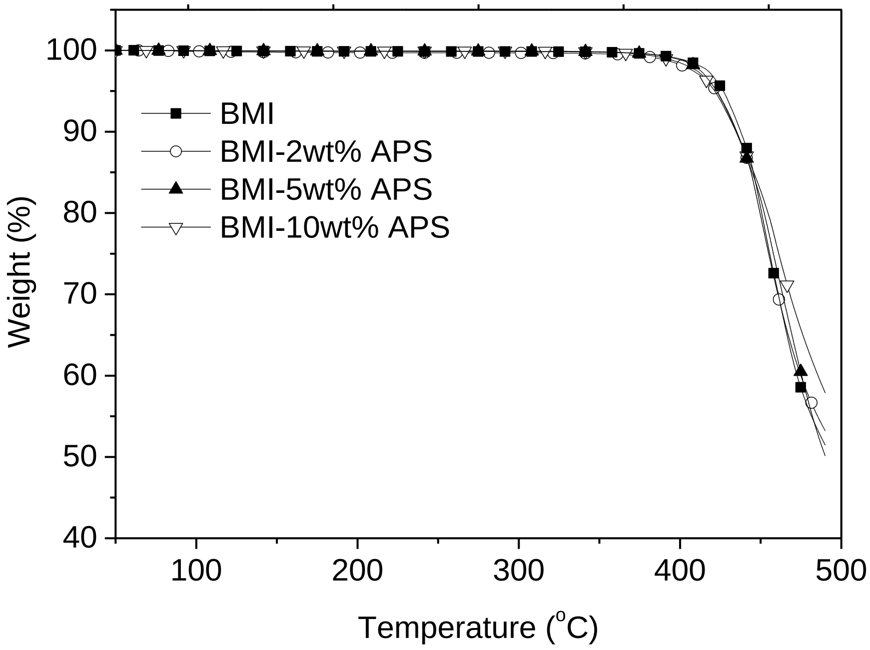

Figure 4.23: TGA profiles of non-stoichiometric ratio of BMPM/DABPA resin with APS

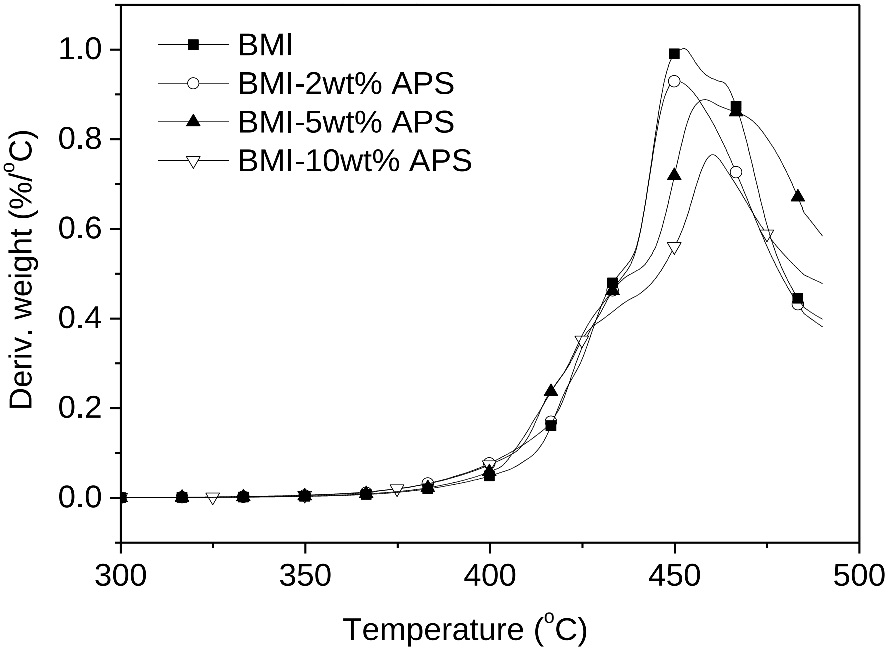

Figure 4.24: Derivative of TGA curves for non-stoichiometric ratio BMPM/DABPA resin with APS

4.3.2.2.4 Moisture uptake of cured BMI network based on BMPM/DABPA non-stoichiometric ratio with APS

Moisture uptake of BMI network based on BMPM/DABPA non-stoichiometric ratio with APS as a function of the square root of time normalized to the specimen thickness was shown in Figure 4.24. The study chose 2 and 10wt% APS as representative study. Since above stoichiometric BMPM to DABPA study showed that 2wt% APS can slight change the network structure when 10wt% APS would significantly affect the reaction and network formation of BMI. The initial rate of water uptake was almost the same between BMI control system and BMPM/DABPA non-stoichiometric ratio with 2 and 5wt% APS. The equilibrium moisture content of BMI with 2wt% APS was higher than the control system while BMI with 10wt% APS showed lower moisture uptake. This was due to the fact that not every single amine groups in APS will react with BMPM. With higher amount of APS in the network, it will make the system more BMPM rich. When BMPM was rich in the network, the final crosslink density will be higher. With higher crosslink density, the network will absorb less water due to the inhomogeneity of the network. Although the APS should increase the free volume area due to the POSS cage, the moisture uptake was a combination effect of both free volume due to APS and crosslink density due to BMPM.

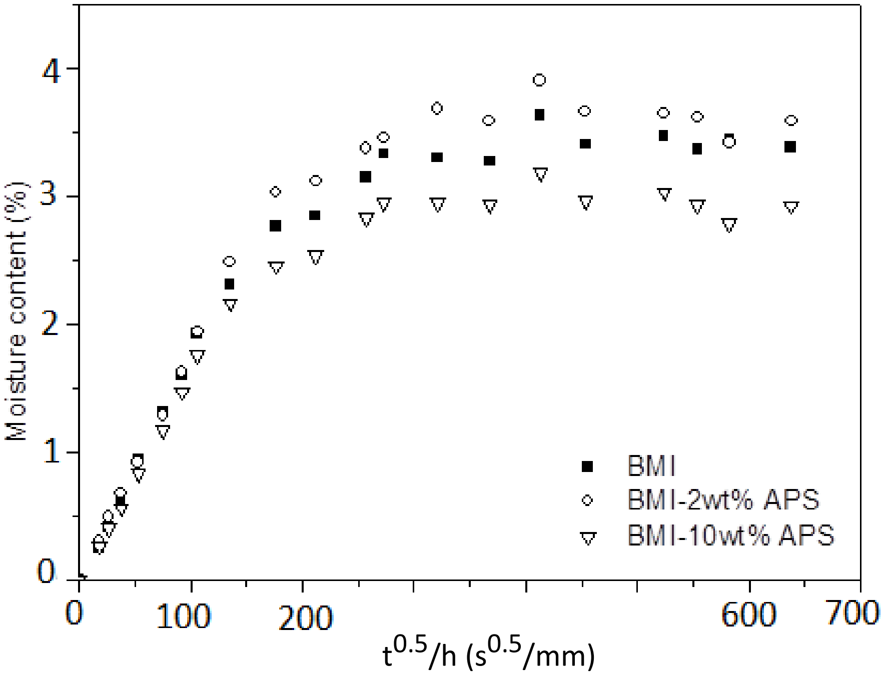

Figure 4.25: Moisture absorption curves of cured BMI consisted by non-stoichiometric ratio of BMPM/DABPA resin with 2 and 10wt% APS at 80°C

4.4 Conclusions

The major finding in this chapter involved with two different kinds of POSS, OSTS and APS, addition on the thermal mechanical properties of BMPM/DABPA based bismaleimide thermoset. Cure reaction and mechanism, glass transition temperature of cured network, thermal degradation stability and moisture uptake of cured BMI/POSS system were investigated with different weight content of POSS in the system. For BMI/APS system, molar ratio of BMPM to DABPA was further investigated on the thermal mechanical properties of BMI network.

In BMI/OSTS study, the effect of mixing sequence of OSTS into BMI system was investigated based on BMI/additional 2wt% OSTS. No significant effect of POSS on the thermal mechanical properties of BMI network was observed. However, by mixing OSTS with DABPA first, higher content of OSTS can be homogenously dispersed in BMI network. With more content of OSTS in the system, the thermal mechanical property of BMI/OSTS nanocomposites was systematically enhanced. This was due to the free radical polymerization of OSTS with BMPM. The bulky POSS cage would retard the chain movement, thus increase glass transition temperature of BMI system. The inorganic natures of POSS cage also protect the BMI network from degradation under both nitrogen and air condition. Especially for BMI/additional 10wt% OSTS which char yield under air condition was 30wt% higher than the control system. The inclusion of OSTS in the network also decrease the possibility of water molecule locked in the system, which in turn enhanced the service life of this BMI composite.

In BMI/APS study, different amount of APS was added into BMI network to compare its effect on the thermal mechanical properties of the network with OSTS. Major difference between APS and OSTS is the reaction with BMPM. APS can reaction with BMPM through Michael addition reaction that can occur around 150^{o}C. OSTS reacted with BMPM through free radical polymerization, which requires higher temperature up to 200^{o}C when BMPM can generate free radicals. APS addition at 5wt% significantly improved the glass transition temperature of the network, around 30^{o}C higher than the control system. With higher content of APS, glass transition temperature start to decrease, which was due to the reaction between APS and BMPM made the system DABPA rich. Thermal degradation behavior of BMI/additional APS did not show significant improvement as the BMI/additional OSTS system. This might due to the fact that the functional groups on OSTS were aromatic while the functional groups on APS were allylic groups. Besides, the C-N bonds in APS were weaker than C-C bonds in OSTS. To compensate the amount of BMPM consumed by APS, higher molar ratio of BMPM to DAPBA was also investigated with 2 and 10wt% APS. From DSC, DMA and TGA analysis, it turned out that the properties of BMI network was more relied on APS than the molar ratio between BMPM to DABPA.

REFERENCES

REFERNECES

1. Zhuo, D.X., Gu, A.J., Liang, G.Z., Hu, J.T. and Yuan, L., Novel high performance functionalized ladderlike polyphenylsilsesquioxane/bismaleimide hybrids with very good flame retardancy, thermal, and dimensional stability, Journal of materials science, vol.46, pp7649-7659, 2011.

2. Guo, Q.P., Zheng, H.F., Zheng, S.X., Mi, Y.Q. and Zhu, W., Phase behavior, mechanical properties and thermal stability of thermosetting polymer blends of unsaturated polyester resin and poly(ethylene oxide), Journal of materials science, vo..34, pp123-128, 1999.

3. Jang, J.Y., Nam, S.J., Chung, D.S., Kim, S.H. and Park, C.E., High Tg cyclic olefin copolymer gate dielectrics for N,N'-ditridecyl perylene dilmide based field-effect transistors: improving performance and stability with thermal treatment, Advanced functional materials, vol.20, pp2611-2618, 2010.

4. Chen, X.L., Yu, J., Guo, S.Y., Lu, S.Q., Luo, Z. and He, M. Surface modification of magnesium hydroxide and its application in flame retardant polypropylene composites, Journal of materials science, vol.44, pp1324-1332, 2009.

5. Ho, T.H., Hwang, H.J., Shieh, J.Y. and Chung, M.C., Thermal, physical properties and flame retardant properties of phosphorus containing epoxy cured with cyanate ester, Reactive and functional polymers, vol.69, pp176-182, 2009.

6. Chang, C.W., Lin, C.H., Lin, H.T., Huang, H.J. and Hwang, K.Y., Development of an aromatic triamine-based flame-retardant benzoxazine and its high-performance copolybenzoxazines, European polymer journal, vol. 45, pp680-699, 2009.

7. Mackay, M.E., Tuteja, A., Duxbury, P.M., Hawker, C.J., Horn, B.V., Guan, Z.B., Chen, G.H. and Krishnan, R.S., General strategies for nanoparticle dispersion, vol.311, pp1740-1743, 2006.

8. Belva, F., Bourbigot, S., Duquesne, S., Jama, C., Bras, M.L., Pelegris, C. and Rivenet, M., Heat and fire resistance of polyurethane-polydimethylsiloxane hybrid materials, vol.17, pp304-311, 2006.

9. Zhu, Y., Sun, D.X., Zheng, H., Wei, M. and Zhang, L.M., Improvement in properties of epoxy based electrophoretic coating by silica/polyurethane nanocomposites, Journal of materials science, vol.42, pp545-550, 2007.

10. Liang, K.W., Toghiani, H., Li, G. Z., Pittman, C.U., Synthesis, morphology, and viscoelastic properties of cyanate ester/polyhedral oligomeric silsesquioxane nanocomposites, Journal of polymer science Part A: polymer chemistry, vol.43, pp3887-3898, 2005.

11. Li, Y., Gu, A.J. and Liang, G.Z., Microcapsule-modified bismaleimide resins, Composites science and technology, vol.68, pp2107-2113, 2008.

12. Baker, E. Gidden, J., Anderson, S. E. and Haddad, T.S., Isomeric structural chacterization of polyhedral oligomeric silsesquioxane with styryl and epoxy phenyl capping agent, Nano Letters, vol.4, pp779-785, 2004.

13. Bizet, S., Galy, J. and Gerard, J. F., Structure-property relationships in organic-inorganic nanomaterials based on methacryl-POSS and dimethacrylate networks, Macromolecules, vol.39, pp2574-2583, 2006.

14. Cardoen, G. and Coughlin, E. B., Hemi-telechelic polystyrene-POSS copolymers as model systems for the study of well-defined inorganic/organic hybrid materials, Macromolecules, vol.37, pp5123-5126, 2004.

15. Chen, Q., Xu, R.W. and Zhang, J., Polyhedral oligomeric silsesquioxane (POSS) nanoscale reinforcement of thermosetting resin from benzoxazine and bisoxazoline, Macromolecular rapid communications, vol.26, pp1878-1882, 2005.

16. Zhang, J., Xu, R.W. and Yu, D.S., A novel and facile method for the sythesis of octa(aminophenyl)silsesquoixane and its nanocomposites with bismaleimide diamine resin, Journal of applied polymer science, vol.13, pp1004-0, 2007.

17. Ozawa, T., Kinetics of non-isothermal crystallization, Polymer, vol.12, pp150-158, 1971.

18. Stenzenberger, H.D., Koenig, P. and Canning, M.S. Toughened bismaleimides: concepts, achievements, directions, International Sampe Technical Conference, vol.19, pp372-385, 1987.

19. Chattha, M.S. and Dickie, R.A., Dynamic mechanical analysis of bismaleimidodiphenyl methane and diallylbisphenol A crosslinked polymers, Journal of applied polymer science, vol.40, pp411-416, 1990.

20. Mijovic, J. and Andjelic, S., Study of the mechanism and rate of bismaleimide cure by remote in-situ real time fiber optic near-infrared spectroscopy, Macromolecules, vol.29, pp239-246, 1996.

21. Boris, A.R, Emma, A.D, Roger, M. and Eugene, S., High performance bismaleimide matrices: cure kinetics and mechanism, Polymers for advanced technologies, vol13, pp837-844, 2002.

22. Roger, M., Eugene, S and Jason, E.L. Handbook of Thermal Analysis and Calorimetry, vol.3, 2002.

23. R.J. Morgan, E.E. Shin, J.E.Licoln and J.Zhou, Higher temperature polymer matrix-carbon fiber composites, Proceedings of 43rd International SAMPE symposium, Anaheim, CA, pp106-119, 1998.

24. Barton, J.M., Effect of absorbed water on the thermal relaxation of biaxially stretched crosslinked poly(methylmehtacrylate), Polymer, vol.20, 8-1024, 1979.

25. Diamant, Y., Marom, G. and Broutman, L.J., The effect of network structure on moisture absorption of epoxy resin, Journal of applied polymer science, vol.26, pp3015-3025, 1981.

26. Gordon, G.A. and Ravve, A., Oxygen transmission through highly crosslinked polymers, Polymer engineering and science, vol.20, pp70-77, 1980.

27. Liang, G.Z., Hu, X.L., Aluminum borate whiskers reinforced bismaleimide composites. 1: preparation and properties, Polymer international, vol.53, pp670-674, 2004.

28. Wang, C.S., Leu, T.S. and Hsu, K.R., Novel bismaleimide with naphthalene side group. 1. From 1-naphthaldehyde and 2,6-dimethylaniline, Polymer, vol.39, pp2921-2927, 1998.

29. Grenier, M.F. and Cunha, L.D., Influence of steric hindrance on the reactivity and kinetics of molten state radical polymerization of binary bismaleimide-diamine systems, Polymer, vol.39, pp1799-1814, 1998.

30. Kim, D.S., Han, M.J., Lee, J.R. and Chang, J.Y., Cure behavior and thermal stability of an epoxy : new bismaleimide blends for composites matrices, Polymers for advanced technologies, vol.5, pp287-291, 1994.

31. Tungare, A.V. and Martin G.C., Analysis of the curing behavior of bismaleimide resins, Journal of applied polymer science, vol.46, 1125-1135, 1992.

32. Kim, K.M., Ogoshi, T. and Chujo, Y., Controlled polymer hybrids with ladderlike polyphenylsislsesquioxane as a template via the sol-gel reaction of phenyltrimethoxysilane, Journal of polymer science part a : polymer chemistry, vol.43, 473-478, 2005.

33. Li, G.Z., Jin, Y., Shi, L.H., Ye, M.L. and Bai, F., Miscibility of polystyrene (PS)/polyphenylsilsesquioxane (PPSQ) blends, vol.34, pp1079-1084, 1996.

CHAPTER 5: COMBINED EFFECT OF N-PHENYLAMINOPROPYL POSS AND TRIGONOX®101 ON CURE AND THERMAL PROPERTIES OF 4, 4'-BIS-MALEIMIDODIPHENYLMETHANE AND O, O'-DIALLYL BISPHENOL A BASED BISMALEIMIDE NETWORK

5.1 Introduction

The combination of organic and inorganic materials is old challenge in polymer research. Inorganic fillers such as minerals and clays were added into the polymer system to improve thermal stability and mechanical properties. These new composites materials can be applied in many fields, such as optics, electronic and so on [1-7]. In composites, the interface between two different materials is very important to durability. In general, the major goal is always to form a material with improved properties.

Molecular level mixing between two different materials has been under research since the late 1980s, especially the molecular level combination between polymer and inorganic materials [8-15]. Nanoscopic inorganic fillers, Polyhedral Oligomeric Silsesquioxanes (POSS), has received a lot of attention in recent years. POSS molecules with organic functional groups are compatible with polymers，providing vast possibilities for designing new hybrid materials [16-24]. Although the combination of POSS into polymer did exhibit dramatic physical and chemical properties superior to their micro-phase counterpart, enhancement on thermal mechanical properties of polymer by POSS addition was still limited.

The use of peroxides in polymer has been studied for decades. Peroxides were used to initiate polymerization, attach functional groups onto polymer chain as well as enhance high temperature performance of thermoset [25-32]. Polymer and peroxide reaction are mainly consisted by competing mechanisms. The reaction is determined by polymer nature and concentration as well as type of peroxide [33]. In previous study in Chapter 2 and 3, DCP and Trigonox initiators had different efficiency in initiation crosslink reaction at 150°C. Although initiator was much milder as compared to DCP, the glass transition temperature of BMI was still significantly increased. This incensement in Tg was due to the higher crosslink density by BMPM homopolymerization. However, sometimes, this high Tg made the system less thermally stable due to the un-homogenous network. This was verified by TGA study that BMI/ Trigonox® 101 system did not show any enhancement in thermal stability. On the other side, in Chapter 4, it was found that APS could enhance the Tg of BMI by reaction between APS and BMPM. Besides, thermal stability was also enhanced due to the protection of APS POSS cage on the polymer during degradation. Thus, it was very interesting to investigate the combination of APS and Trigonox®101 on the thermal properties of BMI network. It was possible that this combination can enhance the thermal property in a synactic way.

In this chapter, 0.15wt% Trigonox®101 was chose to add into BMI/APS system. The reason to choose this lower content of Trigonox®101was that BMI with 0.3wt% Trigonox®101 still showed a relatively high Tg, which means that the crosslink density was still increased to some degree by this content of Trigonox®101 in BMI network. Besides, 2 and 5wt% APS was chose to combine with Trigonox®101 was due to finding that the thermal property of BMI will start to deteriorate with over amount of APS.

5.2 Experimental Techniques

5.2.1 Materials

Bismaleimide resin (BMI) in this study was consisted by 4, 4'- bisamleimidodiphenyl methane (BMPM) and O, O'-Diallyl bisphenol A (DABPA) (Huntsman Co.) mixed together with 1:1 molar ratio. Additional 2 and 5wt% of N-Phenylaminopropyl POSS (APS) (Hybrid Plastic Co.) was mixed into the BMI resin. The BMI-APS system was then low temperature cured with 0.3wt% Trigonox® 101. All components were used as received with no further purification. All components were used as received with no further purification. The structures of these components were shown in Figure 5.1.

5.2.2 Sample preparation

The amber viscous liquid of DABPA monomers was poured into a glass beaker with magnetic stir bar. It was heated on a hot plate at 150°C until the viscosity decreased. Corresponding amount of yellow crystalline BMPM powder was then added in slowly and the BMPM-DABPA mixture was stirred for about 30min until a homogenous solution was obtained. Next, the mixture was cooled down to 100°C, Trigonox® 101 was added into the mixture and quickly stirred in. Finally, BMI resin panels were prepared by pouring the mixture into aluminum round disk. All panels were cured in a convention air oven at 150°C for 2h and 250°C for 6h. A diamond saw was utilized to cut cured BMI resin panel into desired size. Surface oxidation and porosity on the resin were removed by polishing with grit paper. The final specimen thickness was around 1.5mm. All samples were then cleaned with de-ionized water, followed by drying in a convention air oven at 80^{o}C until no weight change.

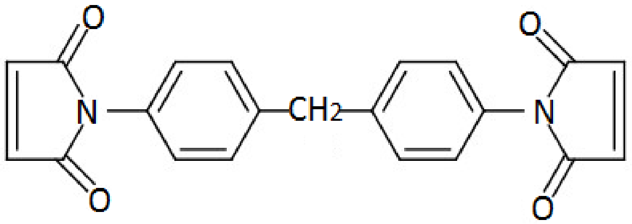

4, 4’- bisamleimidodiphenyl methane (BMPM)

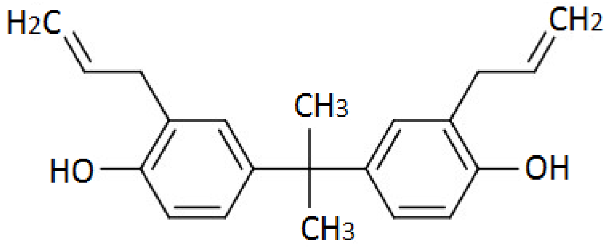

O, O’-diallyl bisphenol A (DABPA)

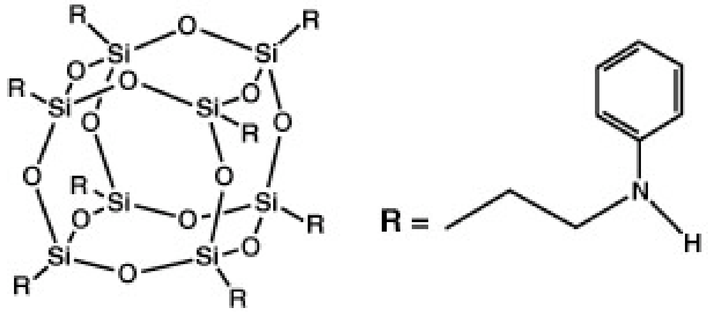

N-Phenylaminopropyl POSS (APS)

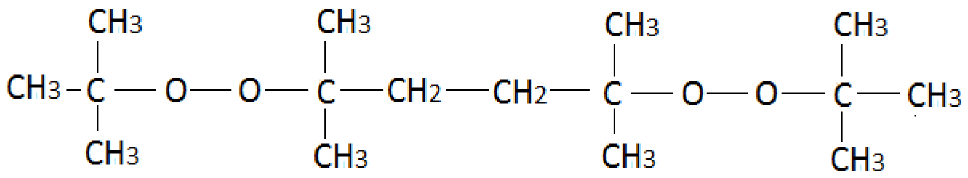

$$CH_3-C(CH_3)_2-O-O-C(CH_3)_2-CH_2-CH_2-C(CH_3)_2-O-O-C(CH_3)_2-CH_3$$

2,5-Dimethyl-2,5-di(tert-butylperoxyl) hexane (Trigonox$^{®}$101)

Figure 5.1: Schematic structure of BMPM, DABPA, APS and Trigonox$^{®}$101

5.2.3 Characterization techniques

DSC analysis of BMPM/APS/ resin was studied using around 10mg mixture in a Mettler Toledo DSC-1. Dynamic heating rate of 10^{o}C/min was used to determine the heat of reaction during curing process. The heating range was from 50-350^{o}C with nitrogen gas at a flow of 50ml/min. The extent of cure α at any time was defined as

$$\alpha = \frac{\Delta H}{\Delta Hr}$$

where ΔH is the partial heat of reaction at any determined time while ΔH_r is the overall heat of reaction.

DMA was carried out on a Rheometric Solid Analyzer III with a 350g transducer. BMI/APS/ Trigonox$^®$101 samples were cut into rectangular bars with a width of 5mm and thickness of 1.5mm. Torsion mode was applied to the sample. Experiments were performed from 50 to 400^{o}C at the frequency of 10rad/s with 5^{o}C/min heating rate. From the DMA spectra, change in storage modulus, G', as a function of temperature can be obtained. Tg was determined as the temperature when maximum drop of G' occurs.

Thermal gravimetric analyzer, TA Q500, was used to investigate the thermal and oxidative stability of the BMI/APS/ Trigonox$^®$101 thermosets. All the thermal analysis was conducted from 50 to 500^{o}C at a heating rate of 20^{o}C/min. The onset degradation temperature was determined as the temperature at 5wt% weight loss.

5.3 Results and Discussion

5.3.1 Reaction in BMI/APS/ Trigonox®101 system by DSC

From previous study, BMI with additional 5wt% APS showed the highest glass transition temperature while 2 and 10wt% APS showed about the same lower Tg than the 5wt% system. Meanwhile, study in Chapter 3 concluded that with 0.15wt% Trigonox®101, the BMI network showed the best thermal performance. Thus, it is very interesting to investigate the combined effect of APS and Trigonox®101 on the thermal properties of BMI network. The first study would be DSC reaction analysis that can give some information on the reaction mechanism and the rate of reaction in the network. Figure 5.2 showed dynamic DSC curves of BMI with 2 and 5wt% APS co-curing with 0.15wt% Trigonox®101. No melting endotherm appeared implying that the hybrid resin was noncrystalline. As can be seen in the figure, two peaks were shown in both BMI-additional 2 and 5wt% APS with Trigonox system. However, the first peak that was dedicated as cure reaction initiated by Trigonox®101 was much lower in BMI with 5wt% APS system. Heat of reaction as well as the percentage of cure after the first reaction peak was summarized in Table 5.1. It was clear that in BMI-additional 5wt% APS system, the first reaction peak was almost eliminated. On the other hand, BMI-additional 2wt% APS system also showed relatively lower percentage of cure for the first reaction peak as compared to BMI with 0.15wt% Trigonox®101 system. This might be due to the reaction between the secondary amine in APS with free radical generated by Trigonox®101. It was also found in literature that secondary aromatic amines are extremely effective hydrogen donors [35]. So, it was understandable that the much lower heat of reaction of first reaction in BMI-additional 5wt% APS and Trigonox®101 system was due to the terminated free radicals by APS.

Table 5.1: Heat of reaction for BMI with additional 2 and 5wt% APS with 0.15wt% Trigonox®101

System	Overall (J/g)	Trigonox®101 peak		BMPM peak
		Heat of reaction (J/g)	Percent of cure (%)	Heat of reaction (J/g)
Control	368	/	/	339
0.15wt%	375	146	39	202
2wt%APS/	363	127	35	203
5wt%APS/	315	23	7	268

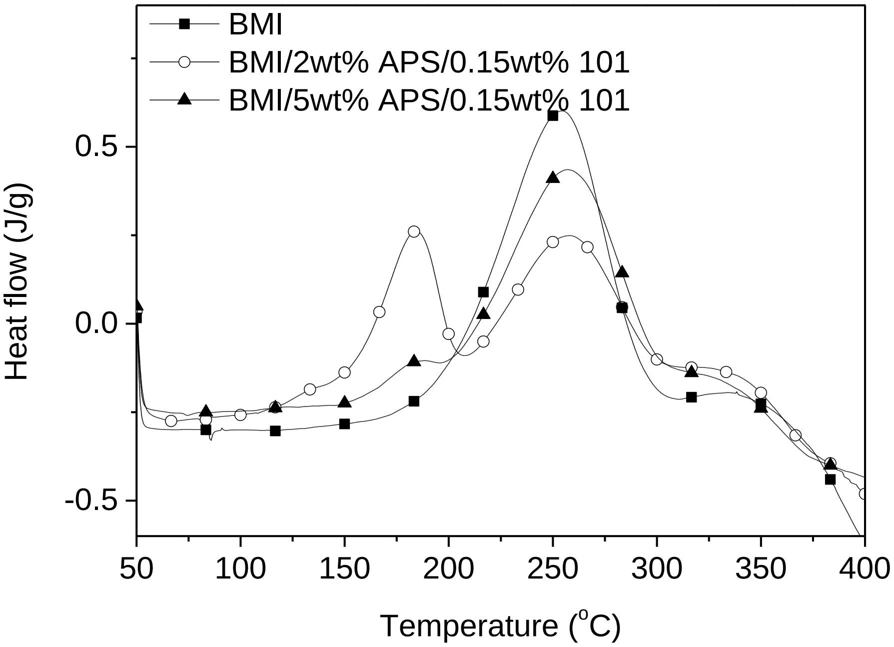

Figure 5.2: Dynamic DSC curves of BMI control system and BMI-additional 2 and 5wt% APS with 0.15wt% Trigonox®101 at 10°C/min heating rate

As can be seen in Table 5.1, the heat of reaction in BMI/5wt% APS/ Trigonox® 101 system has much higher heat of reaction underneath the BMPM reaction peak than 2wt% APS system. This is another indication that Trigonox® 101 did not effectively initiate the crosslink reaction under the lower temperature range. The crosslink reaction was mostly initiated by BMPM itself as the reaction mechanism in the control system. On the other hand, the similar heat of reaction of BMI/2wt%APS/0.15wt% Trigonox® 101 system with the BMI/0.15wt% Trigonox® 101 system indicated that the reaction mechanism between these two networks was similar. The slightly lower heat of reaction can be due to the terminated of free radical by APS. But it could also because of the APS reaction with BMPM that will slow down the crosslink reaction. This can be seen in Figure 5.3, that the reaction peak in BMI/2wt% APS/0.15wt% Trigonox® 101 was slightly broader than BMI/0.15wt% Trigonox® 101.

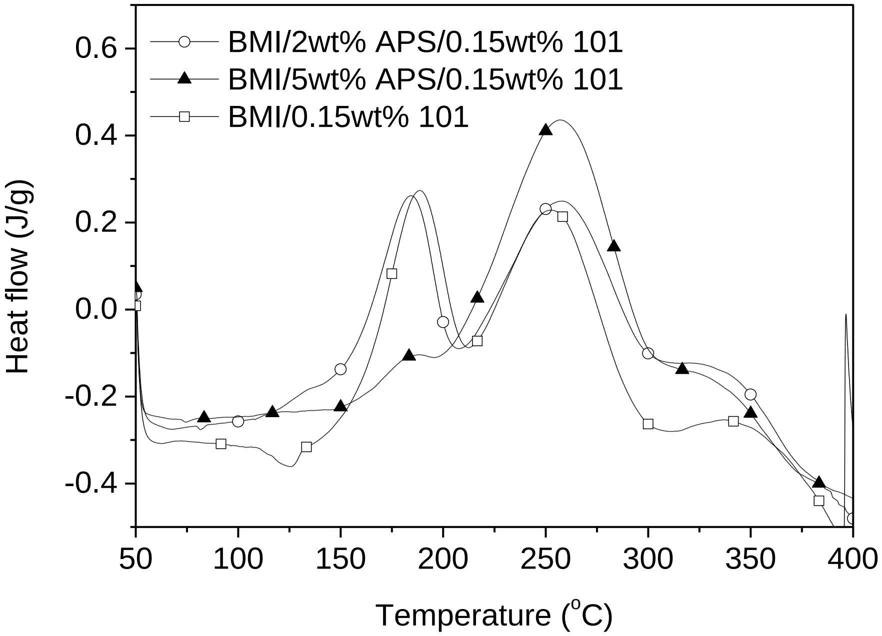

Figure 5.3: Dynamic DSC curves of BMI with additional 2 and 5wt% APS combined with 0.15wt% Trigonox® 101 and BMI with 0.15wt% Trigonox® 101 at 10°C/min heating rate

5.3.2 Glass transition temperature of BMI/APS/ Trigonox®101network

The curing procedure of the BMI/APS/ hybrid resin was chosen as follows: 150°C for 2h and 250°C for 6h based on curing behavior from DSC analysis. It was the same cure cycle as we chose for BMI/ system. The DMA data of the cured BMI/APS/ hybrid resins were shown in Figure 5.4. The glass transition temperature summarized in Table 5.2 was obtained as the onset point of storage modulus start to decrease.

Table 5.2: Glass transition temperature of cured BMI and additional 2 and 5wt% APS with Trigonox®101 system

System	Tg (°C)
BMI	255
2wt%APS/Trigonox®101	295
5wt% APS/Trigonox®101	293
BMI/0.15wt% Trigonox®101	342

As can be seen from the data in Table 5.2 and Figure 5.4, glass transition temperature of cured BMI/APS/Trigonox®101 system was higher than BMI control system, but lower than BMI/ Trigonox®101 system. It was very interesting that BMI/2wt%APS/ Trigonox®101 showed an early decreased storage modulus around 170°C.

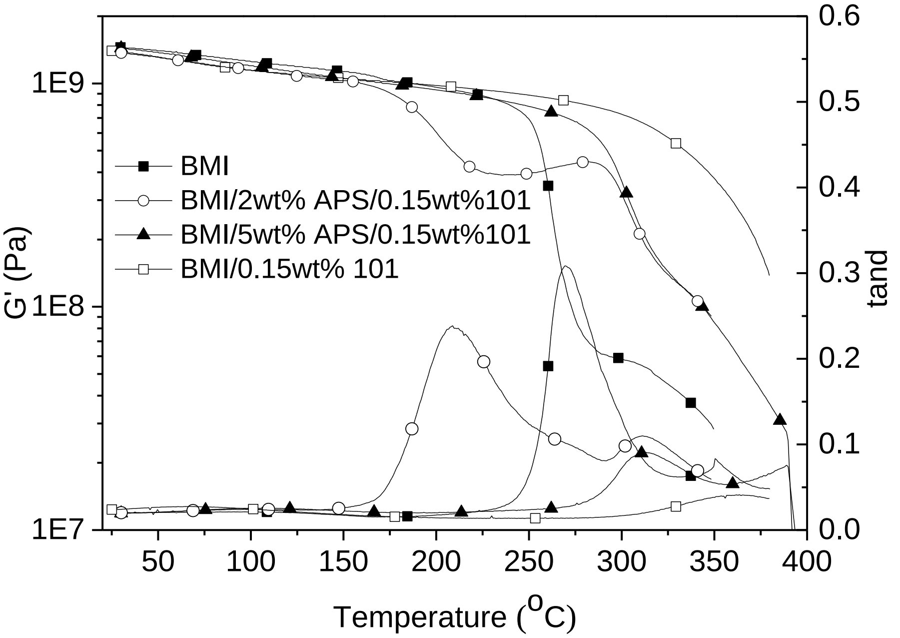

Figure 5.4: Shear modulus and tanδ vs. temperature of BMI, BMI and additional 2 and 5wt% APS with 0.15wt% Trigonox® 101 and BMI with 0.15wt% Trigonox® 101

With the increase of temperature, the storage modulus increased later again. This was mainly due to the competition reaction between Trigonox® 101 and APS. In 2wt% APS system, there were not as much APS as BMI/5wt%APS/ Trigonox® 101 system. As learned from the DSC analysis above, APS can terminate the free radicals. Thus, this early decreased storage modulus was due to the incomplete reaction initiation by Trigonox® 101 at 150°C. When the system was heated up to 200°C, the network was further crosslinked by BMPM free radicals. As a result, the storage modulus started to increase again.

When in BMI/5wt% APS/Trigonox®101 system, this early decreased storage modulus was not observed. This can explained by the fact that Trigonox®101 was more consumed APS at the lower temperature range. This system cure at 150°C for 2h, after this low temperature cure, Trigonox®101 might form some high crosslink network but not as high as BMI/ Trigonox®101 system. Thus, the further curing at 250°C allowed some further crosslink reaction that contribute the slightly increased modulus. Another data difference should be concerned is that the Tg difference between the BMI/2wt%APS/Trigonox®101 and BMI/5wt%APS/Trigonox®101 system was not as significant as BMI with additional APS system. This enhancement in Tg was due to the competition ability of APS and Trigonox®101 in changing the BMI network. The way that APS change the network in order to enhance the Tg was to chemical bonded to BMI network through Michael addition reaction and slow down the network chain mobility. On the other side, the way that Trigonox®101 enhance the Tg of BMI network was to increase the crosslink density of the system due to the early initiation step induced BMPM homopolymerization. When these two mechanisms compete with each other, especially for BMI/5wt% APS/ Trigonox®101 system, it seems that this combination gave the network the best thermal mechanical property.

5.3.3 Thermal stability of BMI/APS/ Trigonox®101 network

The degradation behavior of cured BMI/APS/ Trigonox®101 was investigated by TGA analysis under N_2 atmosphere. TGA curves of these systems were shown in Figure 5.5. The typical data, T_{d1}, T_{d2}, T_{d3} and T_{d4}, temperature at 5, 10, 15 and 20% weight loss were summarized in Table 5.3. Single step decomposition was observed, which indicated that combining APS and Trigonox®101 still did not alter the decomposition mechanism of the BMI system. It can be seen that all composites have similar decomposition temperature values that also indicated that similar degradation mechanism.

When comparing the char yield of BMI/5wt% additional APS/0.15wt% Trigonox®101 with BMI/additional 5wt% APS, it was decreased up to 8%. This was another indication that Trigonox®101 did contribute to the higher Tg. The relatively faster homopolymerization of BMPM during 150°C curing stage that made the system less homogenously crosslinked. The onset degradation of BMI with APS and Trigonox®101 system was lower than BMI control system. However, when observing the derivative of BMI/APS/ as shown in Figure 5.6, it can be seen from the curve that when APS was in the system, the maximum weight loss rate was suppressed. This was due to the protection of the network by POSS that was inorganic in nature. The BMI/5wt% APS/ Trigonox®101 showed the lowest maximum degradation rate as can be seen in the Figure.

Table 5.3: Degradation temperatures of cured BMI resin with additional 2 and 5wt% APS with 0.15wt% Trigonox® 101

System	T_{d1}(°C)	T_{d2}(°C)	T_{d3}(°C)	T_{d4}(°C)	Char Yield (%)
BMI	427	436	445	451	51
2wt % APS	423	433	442	448	51
5wt% APS	417	429	438	446	47

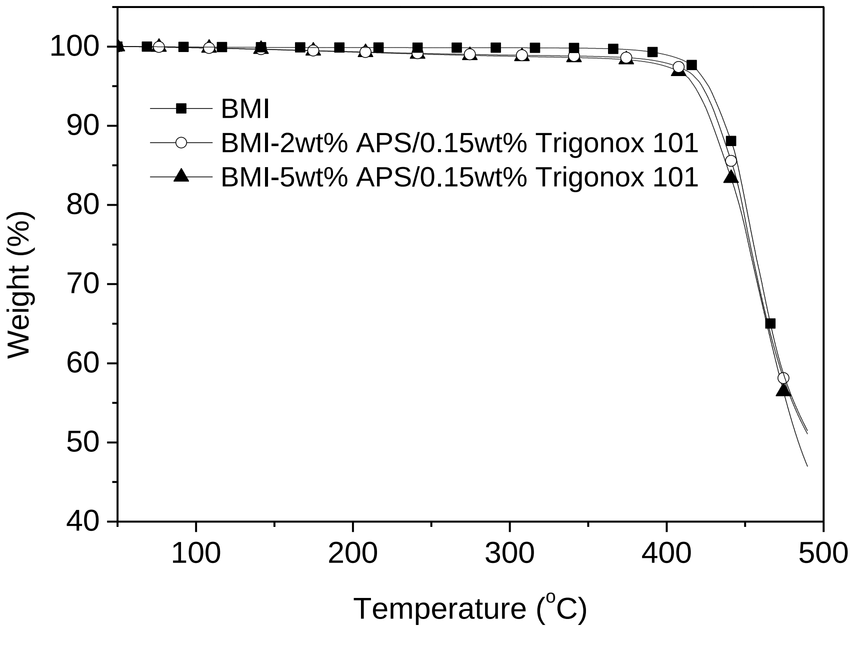

Figure 5.5: TGA profiles of cured BMI resin with additional 2 and 5wt% APS with 0.15wt% Trigonox® 101

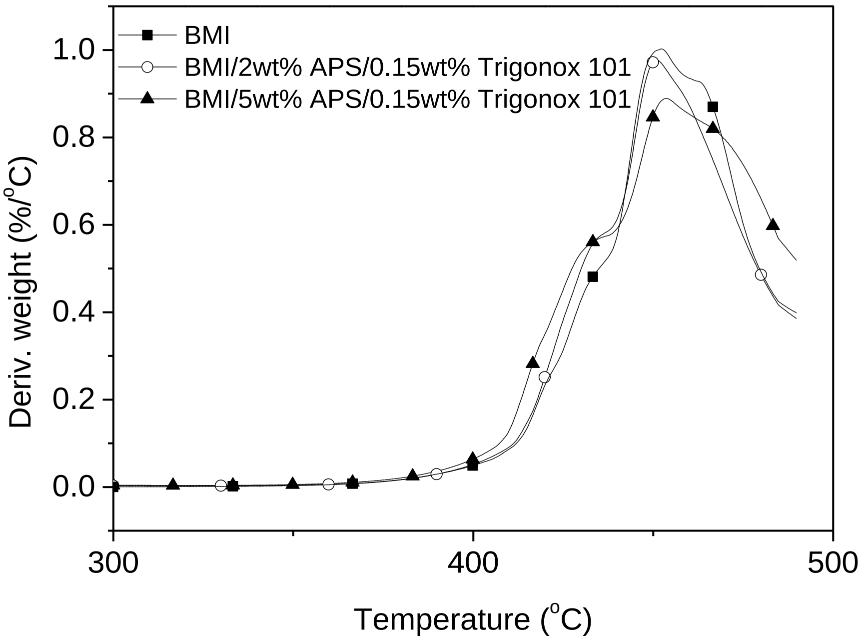

Figure 5.6: Derivative of TGA curves for cured BMI resin with additional 2 and 5wt% APS with 0.15wt% Trigonox®101

5.4 Conclusions

In this study, APS and Trigonox®101 was combined together in order to investigate the synactic effect of both addition on the thermal properties of BMI network. From DSC analysis, it was found that there were reaction between APS and Trigonox®101. As a result, the termination of Trigonox®101 by APS affected the curing step at 150°C. DMA results showed that Tg of BMI/APS/ system was lower than BMI/ system but higher than BMI/APS system. This indicated that the thermal mechanical property of BMI was enhanced by the combination of APS and Trigonox®101. BMI with 5wt% APS and 0.15wt% Trigonox®101 showed the best thermal mechanical property while BMI with 2wt% APS and 0.15wt% Trigonox$^{®}$101 showed an early decreased shear modulus which was due to the un-complete cure at 150^{o}C. Thermal stability of BMI/APS/ Trigonox$^{®}$101 was not as good as BMI/APS system, but it was better than BMI/ Trigonox$^{®}$101 system. The derivative TGA curves gave information on the network homogeneity. With APS in the system, the degradation rate and maximum degradation was slowed down as compared with BMI/ Trigonox$^{®}$101 system. In general, the thermal mechanical and thermal stability of BMI/APS/ was enhanced by the combination of APS and Trigonox$^{®}$101.

REFERENCES

REFERENCES

1. Cheetham, A.K., Better ceramics through chemistry VI, Materials research society symposium, vol.346, 1994.

2. Patrick, J and Clement, S., Hybrid organic-inorganic materials: a land of multidisciplinartiy, Journal of materials chemistry, vol.6, pp511-525, 1996.

3. Clement, S. and Francois, R. Proceedings of the first european workshop on hybrid organic inorganic materials, New journal of chemistry, vol.8, 1994.

4. Clement, S., Kenneth, J.S. and Susumu, K., Recent progess in hybrid materials science, Chemical society reviews, vol.40, pp471-472, 2011.

5. Paul, D.R. and Robeson, L.M., Polymer nanotechnology: nanocomposites, Polymer, vol.49, pp3187-3204, 2008.

6. Jean, P.B., Claude, C. and Catherine, R., Preparation and characterization of new organic-inorganic hybrid materials in incorporating phosphorous centres, Journal of materials chemistry, vol.8, pp1749-1759, 1998.

7. Pedro, G.R. and Clement, S., Hyrbid materials, functional properties, from maya blue to 21st century materials, New journal of chemistry, vol.29, pp57-58, 2005.

8. Chujo, Y., Saegusa, T., Organic polymer hybrids with silica gel formed by means of the sol-gel method, Advances in polymer science, vol.1, pp1-29, 1992.

9. Sanchez, C. and Ribot, F., Design of hybrid organic-inorganic materials synthesized via sol-gel chemistry. New journal of chemistry, vol.18, pp1007-1047, 1994.

10. Wilkes, G., Orler, B. and Huang, H. Ceramers: hybrid materials incorporating polymeric/oligomeric species into inorganic glasses utilizing a sol-gel approach, Polymer preprints, vol. 262, pp300-302, 1985.

11. Schubert, U., Hiising, N. and Lorenz, A., Hybrid inorganic-organic materials by sol-gel processing of organofunctional metal alkoxides, Chemistry of materials, vol.7, pp2010-2027, 1995.

12. Novak, B.M, Hybrid nanocomposite materials between inorganic glasses and organic polymers, Advanced materials, vol.6, pp422-433, 1993.

13. Loy, D.A. and Shea, K.J., Bridged polysilsesquioxanes highly porous hybrid organic-inorganic materials, Chemical reviews, vol. 95, pp1431-1442, 1995.

14. Mark, J.E., Novel reinforcement techniques for elastomers, Journal of applied polymer science. Applied polymer symposium, vol.60, pp262-273, 1992.

15. Mark, J.E, Lee, C.Y. and Bianconi, P.A., Hybrid organic-inorganic composites, American chemical society symposium series, vol.565, 1995.

16. Lee, A. and Lichtenhan, J.D., Viscoelastic responses of polyhedral oligosilsesquioxane reinforced epoxy systems, Macromolecules, vol.31, pp4970-4974, 1998.

17. Lichtenhan, J.D., Otonari, Y.A. and Carr, M.J., Linear hybrid polymer building blocks: methacrylate-functionalized polyhedral oligomeric silsesquioxane monomers and polymers, Macromolecules, vol.28, pp8435-8437, 1995.

18. Haddad, T.S. and Lichtenhan, J.D., Hybrid organic–inorganic thermoplastics: styryl-based polyhedral oligomeric silsesquioxane polymers, Macromolecules, vol.29, pp7302-7304, 1996.

19. Romo, U.A, Mather, P.T., Haddad, T.S. and Lichtenhan, J.D., Viscoelastic and morphological behavior of hybrid styrylbased polyhedral oligomeric silsesquioxane (POSS) copolymers, Journal of polymer science, part b: polymer physics, vol.36, pp1857-1872, 1998.

20. Fu, B.X., Hsiao, B.S. and Lichtenhan, J.D., Structural development during deformation of polyurethane containing polyhedral oligomeric silsesquioxanes (POSS) molecules, Polymer, vol.42, pp599-611, 2000.

21. Mather, P.T., Jeon, H.G., Haddad, T.S. and Lichtenhan, J.D., Mechanical relaxation and microstructure of poly(norbornyl-POSS) copolymers, Macromolecules, vol.32, pp1194-1203, 1999.

22. Pyun, J. and Matyjaszewski, K., Synthesis of hybrid polymers using atom transfer radical polymerization: homopolymers and block copolymers from polyhedral oligomeric silsesquioxane monomers, Macromolecules, vol.33, pp217-220, 2000.

23. Pyun, J. and Matyjaszewski, K., Synthesis of nanocomposites organic/inorganic hybrid

materials using controlled/living radical polymerization, Chemistry of materials, vol.13, pp3436-3448, 2001.

24. Tsuchida, A., Bolln, C., Sernetz, F.G. and Frey, H., Ethene and propene copolymers containing silsesquioxane side groups, Macromolecules, vol.30, pp2818-2824, 1997.

25. Peter, R.D., Peroxide vulcanization of elastomers, Rubber chemistry and technology, vol.74, pp451-492, 2001.

26. Milan, L. Ludmila, H, Eberhard, B. and Manfred, R., Course of degradation and build up reactions in isotactic polypropylene during peroxide decomposition, Journal of applied polymer science, vol.78, pp886-893, 2000.

27. Yu, Q. and Zhu, S., Peroxide crosslinking of isotactic and syndiotactic polypropylene, Polymer, vol.40, pp2961-2968, 1999.

28. Braun, D., Richter, S., Hellman, G.P. and Ratzsch, M., Peroxy initiated chain degradation, crosslinking, and grafting in PP-PE blends, Journal of applied polymer science, vol.68, pp2019-2028, 1998.

29. Borsig, S.E., Lazar, M. and Ratzsch M., Peroxides grafting of powder polypropylene by butyl acrylate, Journal of marcromolecular science, part a: pure and applied chemistry, vol.36, pp1783-1795, 1999.

30. Parent, J.S., Geramita, S., Ranganathan, S. and Whitney, R.A., Silane modified poly(ethylene-co-vinyl acetate): influence of comonomers on peroxide initiated vinylsilane grafting, vol.76, pp1308-1314, 2000.

31. Olga, P.G. and Jozsef, K.K., Melt grafting of maleic anhydride onto an ethylene-propylene-diene terpolymer (EPDM), European polymer journal, vol. 36, pp1419-1429, 2000.

32. Dluzneski, P., Peroxide vulcanization of elastomers, Rubber chemistry and technology, vol.74, 451-460, 2001.

33. Neal, J. E., Hand book of adhesive technology, Taylor & Francis Group, Marcel Dekker, 1994.

CHAPTER 6: CONCLUSIONS AND RECOMMENDATION

6.1 Primary findings

For BMPM/DABPA based BMI resin, the thermal properties are closely associated with how the network was formed. The incorporation of DABPA with BMPM enhanced the toughness of BMI thermoset, but also affects the thermal stability of the cured network [1,2]. The major crosslink reaction of BMPM/DABPA thermoset is self-initiated by BMPM. When BMPM was heated up to 200°C, it will form free radicals and transfer to BMPM or DABPA forming crosslinked network. Due to this high temperature, their usage in the repair of conventional composites process was limited [3].

Reaction initiator can effectively reduce the initial cure temperature. The initiators can either be peroxides that can form free radicals and initiate the cure reaction or some tertiary amines, imidazoles that can induce the bismaleimide to undergo the anionic reaction [4-7]. In this project, influence of different kind and amount of peroxide initiators on the reaction of bismaleimide was evaluated. This kind of study was an important step for process optimization as well as for the understanding of structure-property relations in the final thermoset network.

The incorporation of peroxide into BMI can significantly decrease the onset reaction temperature. However, this may also introduce high crosslink density as well as inhomogeneous network due to the fast homopolymerization of BMPM. Three different kinds of peroxides were chose to investigate with BMI, which was Dicumyl peroxide (DCP),

It was shown that the addition of DCP significantly lowered the onset cure temperature of

BMI thermoset up to 50°C. The rate of curing was much faster for BMI cured by DCP. This also indicated that fast crosslink reaction was introduced by DCP. With higher content of DCP in BMI network, more chemical reaction occurred at the lower temperature range while reaction at higher temperature was inhibited. DMA analysis shows that storage modulus and crosslink density of BMI cured by DCP was significantly higher than control system. Tg was significantly increased even with only 0.62mole% initiator in the system. Thermal stability of BMI was independent of the DCP concentration. Although onset of degradation temperature of initiator system was slightly higher than the control, the degradation rate was mostly higher than the control. This was due to the inhomogeneity of network by initiator. Moisture uptake was significantly less for initiator system, which is also related with the inhomogeneity of the network. Overall, thermal properties of BMI were enhanced with DCP addition. A minor amount of DCP is sufficient for improving the thermal and moisture uptake properties of BMI network.

A series of BMI catalyzed by Trigonox peroxides were studied to determine the effect of initiator type and initiator concentration on the cure reaction and thermal characteristics of BMPM-DABPA based BMI Thermoset. It was shown that the addition of Trigonox®101 and 301 can also significantly lowered the onset cure temperature of BMI. The rate of curing was more efficient for BMI cured by Trigonox®101 compared with system cured by Trigonox®301. The same as BMI with DCP, only a small amount of Trigonox peroxide was enough for the network. Since Trigonox®301 showed a third reaction peak that was not a beneficial reaction to the network and it also had higher initiation temperature than Trigonox®101, thus

Trigonox®101 was considered as a better initiator to trigger the BMI crosslink reaction at lower temperature.

DMA analysis showed that storage modulus and crosslink density of BMI cured by both Trigonox®101 and 301 was significantly higher than control system while BMI Trigonox®301 system had slightly lower Tg than BMI/Trigonox®101's. Thermal stability of BMI was slightly enhanced also by initiator addition. Although the onset degradation temperature of initiator system was slightly higher than the control, the degradation rate was also mostly higher than the control system. This was due to the inhomogeneity of network due to initiator addition. Moisture uptake was significantly less for BMI/ Trigonox®101 or 301 systems as compared to the control network, which was also related with the inhomogeneity of the network.

Thermal mechanical properties of BMI were affected by different molar ratio of BMPM to DABPA. The DSC study showed that Trigonox®101 did give the system higher heat of reaction when DAPBA was rich in the system. This indicated that the hypothesis of hydrogen abstraction by Trigonox®101 could be true. However, thermal mechanical property of DAPBA rich system was not very promising showing a much lower Tg than the 1 to 1 molar ratio control system with initiator. This indicated that this off ratio might be too much, that some part of DABPA was left over and unreacted. On the other side, thermal resistance study showed that DABPA rich network had the most similar degradation curve as the control system without any initiator. This might be another indication of network similarity.

Although peroxides can effectively decrease onset reaction temperature, the thermal stability of BMI network was not significantly enhanced. BMI with two different kinds of POSS, OSTS and APS was then investigated in order to further enhance the thermal properties of BMI. In BMI/OSTS study, the effect of mixing sequence of OSTS into BMI system was investigated based on BMI/additional 2wt% OSTS. No significant effect of POSS on the thermal mechanical properties of BMI network was observed. By mixing OSTS with DABPA first, higher content of OSTS can be homogenously dispersed in BMI network. With more content of OSTS in the system, the thermal mechanical property of BMI/OSTS nanocomposites was systematically enhanced. This was due to the free radical polymerization of OSTS with BMPM. The bulky POSS cage would retard the chain movement, thus increase glass transition temperature of BMI system. The inorganic natures of POSS cage also protect the BMI network from degradation under both nitrogen and air condition. Especially for BMI/additional 10wt% OSTS which char yield under air condition was 30wt% higher than the control system. The inclusion of OSTS in the network also decrease the possibility of water molecule locked in the system, which in turn enhanced the service life of this BMI composite.

In BMI/APS study, it was found that APS can reaction with BMPM through Michael addition reaction that can occur around 150^{o}C. APS addition at 5wt% significantly improved the glass transition temperature of the network, around 30^{o}C higher than the control system. With higher content of APS, glass transition temperature start to decrease, which was due to the reaction between APS and BMPM made the system DABPA rich. Thermal degradation behavior of BMI/additional APS did not show significant improvement as the BMI/additional OSTS system. This might due to the fact that the functional groups on OSTS were aromatic while the functional groups on APS was longer allylic groups. Higher molar ratio of BMPM to DAPBA was also investigated with 2 and 10wt% APS. From DSC, DMA and TGA analysis, it turned out that the properties of BMI network was more relied on APS than the molar ratio between BMPM to DABPA.

At the end, APS and Trigonox®101 was combined together in order to investigate the synactic effect of both addition on the thermal properties of BMI network. From DSC analysis, it was found that there were reaction between APS and Trigonox®101. As a result, the termination of Trigonox®101 by APS affected the curing step at 150°C. DMA results showed that Tg of BMI/APS/Trigonox®101 system was lower than BMI/Trigonox®101 system but higher than BMI/APS system. This indicated that the thermal mechanical property of BMI was enhanced by the combination of APS and Trigonox®101. BMI with 5wt% APS and 0.15wt% Trigonox®101 showed the best thermal mechanical property while BMI with 2wt% APS and 0.15wt% Trigonox®101 showed an early decreased shear modulus which was due to the un-complete cure at 150°C. Thermal stability of BMI/APS/ Trigonox®101 was not as good as BMI/APS system, but it was better than BMI/ Trigonox®101 system. The derivative TGA curves gave information on the network homogeneity. With APS in the system, the degradation rate and maximum degradation was slowed down as compared with BMI/ system. In general, the thermal mechanical and thermal stability of BMI/APS/Trigonox®101 was enhanced by the combination of APS and Trigonox®101.

6.2 Suggestions for future work

Since the addition of initiator into BMI system will efficiently decrease the onset reaction temperature, further investigation on the minimum content of initiator should be conducted. Due to the fast homopolymerization of BMPM by initiator addition, lower amount of initiator in the network may slow down the reaction rate and give the system a more homogenous network in the end. As a result, the cured network would have better mechanical properties.

Molar ratio change of BMPM to DABPA does affect the thermal stability of cured BMI network. Future investigation on the change of molar ratio effect on the BMI with initiator network should be continued. When BMPM to DABPA was too off ratio, the amount of unreacted DABPA would be increased. As from this project study, more BMPM in the network was more preferred for future study. Combined with the above-founded lowest amount of initiator for the network, more BMPM can be left over to incorporate DAPBA into the network. As a result, the network structure of BMI with initiators would be more homogenous as the BMI control system.

Last but not the least is the combination study of initiator with POSS on thermal properties of BMI. The POSS selected should not consume free radicals but should also be capable of enhance Tg of BMI by chemical reaction. The reaction between POSS and BMI should not be too fast and affect the crosslink reaction between BMPM and DABPA. In order to enhance degradation behavior of BMI/POSS network, POSS with aromatic groups should be selected which itself have good thermal stability.

REFERENCES

REFERENCES

1. Jason, E.L. Michigan State University, Ph.D. thesis, 2001.

2. Wilson, D., Stenzenberger, H.D. and Hergenrother P.M., Polyimides, New York: Chapman and Hall Inc, 1990.

3. Boey F., Xiong, Y. and Rath, S.K., Glass transition temperature in the curing process of bismaleimide modified with diallylbisphenol A, Journal of applied polymer science, vol.91, pp3244-3247, 2004.

4. Stenzenberger H., Polyimides in structural adhesives, A. J. Kinloch, Ed., Elsevier, London, 1986.

5. Varma, I.K., Gupta, S.P., and Varma, D.S., Effect of triallyl cyanurate on the properties of bismaleimide, Journal of applied polymer science, vol.33, pp151-164, 1987.

6. Kwiatkowski, G.T., Robeson, L.M. and Bedwin, A.W., Thermosetting diphenyl sulfone -based maleimides, Journal of polymer science: polymer chemistry edition, vol.13, pp961-972, 1975.

7. Acevedo, M., Abajo, J.D. and Campa, J.G., Kinetic study of the crosslinking reaction of flexible bismaleimides, Polymer, vol.31, pp1955-1959, 1990.